Universidade dos Açores

CLIMATIC PATTERNS AND PHYSICAL CONTROLS OF CHLOROPHYLL-A IN THE NORTHEAST ATLANTIC

André dos Santos Franca Gaspar Valente
Doutoramento em Ciências do Ambiente

Tese orientada pela Prof. Doutora Maria Manuela Fraga Juliano e co-orientada pelo Prof. Doutor Eduardo Manuel Vieira de Brito de Azevedo

Angra do Heroísmo
2013

Universidade dos Açores

CLIMATIC PATTERNS AND PHYSICAL CONTROLS OF CHLOROPHYLL-A IN THE NORTHEAST ATLANTIC

André dos Santos Franca Gaspar Valente
Doutoramento em Ciências do Ambiente

Tese orientada pela Prof. Doutora Maria Manuela Fraga Juliano e co-orientada pelo Prof. Doutor Eduardo Manuel Vieira de Brito de Azevedo

Angra do Heroísmo
2013

ACKNOWLEDGEMENTS

I would like to thank to Prof. Eduardo Brito de Azevedo for providing me the opportunity to enroll in this PhD and for always being so helpful. To my advisor Prof. Manuela Juliano for all her support, understanding and sympathy. For both, I want to express my gratitude for allowing me to pursuit my research questions. To Dr. Rui Caldeira for his time and crucial role in the first years. I want to thank my girlfriend Ulgen Kopuz for all her love, support, encouragement and key role in the decisive moments of the writing process. To my friends Joao Rego and Sergio Muacho, for the life and science discussions, and Miguel Conceicao, Orlando Santos and Hugo Afonso for their long-lasting friendship. To all my colleagues, with special thanks to Francisco Reis, Ricardo Tome, Vasco Avila, Sonia Ameijeiras and Joana Reis, for their disponibility, friendship and scientific discussions. To all the "Terceirense" community for their unique hospitality and sociability, which never made me feel alone. To "Santa Catarina", an endless source of happiness and escape. To the Azores nature, which gave me the necessary escape from computer radiation. To my laptop, the source of radiation, that resisted until the end. To my flat-mate Paulo Silveira, for his company and amazing personality. To all the amazing people I was fortunate to meet in this incredible journey that profoundly mark my life. Finally, I dedicate this thesis to my mother and all my family that always supported me.

This work was made possible by the financial support from the "Plano Integrado para a Ciência e Tecnologia, Eixo 3.1. – Bolsas de Apoio à Investigação Científica e Tecnológica do Programa de Apoio à Formação Avançada (FORMAC)", which is greatly appreciated.

ABSTRACT

Chlorophyll-a concentration is one of the most commonly used indicators of phytoplankton biomass, the basis of the marine food chain. Patterns of chlorophyll-a can be driven by many environmental factors, such has meteorological and oceanographic processes that regulate the available light and nutrients for phytoplankton growth. The identification of physical mechanisms responsible for observed chlorophyll-a patterns is key to predict and understand the effect of climate on phytoplankton. Satellite data, with their unprecedented spatial and temporal coverage, provides an unique source of observations to elucidate on these physical-biological interactions. This study describes the distribution and variability of chlorophyll-a in the Northeast Atlantic using satellite images of ocean colour and identifies underlying physical mechanisms using complementary satellite, in-situ and model data.

Long-term changes in oceanographic properties were firstly analyzed for a better understanding of chorophyll-a variability. Simultaneous reductions in the southward flow and increases in temperature in the upper ocean (0-500 m) were observed in the eastern basin. These results support the hypothesis that the colder and fresher waters of the early 1990's were replaced by warmer and more saline waters after 2000, as a result, at least partially, of stronger subtropical inflows. Positive (and weak negative) wind stress curl was related to the reduction of southward flow providing a link between large-scale changes in atmospheric patterns and the observed warming. After the severe winter of 2009/2010, surface temperature (0-300 m) dropped to the values of 1998-2000, possibly due to an exceptional deep winter mixing.

Regarding the distribution of satellite-derived chlorophyll concentration (SCHL), it was found that the climatological annual pattern was remarkably similar to the nutrient pattern resulting from the combination of the subsurface nutrient field and the mixed layer depth (MLD) field. This suggests that the supply of nutrients during winter has a control over annual SCHL in the region and that this nutrient supply is regulated not only by the depth of winter mixing, but also by the subsurface nutrient field, which in turn is related to ocean circulation and lower in subtropical waters. The seasonal variability of SCHL was different in each group of Azores islands. During winter, a gradual increase of SCHL related to shallower MLD (< 150 m) was typically observed in the Central and Eastern Groups, while a decrease of SCHL related to deeper MLD (> 200 m) was observed in the Western Group. In spring, stronger late blooms were observed in the Western Group, possibly associated with the deep mixing. In the Eastern Group weaker spring blooms could

be attributed to lower winter nutrient supply as a result of shallower MLD, but also to a reduced subsurface nutrient content due to its proximity to the Azores Front. The timing of the seasonal SCHL increase in autumn followed heat losses from the ocean, which indicates surface cooling and the start of convective mixing. Inversely, the timing of SCHL increases in winter and spring occurred during oceanic heat gain, which indicates surface warming and reductions in turbulence. Regarding interannual variability of spring bloom magnitude, a decreasing trend was observed between 1998 and 2009 in the eastern basin. Although west of Azores, stronger winter mixing was related to increased spring bloom magnitude, to the east there was no clear relation. One possible explanation is that subtropical inflows after 2000, changed the subsurface nutrient content in the eastern basin during the period of SCHL observation and caused different biological responses to winter mixing. Finally, SCHL around the islands was slightly higher than surrounding areas, which provides evidence that the Azores islands produce an island-mass effect throughout the year.

This study provides observational evidence of the effect of vertical mixing and horizontal transport on the patterns of chlorophyll-a in the Northeast Atlantic. These results illustrate direct routes between climate and the basis of the marine food chain, contributing to the understanding of the transition region between the subtropical and subpolar biomes, and the physical-biological coupling in the ocean.

RESUMO

A concentração de clorofila-a é um dos mais usados indicadores de biomassa de fitoplâncton, a base da cadeia alimentar marinha. Os padrões de clorofila-a podem ser governados por vários fatores ambientais, tais como processos meteorológicos e oceanográficos que regulam a luz e nutrientes disponíveis para o crescimento do fitoplâncton. A identificação dos mecanismos físicos responsáveis pelos padrões de clorofila-a observados é a chave para prever e entender o efeito do clima sobre o fitoplâncton. Os dados de satélite, com a sua cobertura espacial e temporal sem precedentes, fornecem uma fonte única de observações para esclarecer estas interações físico-biológicas. Este estudo descreve a distribuição e variabilidade de clorofila-a no Atlântico Nordeste utilizando imagens de satélite da cor do oceano e identifica mecanismos físicos associados usando dados complementares de satélite, in-situ e de modelos.

Alterações nas propriedades oceanográficas foram primeiro analisadas para uma melhor compreensão da variabilidade de clorofila-a. Foram observadas reduções simultâneas na circulação para sul e aumentos de temperatura na parte superior do oceano (0-500 m) na bacia oriental. Estes resultados suportam a hipótese de que as águas mais frias e menos salinas do início da década de 1990 foram substituídos por águas mais quentes e mais salinas depois de 2000, como resultado, pelo menos em parte, de pulsos de águas subtropicais. Períodos positivos (e fraco negativos) do rotacional do vento foram relacionados com a redução da circulação para sul proporcionando uma ligação entre alterações nos padrões atmosféricos de larga escala e o aquecimento observado. Após o inverno rigoroso de 2009/2010, a temperatura da superfície (0-300 m) caiu para os valores de 1998-2000, possivelmente devido a uma camada de mistura excepcionalmente profunda.

No que diz respeito à distribuição da concentração de clorofila derivada de imagens de satélite (SCHL), verificou-se que o padrão anual climatológico foi semelhante ao padrão de nutrientes resultante da combinação do campo subsuperficial de nutrientes e do campo da profundidade da camada de mistura (MLD). Isto sugere que o fornecimento de nutrientes durante o inverno, tem um controle sobre a SCHL anual na região, e que este fornecimento de nutrientes é regulado não só pela profundidade da camada de mistura, mas também pelo conteúdo de nutrientes em profundidade, que por sua vez é governado pela circulação oceânica e inferior em águas subtropicais. A variabilidade sazonal de SCHL foi diferente em cada grupo de ilhas dos Açores. Durante o inverno, um aumento gradual de SCHL relacionado com menores MLD (<150 m) foi tipicamente observado nos Grupos Central e Oriental, enquanto que uma diminuição de SCHL relacionada com maiores MLD (> 200

m) foi observada no Grupo Ocidental. Na primavera, um forte "spring bloom" foi observado no Grupo Ocidental, possivelmente relacionado com a profundidade da camada de mistura. No Grupo Oriental, um "spring bloom" fraco pode ser atribuído a um menor fornecimento de nutrientes durante o inverno como resultado de MLD inferiores, mas também a um reduzido conteúdo de nutrientes em profundidade, devido à proximidade com a Frente dos Açores. O momento do aumento de SCHL no outono seguiu perdas de calor do oceano, o que indica arrefecimento à superfície e o início da mistura por convecção. Inversamente, o momento do aumento de SCHL no inverno e primavera ocorreu durante ganhos de calor no oceano, o que indica aquecimento da superfície e reduções de turbulência. Relativamente à variabilidade interanual da magnitude do "sping bloom", foi observada uma tendência decrescente entre 1998 e 2009 na bacia oriental. Embora a oeste dos Açores, a mistura durante o inverno tenha sido relacionada com uma maior magnitude do "spring bloom", para leste não houve uma relação clara. Uma possível explicação é que os pulsos de águas subtropicais depois de 2000, alteraram o conteúdo de nutrientes em profundidade da bacia oriental durante o período de observação de SCHL e causaram diferentes respostas biológicas à mistura de inverno. Finalmente, SCHL em torno das ilhas foi um pouco maior do que nas áreas circundantes, o que fornece evidência de que as ilhas dos Açores produzem um "island-mass effect" ao longo do ano.

Este estudo fornece evidências observacionais do efeito da mistura vertical e do transporte horizontal nos padrões de clorofila-a no Atlântico Nordeste. Estes resultados ilustram rotas diretas entre o clima e a base da cadeia alimentar marinha, contribuindo para a compreensão da região de transição entre os biomas subtropicais e subpolares, e do acoplamento físico-biológico no oceano.

LIST OF ACRONYMS

AC	Azores Current
AMT	Atlantic Meridional transect
ARGO	Array for Realtime Geostrophic Oceanography
AVHRR OI	Advanced Very High Resolution Radiometer Optimum Interpolation
AVISO	Archiving, Validation and Interpretation of Satellite Oceanographic Data
CMCC	Euro-Mediterranean Center on Climate Change (Bologna, Italy)
DCM	Deep Chlorophyll Maximum
EKE	Eddy Kinetic Energy
ETOPO1	1 Arc-Minute Global Relief Model
FNMOC	Fleet Numerical Meteorology and Oceanography Center
GTSPP	Global Temperature-Salinity Profile Program
LEV05	Levy et al. (2005)
MAR	Mid-Atlantic Ridge
MATLAB	MATrix LABoratory
MLD	Mixed Layer Depth
MODIS AQUA	Moderate Resolution Imaging Spectroradiometer aboard the AQUA satellite
NAC	North Atlantic Current
NASA	National Aeronautics and Space Administration
NCEP	National Centers for Environmental Prediction
OSCAR	Ocean Surface Current Analysis - Real Time
Qnet	Net heat flux at air-sea interface

QuickSCAT	Quick Scatterometer
SCHL	Satellite-derived concentration of chlorophyll-a
SeaWiFS	Sea-viewing Wide Field-of-view Sensor
SST	Sea surface Temperature
SODA	Simple Ocean Data Assimilation
TOPS	Thermal Ocean Prediction Model
WOA05	World Ocean Atlas 2005

LIST OF FIGURES

TABLE OF CONTENTS

CHAPTER 1: GENERAL INTRODUCTION

1.1. Motivation

Climate variability significantly impacts phytoplankton in the ocean, over both short (seasonal to interannual) and long-term (decadal) time scales. Changes in light, nutrients, temperature, salinity, freshwater discharge, acidification, wind forcing and currents impact the abundance, distribution, phenology and diversity of these microscopic water plants. They are at the basis of the marine food web and the impact of climate on phytoplankton biomass will have impacts on the rest of the marine ecosystem including on living marine resources used by humans. This has both ecological as well as socio-economic implications.

Just like terrestrial plants, phytoplankton grow and multiply via photosynthesis, a process regulated by light and inorganic nutrients. In the ocean, light is only available at the surface, while nutrients are mostly found in deeper waters where sinking particles decompose. The nutrients are thus unavailable for phytoplankton growth unless some physical mechanism bring the nutrients back to the surface. In the North Atlantic, away from continental margins, the annual supply of nutrients to surface waters is mainly accomplished by the surface mixed layer of the ocean which shoals and deepens in response to seasonal climatological change (Williams et al., 2000). During winter, decreased solar radiation and strong winds, mix surface waters with deeper nutrient-richer waters, providing the necessary nutrients for phytoplankton growth. The amount of nutrients a given mixed layer provides to the surface, is than regulated by the subsurface nutrient concentration or nutricline depth (Yentch, 1989; Longhurst et al., 2006). These two factors together control much of the available nutrients at the surface and consequently the large-scale distribution of phytoplankton biomass which is mainly a result of nutrient limitation (e.g. Falkowski et al., 1992; Marañon et al., 2000). Two major biomes than appear. At low latitudes such as the subtropical gyres, a deep nutricline and weak winter mixing reduces the supply of nutrients to the euphotic layer, which leads phytoplankton to rely on local recycling to sustain their standing stocks and ultimately in low biomass. In contrast, at high latitudes and temperate regions, a shallow nutricline and stronger winter mixing, results in an adequate supply of nutrients to the euphotic layer and higher phytoplankton biomass.

The recent observed global surface warming (about 0.2 ºC per decade) is expected to accelerate in coming decades as we continue to release excess carbon dioxide into the atmosphere. In fact, the

planet may soon be warmer than at any time in the past million years (Hansen et al., 2006). These future scenarios result in a different climate–phytoplankton link to the north and south of the Azores (~ 40 ºN) due to the different production regimes (e.g. Doney, 2006). To the south, in the subtropics (< 35 ºN), a deep nutricline and weak vertical mixing limit phytoplankton growth. In these regions climate warming further inhibits mixing, reducing the upward nutrient supply, lowering productivity and expanding oligotrophic conditions typical of the subtropical gyres into temperate regions (Behrenfeld et al., 2006; Polovina et al., 2008). To the north, phytoplankton are often light-limited because intense vertical mixing carries them hundreds of meters down into darkness where sunlight does not penetrate. In these regions, where nutrients are often available, future warming will contribute to reduce mixing that may actually increase productivity (Reid et al., 1998; Raitsos et al., 2005). The transition between these two production regimes occurs in the midlatitude or intergyre region, where the Azores Archipelago is located. Therefore, this region is of great scientific interest because it will be the first area to be influenced by the expansion of the North Atlantic subtropical gyre (Behrenfeld et al., 2006; Polovina et al., 2008) and where these paradigms can be tested in future.

Very few sufficiently long biological time series exist to assess interannual- to decadal-scale variability in phytoplankton. In the North Atlantic, the exceptions are the Continuous Plankton Recorder (CPR) program and the NASA daily global maps of chlorophyll-a concentration (a proxy for phytoplankton biomass). Both these datasets measure the color of the ocean, therefore providing a qualitative index of phytoplankton biomass. While the CPR dataset goes back to 1948, it has a course temporal and spatial resolution. Conversely, the NASA satellite ocean color datasets have a high temporal-spatial resolution, but only exist since 1997. Most of the studies in phytoplankton variability on interannual and decadal time-scales in the North Atlantic have used these datasets.

To understand how global warming will influence phytoplankton is crucial to scrutinize these long-term biological datasets and understand how their variability responds to physical changes. Only by understanding the mechanisms responsible for past and “normal” variability it is possible to identify abnormal changes and predict future scenarios. In this work, the NASA satellite ocean color datasets and complementary physical datasets are used to describe the oceanographic conditions in the Azores region and how these conditions have influenced phytoplankton variability. In addition to the relevance of this study for a better understanding of the climatic mechanisms responsible for phytoplankton variability, the regional ocean climate around Azores is poorly known, which prompts for more investigation in the area.

1.2. Objectives

My main objectives are 1) describe the physical oceanographic changes in the Azores region during the last two decades, 2) describe the seasonal and interannual variability of phytoplankton chlorophyll-a in the Azores region since 1997 and 3) identify the mechanisms responsible for the observed variability in both the physical and biological fields.

1.3. Structure of the thesis

In this first chapter it is given an introduction for the region of interest in terms of location, currents, temperature, salinity, mixed layer and concentration of chlorophyll-a. In chapter 2 the datasets used in this study are described. In chapter 3 the recent physical changes in the Northeast Atlantic in terms of temperature and salinity in the first 500m, are described in relation to the Azores Archipelago and the responsible mechanisms are investigated. In chapter 4 the climatic patterns and variability of satellite-derived chlorophyll-a concentration since 1997 are analyzed for the Northeast Atlantic and the Azores Archipelago. The mechanisms responsible for the observed biological variability are also investigated. In chapter 5 a resume of the major findings is provided.

1.4. Scientific Background

1.4.1. Region of interest

The region of interest is the Azores Archipelago and the midlatitude region of the Northeast Atlantic, between 30-50 ºN and 15-45 ºW (boxes in Figure 1-1). The bathymetry of the region is defined by two large topographic features: the Azores Plateau and the Mid-Atlantic Ridge (MAR). The Azores Plateau is a large bathymetric anomaly in the central North Atlantic from where the islands emerge. It has a triangular shape and is defined by the bathymetric curve of 2000 m. The MAR is an underwater mountain range along the floor of the Atlantic Ocean, with a deep rift valley running along the axis of the ridge. The MAR marks the boundary between the east and west basins of the Atlantic Ocean.

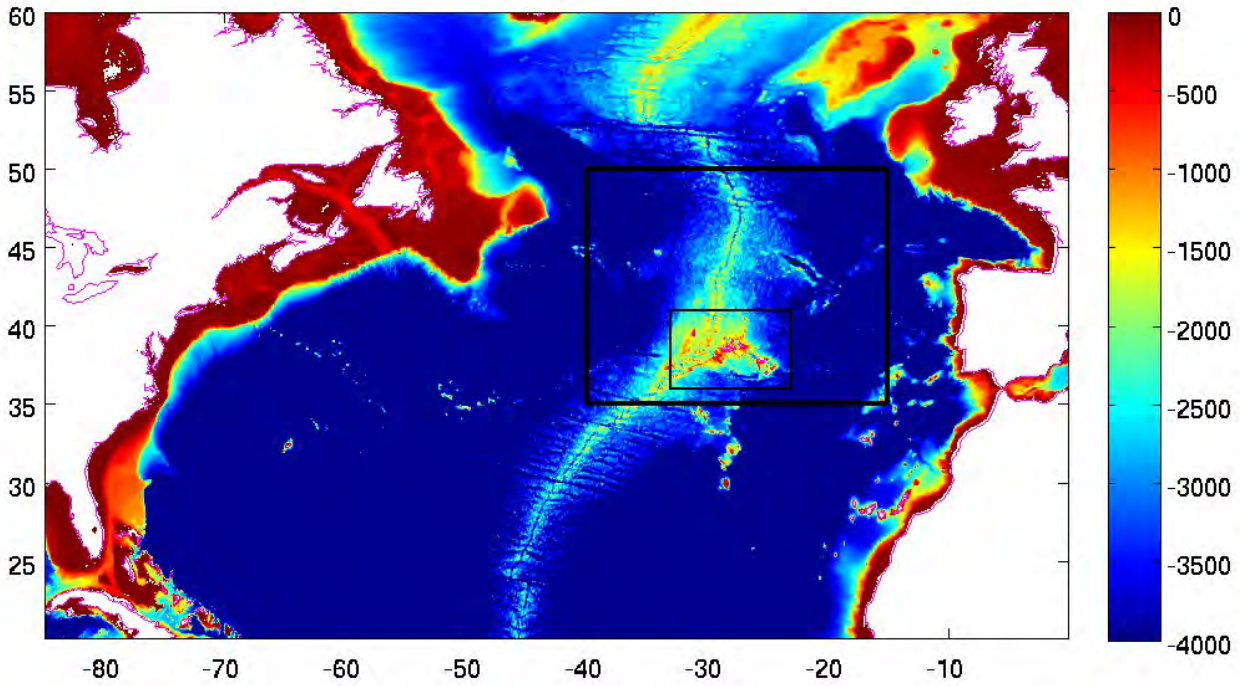

Figure 1-1 North Atlantic bathymetry (m) from ETOPO1 (Amante and Eakins, 2009). The boxes indicate the midlatitude region of the Northeast Atlantic and the region of the Azores Archipelago.

The Azores Archipelago is centered at 28 ºW and 38 ºN, spanning over seven degrees in longitude (25-32 ºW) and three degrees in latitude (37-40 ºN). A straight line connects the Azores with New York (United States of America) and Lisbon (Portugal). The archipelago is composed of nine islands, divided into three groups: Western, Central and Eastern (Figure 1-2). The Eastern group is formed by Santa Maria and São Miguel islands, the Central group includes Terceira, Graciosa, São Jorge, Pico and Faial islands and the Western group is constituted by Flores and Corvo islands. The Azores islands have steep slopes and narrow shelves. Seamounts are common topographic features in the area.

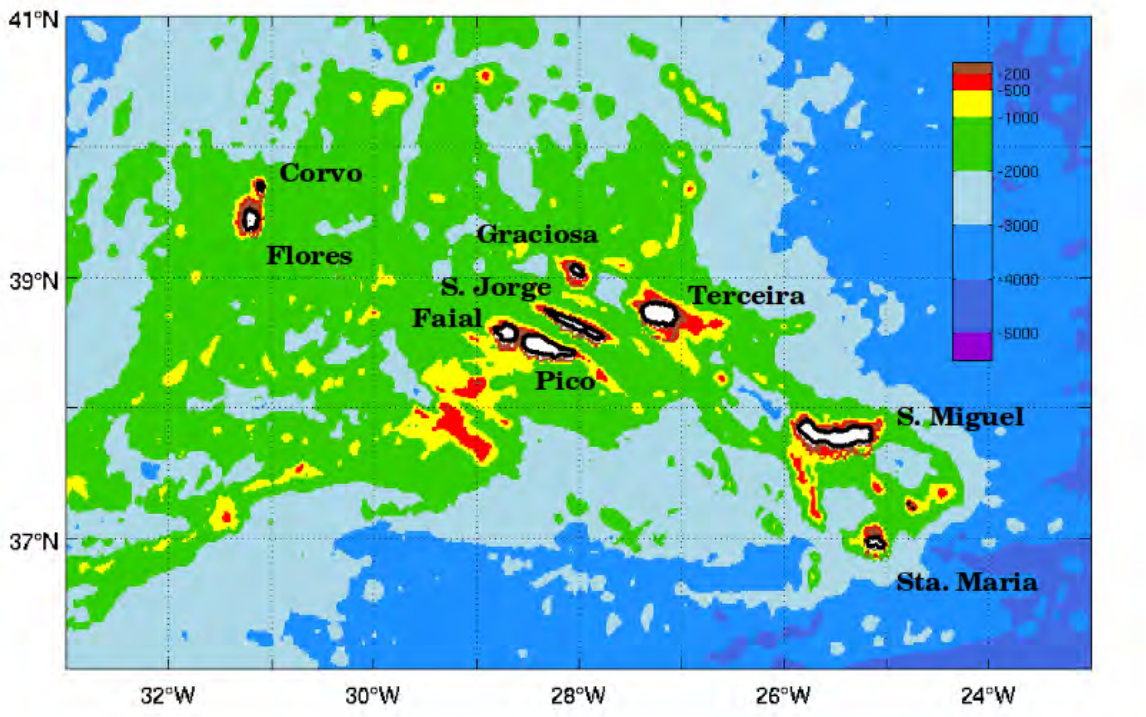

Figure 1-2 Azores islands and bathymetry from ETOPO1 (Amante and Eakins, 2009)

1.4.2. Currents

The mean circulation of the North Atlantic Ocean is characterized by two large gyres: the subpolar gyre with a cyclonic circulation and the subtropical gyre with an anticyclonic circulation (Figure 1-3). The southern boundary of the subpolar gyre is the subpolar front (~ 52 ºN) and the northern boundary of the subtropical gyre is the subtropical front (~ 34 ºN). Most of the surface circulation, takes place in these two fronts that have particular current systems names, the North Atlantic Current (NAC) and the Azores Current (AC). Although the AC is often associated to the circulation around 34 ºN, the NAC terminology is looser and is also used to refer circulations between 40-52 ºN. The AC and NAC are the southeastward and northeastward extensions of the Gulf Stream, respectively. Both these currents make their crossing from the western to the eastern basin through particular fracture zones (gaps) in the Mid-Atlantic Ridge. The AC traverses the Mid-Atlantic Ridge in the vicinity of the Oceanographer Fracture Zone (34 ºN), while the NAC crosses through several gaps between 40-52 ºN (Bower and Von Appen 2008).

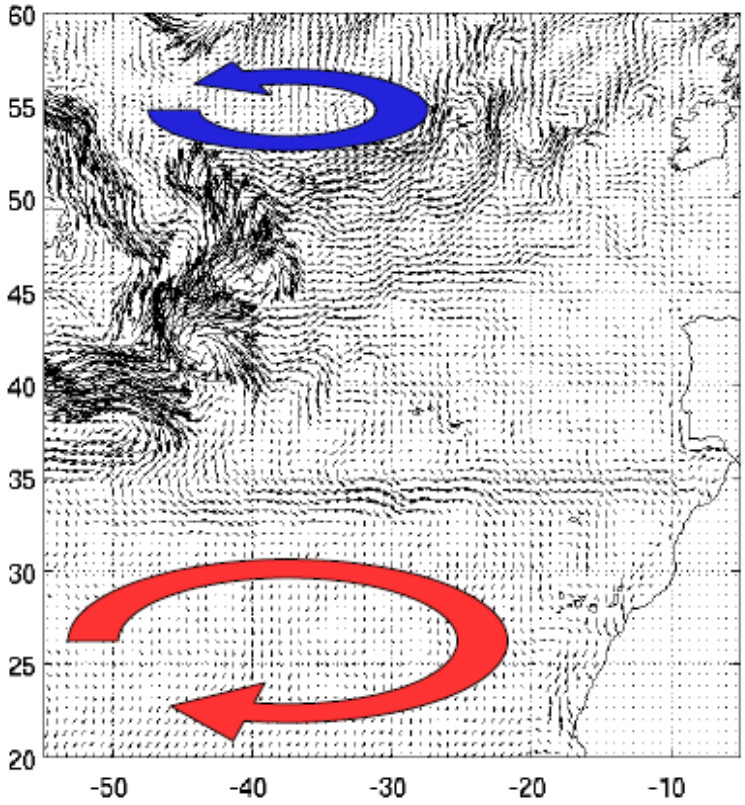

Figure 1-3 Average mean circulation in the Northeast Atlantic derived from satellite altimetry weekly data between 1993 and 2009 (AVISO; CLS, 2009). Smoothed using 1º window moving average.

The NAC does not cross the North Atlantic Ocean as a broad eastward current, but rather as several narrow current bands (jets) that meander across the North Atlantic in the latitudinal band 40–53 ºN (Bower and Von Appen 2008). While most of the NAC recirculates northward, some of the jets veer southward and the average flow develops a southward component below a line between 40 ºN, 35 ºW and 45 ºN, 8 ºW (Reverdin at al., 2003). Given the spatial shifting and temporary nature of the jets, weak currents, meandering regions and mesoscale eddies, it is difficult to make a definitely picture of the area.

To the south, the AC can be seen as a narrow (50-100 km) jet-like eastward current centered around 34 ºN reaching the Gulf of Cadiz. The AC is present throughout the year and meanders all along its path, which leads to the formation of mesoscale eddies (100–200 km) and recirculation patterns on both sides of the jet (Alves et al., 2002). Associated to the main jet there is a strong termohaline front where two bodies of water converge. Fresher and colder northern waters masses are found to the north of the front, while saltier and warmer waters originating from the center of the Subtropical

Gyre (Sargasso Sea) are located on the southern side (Gould, 1985). The Azores islands are not in the direct eastward path of the main jet, but are affected by the recirculation patterns and eddies originated from the meandering (e.g. Alves et al., 2002). Due to convergent southward and northward flows from the NAC and AC, respectively, strong thermal gradients are typical of the region (Lafon et al., 2004).

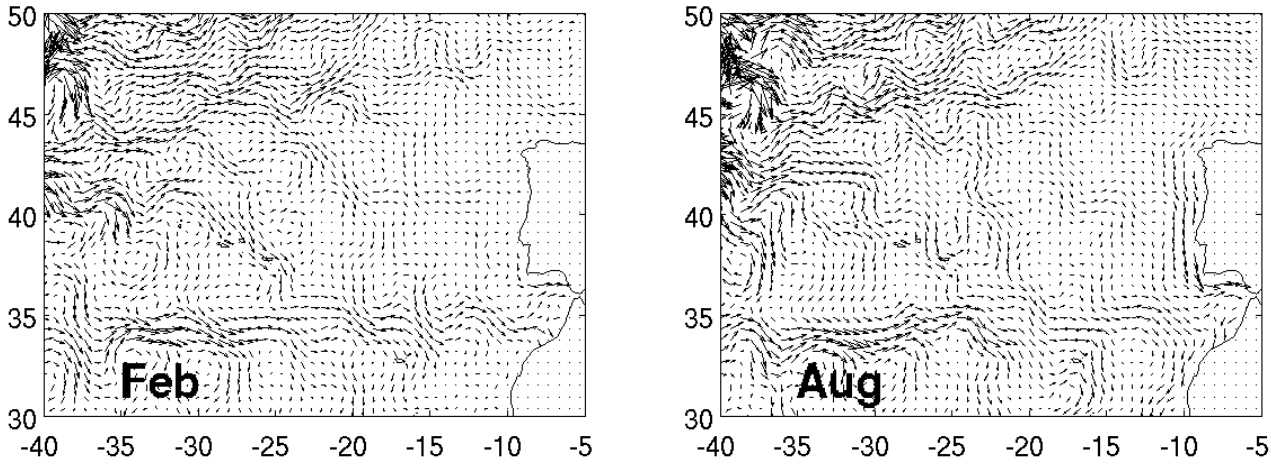

Figure 1-4 Average mean circulation in February and August derived from satellite altimetry weekly data between 1993 and 2009 (AVISO; CLS, 2009). Smoothed using 1º window moving average.

The seasonal climatological patterns of ocean currents derived from satellite altimetry weekly data between 1993 and 2009 are shown in Figure 1-4. Regarding the main circulation patterns, there are no substantial changes throughout the year. It should be noted that the satellite-derived velocities shown in Figure 1-4, only refer to the geostrophic currents, which are more evident at deeper waters. At the surface, increased winds during winter drag the surface water (Ekman currents) and produce stronger surface currents than in summer.

1.4.3. Temperature and salinity

The summer (July-September) climatological field of temperature and salinity at 200-300 m is shown in Figure 1-5. Data was obtained from the WOA05 climatology (Locarnini et al., 2006; Antonov et al., 2006). The spatial patterns of temperature and salinity show the same patterns of the average circulation. It can be seen the Gulf Stream dividing into the AC and NAC at ~50 ºW. The

tendency of waters to move southward in the Azores region, is seen by northwest-southeast orientation of the isolines. Latitudinal and longitudinal gradients can be observed throughout the Azores region. Seasonally, the patterns observed in Figure 1-5 do not change substantially, except if winter mixing reaches 200-300 m.

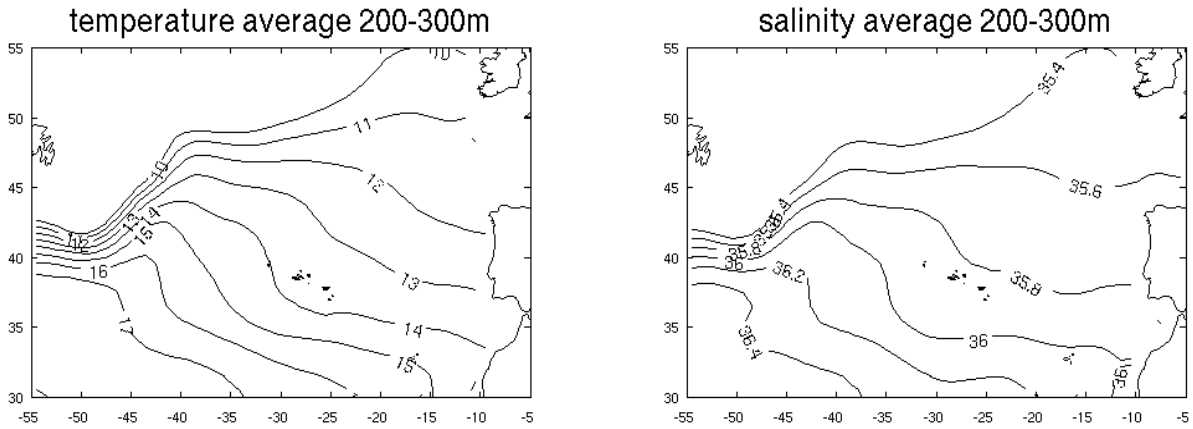

Figure 1-5 Climatological mean temperature (ºC) and salinity (psu) at 200-300 m during summer (data from WOA05).

To illustrate seasonal variability it is shown a section of temperature at 20.5 ºN (Figure 1-6). Salinity patterns (not shown) match closely the ones in temperature and deeper waters show the same features independently of the season. The major feature in Figure 1-6 is the depressed isolines between 20-35 ºN. These are the result of large-scale wind patterns that drive an anticyclonic circulation in the subtropical gyre, characterized by a depressed thicker thermocline. Conversely, subpolar gyres are characterized by a cyclonic circulation with a raised thermocline. The changes in temperature around 35 ºN are associated to the subtropical front. The seasonal changes are mainly at the surface where the atmosphere cools and warms the surface layer, dictating the depth of the mixed layer. In summer (August), weak winds, increased air temperature and solar irradiation, lead to an increase in surface temperature and to the establishment of a thermal stratified layer, the seasonal thermocline, resulting in a shallow mixed layer (~30m). During winter (February), surface waters are cooled and convective overturing deepens the mixed layer depth. From 30 ºN to 40 ºN the mixed layer reaches 100-150 m, while to the north of 40 ºN it can reach 200-400 m.

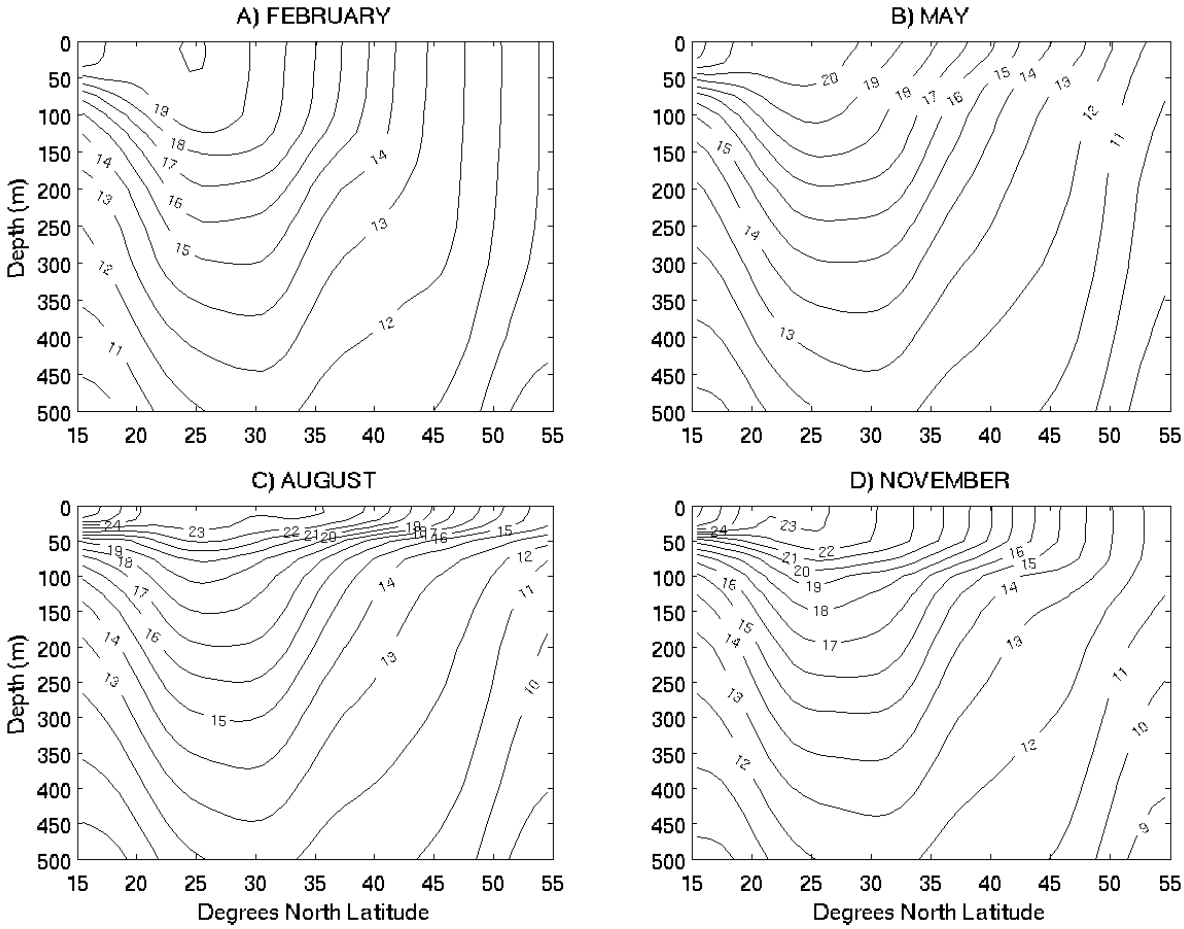

Figure 1-6 Climatological sections of temperature (ºC) at 20.5 ºN (WOA05) in February, May, August and September.

The coupling of the subsurface temperature field, winter mixing and summer thermal stratification, result in the fields of sea surface temperature (SST) shown in Figure 1-7. The SST monthly climatology was derived from the NOAA AVHRR OI SST monthly products (Reynolds et al., 2002). The northward propagation of the isotherms between February and August are a result of the establishment of thermal stratification in spring and summer. The retreat of isotherms between August and February are associated to winter mixing. The reason why the sea surface temperature isotherms during winter, do not show the pronounced northwest-southeast orientation of the waters at 200-300m (Figure 1-5) is a result of deeper winter mixing in the western basin at the Azores latitudes.

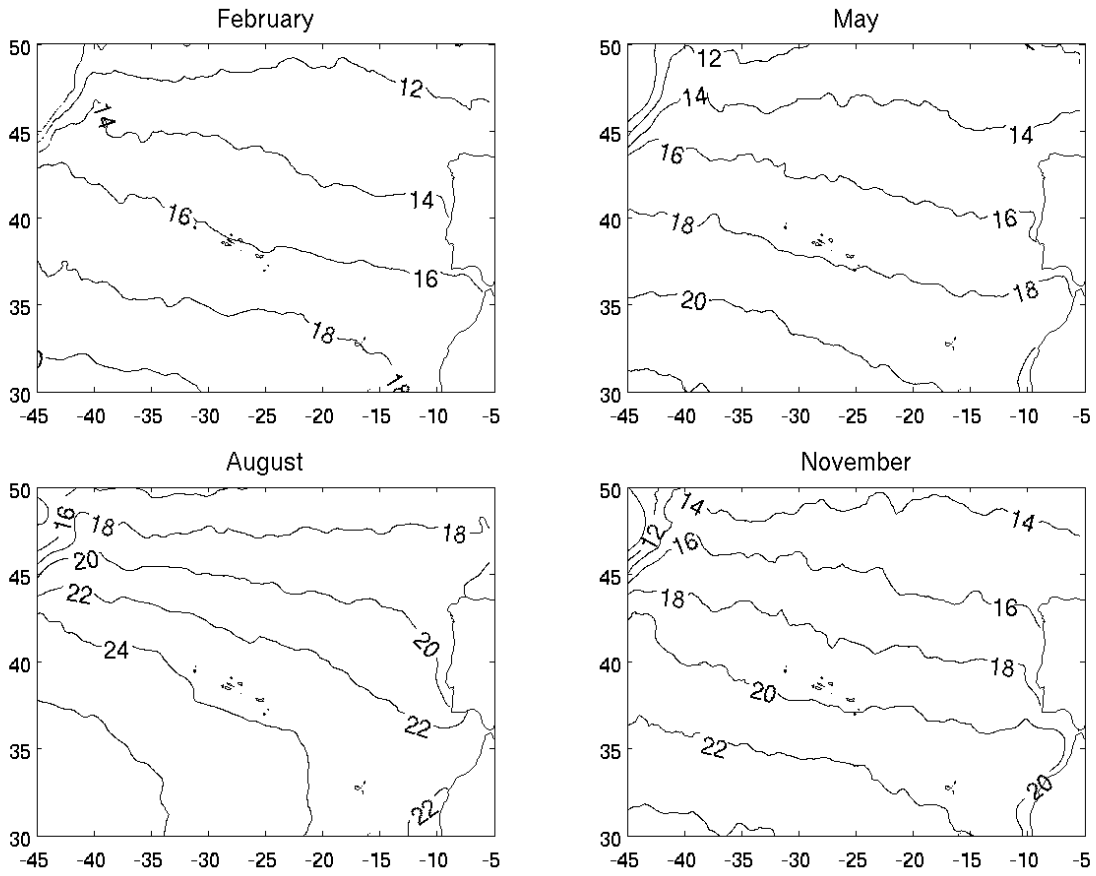

Figure 1-7 Climatological maps of sea surface temperature (ºC) in February, May, August and September derived from the NOAA AVHRR OI SST monthly product between 1998 and 2007 (Reynolds et al., 2002).

1.4.4. Mixed layer depth

The oceanic mixed layer is the layer between the ocean surface and a depth usually ranging between a few to several hundred meters, where both temperature and salinity are constant. This mixed surface layer is generated by waves, winds and surface cooling. The mixing generated by waves is restricted to the first few meters of the surface. The process of wind mixing occurs by vertical changes in the horizontal velocity. When winds are stronger, surface waters are dragged horizontally and the lower layers, which are in rest, are obligated to start moving. Vertical changes in the horizontal velocities, creates small instabilities which mix the water column. The depth of wind-induced turbulence is still a matter of debate, with some authors stating that wind induced mixing is confined to the upper 50 m (e.g. Backaus et al, 2003). The third process and probably the most important is convection or convective overturning. This occurs when surface waters increase their density, through cooling or increased salinity. When surface waters become more dense than

waters immediately below, they sink and mix with deeper waters, deepening the mixed layer. Surface cooling during winter is associated to a net heat loss to the atmosphere, as a result of reduced incoming solar radiation, long-wave heat loss, latent heat loss due to evaporation (dependent on wind speed and humidity) and sensible heat loss (dependent on the air-sea temperature difference). Surface salinity can increase if evaporation is larger than precipitation, but the effect of salinity in density is weaker than the one of temperature. The passage of individual weather systems, or midlatitude depressions, promotes convection due to increased cloudiness and wind speed, and reduced air temperatures. Storms typically travel from SW to NE in a band between the west coast of northeast America and the British islands. This results that storms are particularly harsh in the western basin of the Northeast Atlantic at the latitude of the Azores Archipelago. In general, storms are restricted to those periods characterized by well-defined and deep depressions, i.e. mostly during winter and spring months. The storm track can be seen in Figure 1-8 during February, which shows the climatology of wind speed from high resolution satellite maps (QuickSCAT).

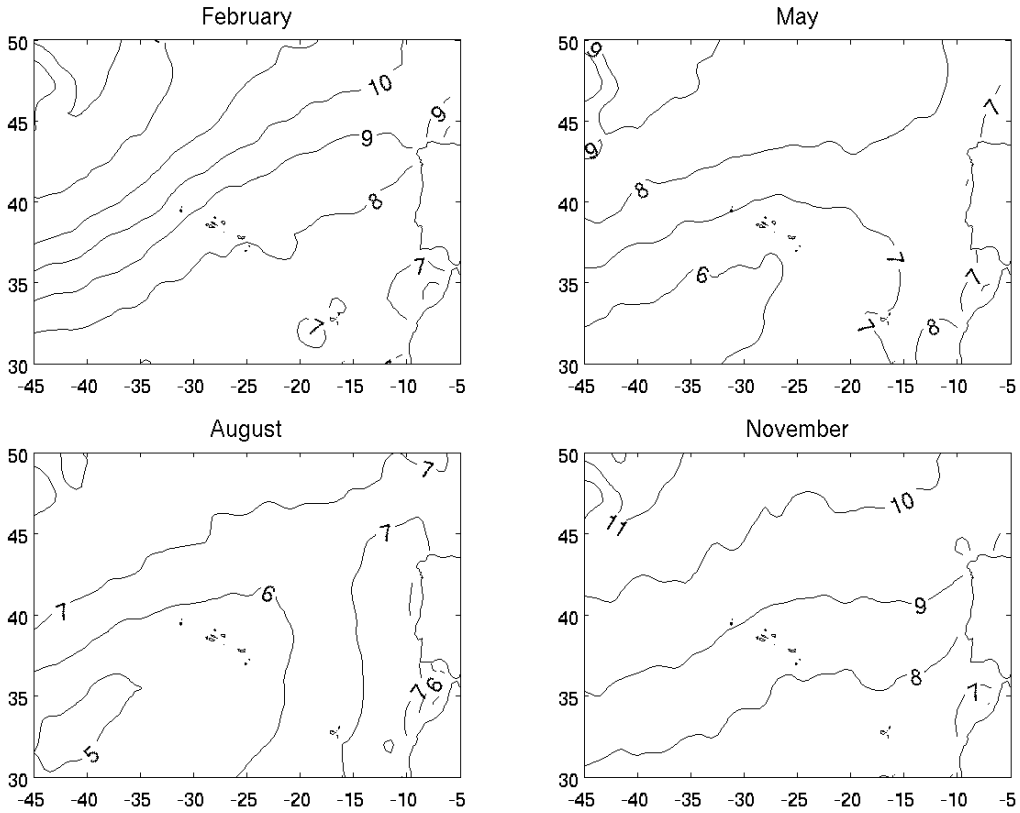

Figure 1-8 Climatology of wind speed in February, May, August and September derived from high resolution satellite maps (QuickSCAT)

Despite the complexity of processes regulating the mixed layer depth (MLD), the following seasonal changes can be generalized. During spring and summer, stronger solar radiation and weaker winds, warm the surface of the ocean which creates a shallow thermally stratified surface layer, the seasonal thermocline. As summer progresses, the surface layer gets progressively warmer, which increases stratification and act as a barrier between deeper and surface waters, like a cap in the ocean. By the end of summer, the seasonal thermocline is completely established and the MLD is around 30 m. In autumn and winter, weaker solar radiation and stronger winds, start eroding the seasonal thermocline and MLD gets progressively deeper, reaching in some regions more than 400 m. In spring, re-stratification starts the cycle once again. The seasonal changes in MLD are shown in Figure 1-9 by the MLD climatology (de Boyer Montégut et al., 2004) and in Figure 1-10 exemplified by the annual changes of an ARGO profile.

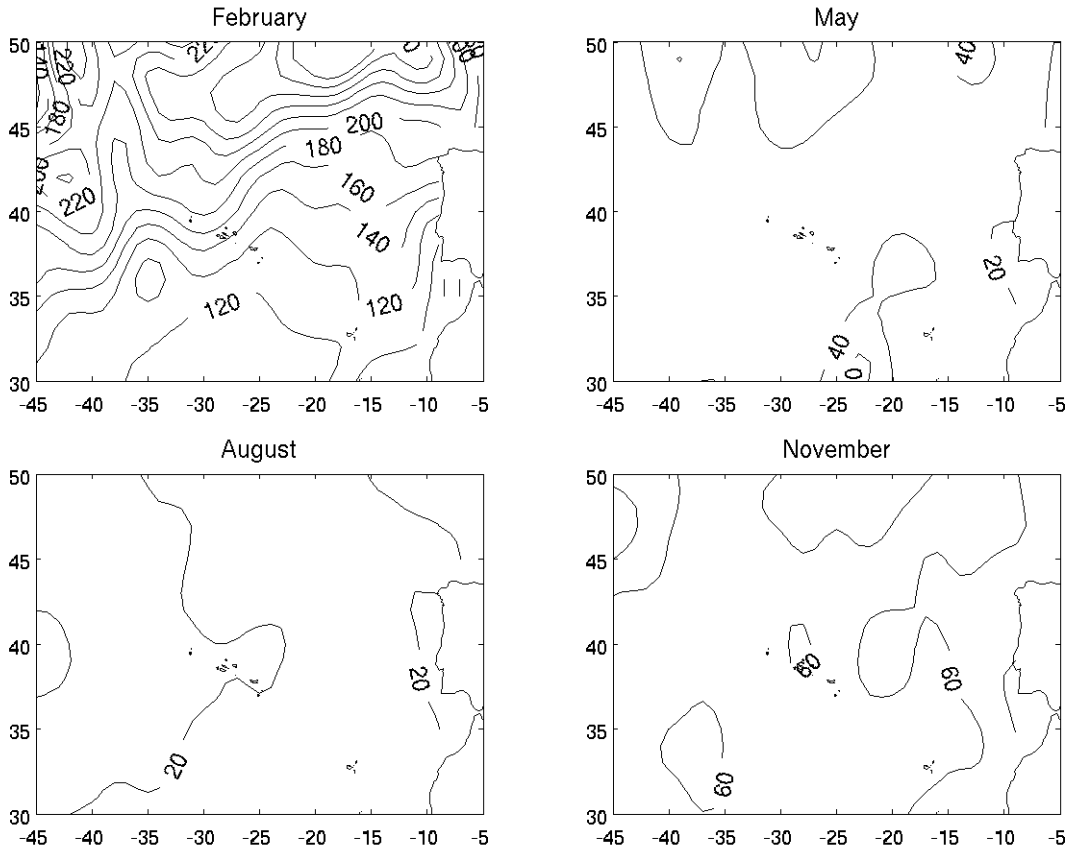

Figure 1-9 Climatological maps of MLD (m) in February, May, August and September from the climatology of de Boyer Montégut et al. (2004) .

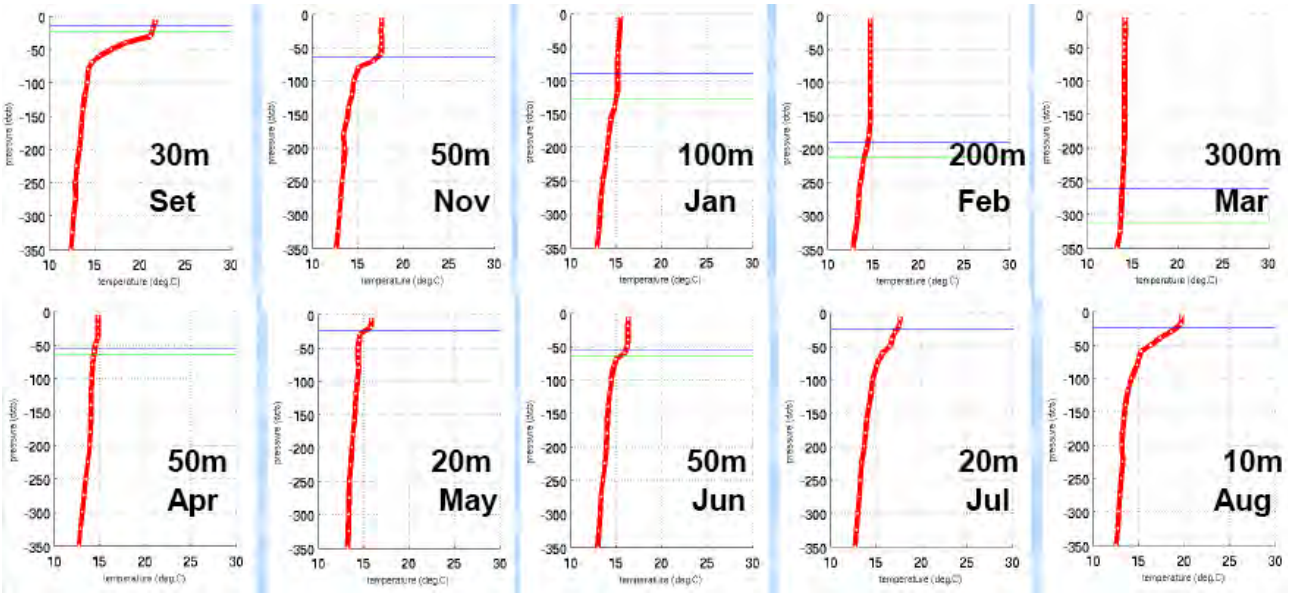

Figure 1-10 Example of the seasonal evolution of the MLD in an ARGO profile.

The period of stratification in spring, is a subject of great debate as a result of its influence on the annual cycle of phytoplankton growth as it is described in the next section. Following the winter period of maximum convection, which produces deep mixed layers, there is a period when the daily average heat flux across the air-sea interface tends to zero. During this period, there is limited convection and the water column is neutrally stable (i.e. with constant density) from the surface to the depth of winter convective mixing. Apart from nocturnal periods of convective mixing, the only other source of energy for deep vertical mixing during this transitional period is the wind, which is much more effective in a neutral stable water column. The depth of wind mixing for the neutrally stable water column is where some authors diverge. Townsend et al (1992) used three Ekman layers which at 42 ºN, given a wind of 54 km/h, would mix 80 m. On the other hand, Backhaus et al (2003) states that any wind induced mixing on a rotating earth is confined to the Ekman layer which, in midlatitudes, has a typical thickness of approximately 50 m. Backaus et al (2003) argues that convection, in contrast to vertical turbulent mixing (caused by winds, surface waves, tides), is the only turbulent process which can account for a significant vertical transport. Taylor and Ferrari (2011) also did not account for wind mixing and suggest that in the transitional period of zero net heat flux, there is a shutdown of wintertime convection, leading to stable, but mixed layers. Another mechanism that can stratify the water column before the heating-induced stratification, is lateral advection near fronts and eddies with large horizontal density contrasts (Mahadevan et al., 2012).

After spring, vertical density stratification exerts a fundamental control on mixing depth, with strong stratification suppressing turbulence and reducing the depth of mixing. The seasonal changes in MLD affect biological productivity by controlling both the supply of nutrients to the upper well-illuminate layer and the light exposure of phytoplankton.

1.4.5. Chlorophyll-a and phytoplankton

Marine life is dependent on the availability of phytoplankton. These are microscopic water plants that form the basis of the food chain in ocean waters. Just like terrestrial plants, they grow and multiply via photosynthesis. Chlorophyll-a is one of the most important pigments of phytoplankton involved in photosynthesis. Traditionally, chlorophyll-a concentration is a proxy for phytoplankton biomass. Despite their microscopic size, phytoplankton contributes to nearly all primary production in the ocean and about half of global primary production. They directly serve has food for zooplankton and small fishes. Indirectly they control the availability of food for higher trophic levels such as large fishes and marine mammals. Moreover, through the process of photosynthesis, they play a major role in the global carbon cycle, by regulating nearly half of the atmospheric oxygen and carbon dioxide. Phytoplankton changes are an undoubted important factor controlling marine ecosystems, fishing resources and global climate. It is arguably to say that without phytoplankton there would be no life in the ocean.

The abundance and distribution of phytoplankton biomass in the ocean is largely controlled by physical forcing. To grow and multiply through the process of photosynthesis phytoplankton needs light, nutrients and carbon dioxide. Because carbon dioxide exists everywhere in the ocean, the other two requirements have to be met at the same time: enough light and nutrients. In the ocean, light is only available in the first meters (~100 m) and nutrients are mostly found in deeper waters where sinking particles decompose. The nutrients are thus unavailable for phytoplankton growth unless some physical mechanism brings the nutrients back to the surface. Ultimately, it is the physical regime that determines the availability of nutrients and consequently the large-scale distribution of phytoplankton biomass which is thought to be mainly a result of nutrient limitation (e.g. Falkowski et al., 1992; Marañon et al., 2000).

In the North Atlantic, away from continental margins, a major mechanisms that determines the supply of nutrients to the surface is the mixed layer depth. The deepening of the mixed layer during winter provides the annual supply of nutrients to phytoplankton growth (e.g. Williams et al, 2000).

An additional factor, is also the sub-surface nutrient field or nutricline, because it determines the amount of nutrients a given mixed layer can supply (e.g. Yentsch, 1989). These two factors together, mixed layer depth and nutricline, control much of the available nutrients at the surface and therefore large-scale distribution of phytoplankton biomass. Other processes that influence nutrient availability in the open ocean include mesoscale and submesoscale features, airborne dust deposition, horizontal transport from the sides and regeneration of nutrients. The major nutrients needed for phytoplankton growth are the macronutrients (nitrate, phosphate and silicate), although in some areas (e.g. Southern oceans) growth is limited by the availability of the micronutrient iron. In the North Atlantic nitrate concentration is typically used as an index of nutrient availability (e.g. Williams et al., 2000; Pelegri et al., 2006).

In regards to seasonal variability of phytoplankton, the well-known subpolar and subtropical regimes explain much of the observed changes. In the subpolar regime, Sverdrup (1953) developed the classical description of the conditions necessary for phytoplankton bloom initiation. Deep mixed layers and low sun angle during winter reduce the mean light available to phytoplankton to a level below that required for growth. Although nutrient concentrations are uniformly high throughout the water column, the deep mixed layer ensures that phytoplankton are only in the sunlit surface layers for a short period of time before being mixed down into deeper, darker water. As spring approaches, the combined effects of longer, warmer days and reduced wind speeds result in the mixed layer swallowing beyond a ‘‘critical depth’’ where the average light intensity is such that phytoplankton growth exceeds losses, and the spring bloom begins. This shallow mixed layer traps the phytoplankton and the nutrients they require for growth, in the sunlit upper water column. Under these conditions phytoplankton grows very quickly, rapidly diminishing the stock of nutrients in the surface layer. Alternative hypotheses for the initiation of spring blooms do not require a mixed layer shoaling, such has when the mixed layer turbulence decreases, allowing phytoplankton to grow within a deep, but weakly mixed layer (Townsend et al., 1992; Taylor and Ferrari , 2011) or the “dilution-recoupling hypothesis” (Behrenfeld, 2010). Recently, Mahadevan et al (2012) proposed a mechanism that involves the shoaling of the mixed layer depth due to the transport of different water masses in a horizontal direction. In the subtropical regime, the “critical depth” model does not apply because the MLD is never deeper than the well-lit layer. Relatively shallow mixed layers and high irradiance year-round result in surface nutrient limitation. In these regions, the bloom may actually commence in fall or winter as the mixed layer deepens (Dutkiewicz et al., 2001; Siegel et al., 2002).

In the Azores little is known about the mechanisms responsible for phytoplankton variability. In a nearby region, to the east of the Azores Archipelago, Levy et al (2005) recently defined a new regime, located between the subpolar seasonally light-limited and the subtropical nutrient-limited regimes: the midlatitude (or transitional) regime where the bloom may have either subpolar or subtropical characteristics. The midlatitude regime is characterized by a single broad bloom weaker than the subpolar spring bloom and stronger than the subtropical fall bloom, which starts in fall as an entrainment bloom and peaks in spring as a restratification bloom. This specific regime is found between 35 ºN and 40 ºN (±2) in the Northeast Atlantic. It corresponds to winter MLDs between Ze (the depth of the euphotic layer) and 2*Ze, i.e., it lays between the region where the winter MLD is greater than Sverdrup's critical depth (subpolar regime) and the region where the mixing is never deeper than the well-lit layer (subtropical regime).

CHAPTER 2: DATA AND METHODS

2.1. Introduction

In this chapter it is described the data used in Chapter 3 and Chapter 4. The variables of interest were: temperature, salinity, ocean currents, wind, mixed layer depth, chlorophyll-a concentration, nitrate concentration and total heat air-sea flux. These variables were obtained from several satellite, in-situ and model datasets. All datasets are freely available for scientific use and were personally downloaded from the Internet. All data processing and analysis was made using MATLAB software and a vast collection of scripts specifically developed for this work. The datasets are described in three sections: satellite, in-situ and models.

2.2. Satellite data

2.2.1. SeaWiFS and MODIS AQUA chlorophyll-a concentration

In this study, the variability of chlorophyll-a concentration was investigated using satellite-derived ocean color data. Satellite-based ocean color instruments measure the spectral radiant flux emanating upward from the top of the Earth's atmosphere at discrete visible and near-infrared wavelengths. Estimates of water-leaving radiances (i.e. ocean color) are than retrieved through the application of an atmospheric correction algorithm to the top-of-atmosphere radiances (e.g. Gordon and Wang, 1994). From ocean color data, is than possible to retrieve information about aquatic coloring agents via the application of bio-optical algorithms (O'Reilly et al., 1998). The most common derived parameter is the concentration of the phytoplankton pigment chlorophyll-a. This was first demonstrated in 1979 by the proof-of-concept Coastal Zone Color Scanner (CZCS). Since 1997, after a gap of nearly 10 years without any ocean color satellite instrument, a number of advanced sensors have been launched. Based on the quality and distribution of their end-products some sensors stand out: the NASA SeaWiFS (Sea-viewing Wide Field-of-view Sensor), the NASA MODIS-AQUA (Moderate Resolution Imaging Spectroradiometer) and the ESA MERIS (Medium Resolution Imaging Spectrometer). Together, these three sensors confirmed a new era for biological oceanography by providing uninterrupted and regular worldwide glimpses of the temporal changes and spatial distributions of phytoplankton biomass. The satellites that carry the sensors have a sun synchronous (i.e. passes in a given region at the same local time every day), near polar orbit at ~700 km altitude and the sensors image the entire Earth every 1 to 2 days.

In this work it was used the NASA weekly images of chlorophyll-a concentration from the SeaWiFS (1997-2010) and MODIS AQUA (2002-2011) sensors. All data was downloaded from http://oceancolor.gsfc.nasa.gov. The product used was “Level 3 standard mapped image (SMI) Weekly Chlorophyll-a Concentration”. The SeaWiFS dataset has a spatial resolution of ~9 km, while the MODIS AQUA as a spatial resolution of ~4 km. The reprocessing versions of the SeaWiFS and MODIS AQUA were R2010 and R2012, respectively. Only data between 1997-2007 was used from the SeaWiFS dataset, since from 2008 onwards the instrument starts having technical problems resulting in consecutive weeks without data. The datasets of SeaWiFS and MODIS AQUA were converted, to suitable MATLAB files for further analysis. Following the procedure of Levy et al (2005), all pixels with values greater than 5μg/L were flagged, in result of being considered unrealistic values. All images were visually inspected and no artifacts were found.

2.2.2. AVISO ocean geostrophic currents

Geostrophic currents are driven by horizontal changes in the pressure field and by the Earth’s rotation. Ocean geostrophic currents do not account for the surface flow induced by wind friction (Ekman currents), therefore their influence is most noticeable in deeper waters. In the northern hemisphere they flow in a cyclonic (anticyclonic) manner around regions of lower (higher) sea surface height. Altimeters aboard satellites measure the sea surface height differences (a few centimeters), from which ocean geostrophic currents can be estimated. The geostrophic currents derived from satellite altimetry were produced by Ssalto/Duacs at Collecte Localization Satellites (CLS), the Centre National d’Etudes Spatiales (CNES) and the French Research Institute for Exploration of the Sea (IFREMER). This product is generated using satellite altimetry data obtained by the Ocean Topography Experiment (TOPEX)/Poseidon, Jason-1, European Remote Sensing Satellite-1 (ERS- 1) and -2 (ERS-2), and Environmental Satellite (Envisat), satellite missions (CLS, 2009). Data is freely available and distributed online at http://www.aviso.oceanobs.com/. All products of geostrophic currents derived from the Delayed Time Maps of Absolute Dynamic Topography (DT-MADT), between 1992-2011, were downloaded. This product is generated every 7 days at a 1/3 ° resolution. The original data was converted, without any masking, to suitable MATLAB files for further analysis. For a complementary analysis, weekly maps of Eddy Kinetic Energy (EKE) were computed using the formula: $EKE=1/2x(U^2+V^2)$. Where U and V are the zonal and meridian components of the geostrophic currents, respectively. All images were visually inspected and no artifacts were found.

2.2.3. OSCAR ocean surface currents

For the analysis of the total currents at the surface it was used the Ocean Surface Current Analysis - Real Time (OSCAR) (http://www.oscar.noaa.gov). This dataset provides operational ocean surface velocity fields from satellite altimeter and vector wind data. The data are available at 5 day intervals with 1 ° spatial resolution. The method combines altimetric geostrophic velocities (described in the previous section) and Ekman drift computed from remotely sensed wind products (SSM/I, NSCAT, QuikSCAT) (Lagerloef et al., 1999). Data is freely available in the project website and the entire dataset between 1993 and 2011 was downloaded. The original data was converted, without any masking, to suitable MATLAB files for further analysis. All images were visually inspected and no artifacts were found.

2.2.4. NOAA AVHRR Optimum Interpolation Sea Surface Temperature

The NOAA/NCEP Reynolds Optimally Interpolated (OI) Sea Surface Temperature (SST) monthly product consists of aggregate global sea surface temperature fields on a 1 degree by 1 degree grid over a month time interval. The OI analysis uses both in-situ SSTs from ships and buoys, and satellite derived SSTs from the NOAA Advanced Very High Resolution Radiometer (AVHRR). Monthly SST fields are derived by a linear interpolation of the weekly optimum interpolation fields to daily fields then averaging the daily values over a month (Reynolds et al., 2002). The version 2 of the dataset (1981-present) was downloaded from http://www.emc.ncep.noaa.gov/research/cmb/sst_analysis/. The original data was converted, without any masking, to suitable MATLAB files for further analysis. All images were visually inspected and no artifacts were found.

2.3. In-Situ data

2.3.1. GTSPP temperature and salinity profiles

The Global Temperature-Salinity Profile Program (GTSPP) (Sun et al., 2010), is a cooperative international project that seeks to develop and maintain a global ocean Temperature-Salinity resource with up-to-date and high quality data. The Global Climate Observing System (GCOS) recognizes the GTSPP as one of the international operational activities that provide essential, sub-surface climate variables of temperature and salinity profile data. This includes observations

collected using water samplers, continuous profiling instruments such as CTDs, thermistor chain data and observations acquired using thermosalinographs. The dataset also includes the drifting profiling floats, known as the Argo Ocean Profiling Network (http://www.argo.ucsd.edu/). Argo is a global array of 3,000 free-drifting profiling floats that measures the temperature and salinity of the upper 2000 m of the ocean. Argo floaters drift with currents at depth and typically every 10 days rise to the surface while measuring temperature and salinity. The data is than transmitted to satellites, which also determine the position of the floats. The quality control procedures consist in checking the data for several types of errors and remove duplicate copies of the same observation.

The “best copy dataset” represents the higher quality data and was downloaded from http://www.nodc.noaa.gov/GTSPP/access_data/gtspp-bc.html.The original data was converted to suitable MATLAB files for further analysis. All profiles were visually inspected for the Azores Archipelago (36-41 °N, 23-33 °W) and only a reduced number of profiles were discarded due to suspicious data. From 1990 to 2011 there were 2995 profiles of temperature. Before 2002 the profiles of salinity were rare. This is due to the fact that ARGO floaters contribute to a greater number of profiles in the GTSPP dataset and only after 2002 these floaters started to measure salinity. The number of temperature profiles available per year in the Azores Archipelago region is shown in Figure 1. The mixed layer depth (MLD) was computed for each profile using the threshold method, for which the MLD is the depth at which temperature or potential density changes by a given threshold value relative to the one at a near-surface reference depth. Since the objective in computing MLD was to have data since 1998 to 2011, it was chosen to calculate MLD on the basis of temperature alone, since the number of salinity profiles before 2002 is very low. It was chosen to use a threshold of 0.3 °C, which means the MLD was defined as the depth temperature changes 0.3 °C from the surface value. This is a more conservative method than other studies that used 0.5 °C (e.g. Spall et al., 2000; Foltz et al., 2003). After visualization it was decided to not use the first value of the profile, since some first values were suspicious. All profiles were visualized and the 0.3 °C threshold typically provides a good estimate of the isothermal layer depth. It is acknowledge that this method does not represents an exact estimate of a layer of constant density, but it will hereafter be referred as the mixed layer depth (MLD). A larger dataset of profiles in the region between 25-60 ºN and 0-50 ºW, was used to visualize the spatial distribution of mixed layer depth and temperature in the entire region of the Northeast Atlantic. In this larger dataset it was not visually inspected each profile.

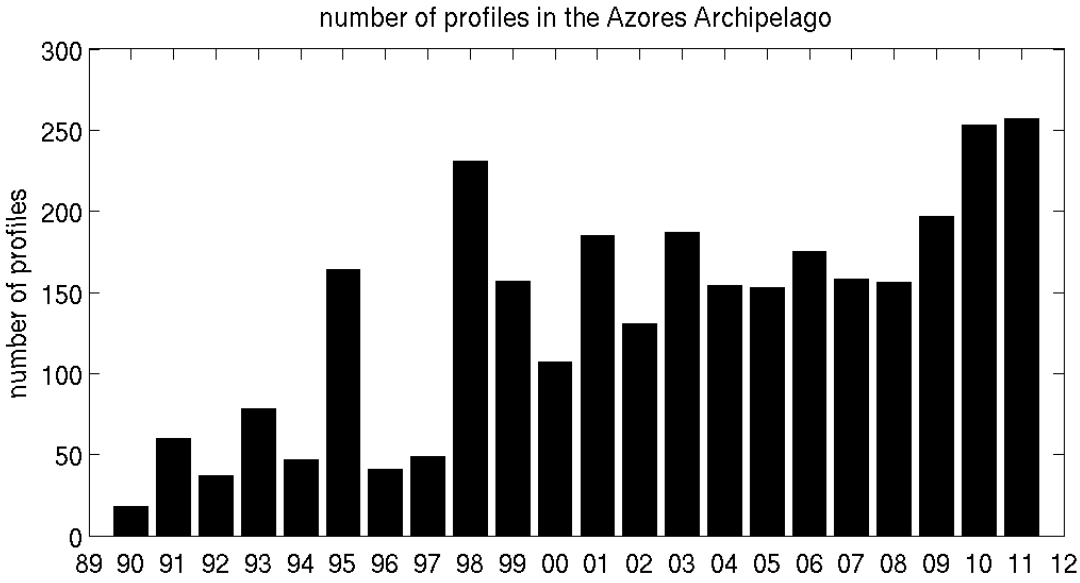

Figure 2-1 Number of temperature profiles from the GTSPP dataset in the Azores Archipelago (36-41 °N, 23-33 °W).

2.3.2. AMT nutrient

The Atlantic Meridional Transect (AMT) is a multi-disciplinary programme operating under the Oceans 2025 programme as a Sustained Observatory. It consists of an annual cruise in October/November from the UK to Punta Arenas in Chile. The transect repeated each year spans a distance of almost 13,500 km through many different ocean provinces. The aim of the AMT project is to study the factors determining the ecological and biogeochemical variability in the planktonic ecosystems of the tropical and temperate Atlantic Ocean and its links to atmospheric processes. The data is available at the British Oceanographic Data Centre (BODC) which is the NERC designated data center responsible for the management of data sets originating from the AMT programme. After signing an agreement all data is available under the data policy of AMT (http://www.bodc.ac.uk/projects/uk/amt/data_policy/). In this work it was used the nitrate concentration data from the cruises AMT 20 (2010), AMT 21 (2011) and AMT 21 (2012).

2.3.3. WOA 2005 climatology

World Ocean Atlas 2005 (WOA05) is a set of objectively analyzed (1° grid) climatological fields of in situ temperature, salinity, dissolved oxygen, apparent oxygen utilization, percent oxygen

saturation, phosphate, silicate, and nitrate at standard depth levels for annual, seasonal, and monthly compositing periods for the World Ocean. The observed oceanographic profile data is interpolated to standard depth levels on both 1° and 5° grids. The data is freely available at http://www.nodc.noaa.gov/OC5/WOA05/woa05data.html. In this work it was used the monthly climatologies of temperature (Locarnini et al., 2006), salinity (Antonov et al., 2006) and nutrients (Garcia et al., 2006) at 1 ° spatial resolution.

2.3.4. de Boyer Montegut et al (2007) mixed layer depth climatology

The dataset of de Boyer Montegut et al (2007), consists in 2 ° resolution global monthly climatology of the mixed layer depth (MLD) based on individual profiles. It differs from previous global climatologies based on temperature or density, since the criterion selected includes both variables. The MLD is defined as the depth at which the value of temperature or density changes by 0.2 °C or 0.03 Kg/m^3, respectively, from a near-surface value at 10 m depth. A validation of the temperature criterion on moored time series data shows that the method is successful at following the base of the mixed layer. The dataset was acquired at http://www.ifremer.fr/cerweb/deboyer/mld. The original data was converted, without any masking, to suitable MATLAB files for further analysis. The dataset was interpolated to the WOA05 climatology grid described above, to allow the analysis performed in Chapter 4.

2.4. Model data

2.4.1. MERCATOR GLORYS2V1 Global Ocean Physics Reanalysis

For the analysis of temperature and salinity changes in the Northeast Atlantic it was used the model outputs of the Mercator Ocean (Toulouse, France) GLORYS2V1 (1993-2009) global ocean reanalysis for the Global Ocean and Sea Ice Physics. The model provides monthly means of temperature, salinity, currents, sea surface height and sea ice parameters, at 1/4 degree horizontal resolution, with 75 vertical levels, forced by ERA-Interim atmospheric variables and covering the 1993-2009 time periods, with Data Assimilation of in-situ Temperature and Salinity profiles as well as satellite-derived Sea Level Anomalies and Sea Surface Temperature. The reanalysis is performed with NEMOv3.1 ocean model in configuration ORCA025_LIM. The ERA-Interim atmospheric surface forcing includes a large scale correction for the downward solar fluxes. The data assimilation technique is a multi-data and multivariate reduced order Kalman filter based on the

Singular Extended Evaluative Kalman (SEEK) filter formulation. The validation results show that the reanalysis has a good skill in estimating and reproducing the observed variability of the main oceanic variables. The identified flaws in relation to Northeast Atlantic region concern surface currents not being strong enough. A complete description of the model configuration, assimilation methods and validation, is provided in Ferry et al (2012).

The MERCATOR GLORYS2V1 reanalysis is part of MyOcean (http://www.myocean.eu/) project. The objective of the MyOcean project is to deliver and operate a rigorous and sustainable Ocean Monitoring and Forecasting system of the GMES Marine Service (OMF/GMS) to users of all marine applications. It delivers ocean state variables that are required to help meet the needs for information of those responsible for environmental and civil security policy making, assessment and implementation. The MERCATOR GLORYS2V1 global ocean reanalysis product is referenced in MyOcean as the product "GLOBAL_REANALYSIS_PHYS_001_009". All monthly fields of Temperature and Salinity, at all depths, from 1993-2009, covering the region of the North Atlantic, were downloaded from http://www.myocean.eu/. The files were converted, without any masking, to MATLAB formats suitable for further analysis. The mixed layer depth (MLD) was subsequently calculated as the depth where the temperature varied by 0.3 °C from the surface temperature. This method was chosen to be consistent with the MLD method used for the in-situ profiles and discussed in the previous section.

2.4.2. CMCC CGLORS Global Ocean Physics Reanalysis

For a complementary analysis of temperature and salinity changes in the Northeast Atlantic it was also used the CMCC (Bologna, IT) CGLORS reanalysis (1993-2010) for the Global Ocean and Sea Ice Physics. The model provides monthly means of temperature, salinity, currents, sea surface height and sea ice parameters, at 1/4 degree horizontal resolution, with 50 vertical levels, forced by ERA-Interim atmospheric variables and covering the 1993-2010 time periods, with Data Assimilation of in-situ temperature and salinity observations, as well satellite-derived sea-surface temperature and sea-ice concentration. The reanalysis is performed with the NEMOv3.2.1 ocean model in configuration ORCA025_LIM. The ERA-Interim atmospheric surface forcing includes a correction of the precipitation and radiative fluxes by means of climatological coefficients derived from space-borne observations. The data assimilation scheme is based on a three-dimensional variational (3DVAR) formulation. The reanalysis shows a good agreement with climatology and external observational datasets. The main problems in relation to Northeast Atlantic region were

found to be weaker currents than those observed. A complete description of the model configuration, assimilation methods and validation, is provided in Storto et al (2012).

The CMCC CGLORS reanalysis is part of MyOcean (http://www.myocean.eu/) project, which is described in the previous section. The CMCC CGLORS global ocean reanalysis is referenced as the product "GLOBAL_REANALYSIS_PHYS_001_011 ". The monthly fields of temperature, at all depth, from 1993-2009, covering the region of the North Atlantic, were downloaded from http://www.myocean.eu/. The files were converted, without any masking, to MATLAB formats suitable for further analysis. The CMCC CGLORS is only used in this work for comparison with the MERCATOR GLORYS2V1 temperature and to provide information of the 2009/2010 winter.

2.4.3. SODA, FNMOC and TOPS mixed layer depth datasets

For the analysis of modeled mixed layer depth (MLD), this work uses the approach, and the datasets, available at the “Ocean Productivity site“. In this website it is proposed a methodology to make a time series of MLD between 1998-2012, from different models. The method is based on comparisons between models and their temporal coverage. The discussion can be found at http://www.science.oregonstate.edu/ocean.productivity/tops.mld.html. The datasets are available at weekly and monthly basis. In this work it was used the weekly data, available at http://orca.science.oregonstate.edu/1080.by.2160.8day.hdf.mld.hycom.php. Following the method available in the website, from 1998 to 2004 it is provided the MLD product “SODA” at 0.5 ° resolution, derived from the Simple Ocean Data Assimilation (SODA) model. The SODA model assimilates temperature and salinity profiles from the World Ocean Atlas as well additional hydrography, sea surface temperature and altimeter sea level (Carton et al., 2000). In 2005, it is used the MLD product “TOPS” at 1 ° resolution, derived from the Fleet Numerical Meteorology and Oceanography Center (FNMOC) Navy Coupled Ocean Data Assimilation (NCODA) system (Cummings, 2005). NCODA assimilates altimeter and sea surface temperature satellite observations as well available in-situ vertical temperature and salinity profiles. From 2006 to 2011 it is used the MLD product “FNMOC” at 0.25 ° resolution, derived from the FNMOC high-resolution ocean analysis for GODAE, which also uses NCODA (Cummings, 2005). These three model datasets of MLD have different methods of calculating MLD. In the “SODA” and “FNMOC” datasets, MLD is calculated at the depth where density varies by 0.125 kg/m^3 over the value at ten meters (Monterey and Levitus, 1997). In the “TOPS” dataset, MLD is calculated at the depth where temperature varies by 0.5 °C of its surface value (Spall et al., 2000). Despite the different MLD methodologies, it is

considered in the “Ocean Productivity site” that in general, both methods compare well in the midlatitudes, but tend to fall apart in the high latitudes.

2.4.4. NCEP/NCAR Global Reanalysis wind and net heat flux

For the analysis of atmospheric forcing (wind and net heat flux) it was used data from NCEP/NCAR Reanalysis Project (Kalnay et al., 1996). The model assimilates data from land surface, ship, aircraft and satellite observations. The products are available at 6 hour intervals, since 1948 and going forward continuously. There are over 80 different variables, (including geopotential height, temperature, relative humidity, U and V wind components, etc.) in several different coordinate systems. The variables of interest for this study are wind and air-sea fluxes. All data is available at http://www.esrl.noaa.gov/psd/data/gridded/data.ncep.reanalysis.html.

Regarding wind it was acquired the daily product of "U-wind at 10 m" and "V-wind at 10 m", between 1990 and 2011. This product is available in a 192x94 Gaussian grid, which means grid points at longitudes are equally separated (1.8750 °), but at latitudes they vary (e.g. -1.9048 ° for ~20 °N and -1.9046 ° for ~70 °N). From this product was computed two other variables used in this study: wind mixing and wind stress curl. The energy transferred through the water column by the wind creates turbulence in the surface layers. A wind-mixing index in the upper layer is usually calculated as the cube of wind speed. This index was used as an indicator of turbulence in the surface layers (Patti et al., 2008). The wind stress curl expresses the rotation of a point in the wind stress field and can be used to estimate the divergence/convergence of Ekman currents. In the Northern Hemisphere, at midlatitudes the westerlies generate equatorward Ekman transport. Since the westerlies decrease towards the pole and equator, so does the equatorward transport. Meridional changes in Ekman transport in turn drive convergence (divergence) of the flow to the south (north) of the latitude where the wind is maximum. The changes in wind that drive these motions can be expressed in terms of the wind stress curl. Positive wind stress curl causes divergence in the Ekman layer and upward Ekman pumping, and negative wind stress curl causes convergence in the Ekman layer and downward Ekman pumping. To calculate the wind stress curl, the wind stress was first calculated for each wind component from the equation: $\tau=\rho air*Cd*W2$, where τ is wind stress (N/m2), ρair is air density (1.22 kg/m3), Cd is the wind-drag coefficient and W is wind speed (m/s). Cd was calculated following Smith (1988). The routine to calculate wind stress (“stresstc.m”) was obtained from the air_sea toolbox (http://woodshole.er.usgs.gov/operations/sea-mat). The curl was than estimated from the finite difference scheme used in MWF (2002).

To calculate net heat flux (Qnet) it was acquired the following daily products: "Net longwave radiation", "Net shortwave radiation", "Sensible heat net flux" and "Latent heat net flux". These products have the same spatial resolution of the wind. Following the method of Henson et al (2006) the net heat flux was calculated as the sum of all components, where a positive flux represents heat entering the ocean. The Qnet dataset was linearly interpolated onto a 0.5 ° resolution grid to provide equally distributed grid points in the Azores region.

CHAPTER 3: PATTERNS OF THE TEMPERATURE AND SALINITY INCREASE DURING THE LAST TWO DECADES IN THE NORTHEAST ATLANTIC, BETWEEN AZORES AND MAINLAND PORTUGAL

3.1. Introduction

Here a description is provided of the changes in temperature and salinity in the midlatitude Northeast Atlantic since 1990. Changes in currents and wind patterns are also investigated and discussed as possible mechanisms. The objective of this chapter is to develop an understanding of the physical changes of the Atlantic Ocean in the Azores region, prior to the analysis of phytoplankton variability of Chapter 4. Here a broad area is studied that corresponds to the midlatitude intergyre region of the Northeast Atlantic (35-50 ºN, 15-40 ºW). This area is bounded to the north and west by the North Atlantic Current (NAC), to the south by the Azores Current (AC) and to the east by the Western Iberian Upwelling System. Along 30 ºW the Mid-Atlantic Ridge (MAR) divides the region into western and eastern basins. The MAR rises up to 2000 m and presents a major barrier to the flow, constraining fluid to the east and west of it. Away from the boundaries of the region of interest, along which the core of the NAC and AC flow, the currents are mainly controlled by mesoscale activity and the NAC secondary branches.

The NAC branches are narrow jet-like features that separate from the main core of the NAC and meander eastward across the entire region. After crossing the MAR at deeper fracture zones, these features can turn northward in direction of the British Isles or southward towards Portugal and the Azores (Bower and Von Appen, 2008). Since the late 1990s, but more pronounced after 2000, an increase in salinity was found in the northeast Atlantic and associated with a large-scale shift in the NAC branches (e.g. Hatun et al 2005; Holliday et al., 2008; Häkkinen and Rhines, 2009; Häkkinen et al., 2011). From drifter trajectories, Häkkinen and Rhines (2009) shown that before 2000, the flow was mainly southeastward in the region and after 2001, there was a shift in the currents and the flow turned northeast towards the British Isles. These changes allowed warm and saline North Atlantic waters to penetrate into the central part of the subpolar gyre and northern latitudes. Changes in wind stress and its curl were suggested as possible mechanisms to the change in currents after 2001 (Häkkinen and Rhines , 2009; Häkkinen et al 2011a). The change in the surface circulation, which redirects part of the saline waters to NE instead of SE, would not need mixing with Mediterranean waters to explain the observed salinity increase in the subpolar gyre (Holliday 2003; Holliday et al; 2008). However, there is evidence that the Mediterranean waters also

penetrated more northward during these salty periods (Lozier and Stewart, 2008; Johnson and Gruber, 2007). Air-sea fluxes were shown to be relatively small and insufficient to explain the changes is salinity near the British Isles (Holliday 2003; Holliday et al; 2008).

The northward flow of warm, saline waters to the central part of the subpolar gyre occurs in a narrow region between the British islands and the subpolar front. Häkkinen and Rhines (2009) show that Gulf Stream waters, as indicated by surface drifters, can have a direct connection to this region and a likely explanation for the significantly higher inflow salinities since 2001. Modelling studies have shown that the transport of warm and saline waters to northern latitudes, through the narrow window near the British islands, is associated to changes in the subpolar gyre intensity and shape (Hatun et al., 2005). Simultaneous with the shift of circulation towards northeast, the subpolar gyre has contracted in the 1990's (Häkkinen and Rhines, 2004) and after 1998, the subpolar front near the British Isles moved westward and the warmer salty waters gradually invaded northern latitudes, with the largest intrusion of salty water in 2002–2004 (Reverdin et al., 2010). Häkkinen et al.'s (2011a) analysis of model results shows three periods (1960s, around 1980, and 2000s) with enhanced warm, saline waters reaching high latitudes, alternating with freshwater events originating at high latitudes. Wind stress curl variability provided a linkage to this subtropical/subpolar gyre exchange. When the wind stress curl climatological pattern is weaker than normal, the ocean response is such that the northward penetration of subtropical waters is enhanced. In this case both the subtropical and subpolar gyres weaken, the polar front moves westward, opening an enhanced northward access of the subtropical waters. The impact of wind stress curl in the gyres proposed by Häkkinen et al (2011a) is sketched here in Figure 3-1.

In the region between the Azores and the Iberian Peninsula, these decadal changes have been less documented when compared to northern latitudes. Nevertheless, Johnson and Gruber (2007) analyzed 4 hydrographic sections at 20 ºW in 1988, 1993, 1998, and 2003. In agreement with the studies at northern latitudes, these authors also observed an increasing influence of warmer, saltier subtropical waters within the permanent pycnocline. Nearly in-phase changes between the near surface and intermediate layers led the authors to suggest that, on decadal scales, surface changes are indicative of large advective changes associated with the ebbing and flowing of more subtropical water to the northern latitudes. In the following sections a description is put forward of how these patterns of temperature, salinity, currents and wind evolved in space and time around the Azores during the last two decades (i.e. between 1990-2010).

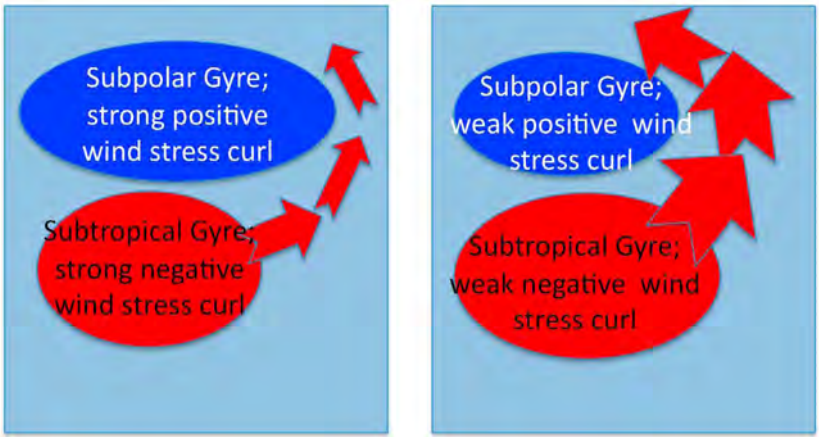

Figure 3-1 Variability of the wind stress curl climatological pattern and its impact on the gyres as proposed by Häkkinen et al (2011a) [author's sketch].

3.2. Temperature and salinity changes

Changes in temperature and salinity for the period 1993-2009 are described in 6 boxes in the Northeast Atlantic from the monthly fields of the model outputs from MERCATOR GLORYS2V1 global ocean reanalysis for the Global Ocean and Sea Ice Physics (Ferry et al., 2012). The time series of temperature and salinity are shown in Figure 3-2 and Figure 3-3, respectively. The 6 boxes are referred as: north-west box (46-51 ºN, 24-34 ºW), north-east box (46-51 ºN, 14-24 ºW), middle-west box (41-46 ºN, 27-37 ºW), middle-east box (41-46 ºN, 17-27 ºW), south-west box (36-41 ºN, 30-40 ºW) and south-east box (34-41 ºN, 20-30 ºW). The geographic location of the boxes is shown in Figure 3-4. Each point in the time series represents the annual averages from January to December at a given depth. Dashed lines show averages between 100-200m (referred to as surface waters) and solid lines represents averages between 400-500m (referred to as deep waters).

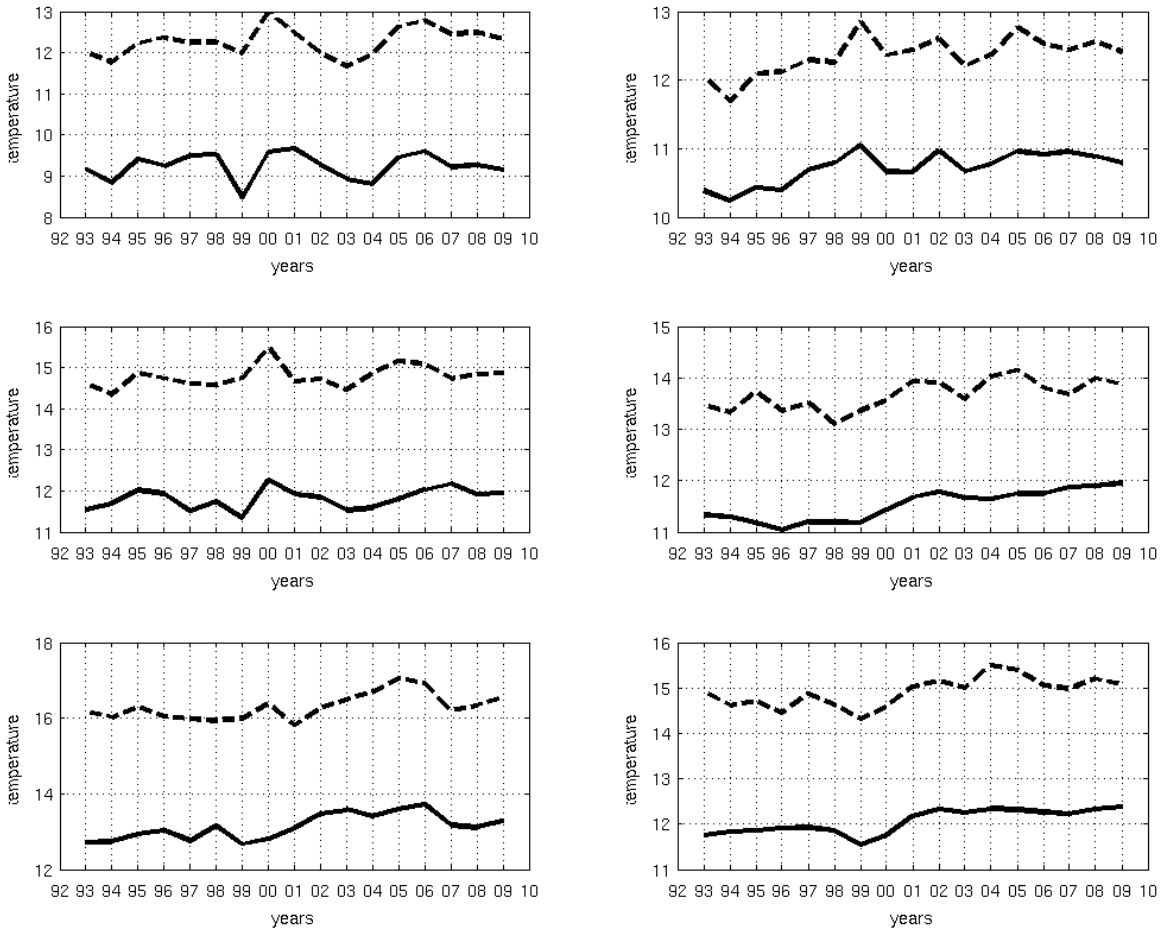

Figure 3-2 Annual averages of temperature (ºC) at 100-200 m (dashed line) and 400-500m (solid l ine), from MERCATOR monthly fields, at the: north-west box (46-51 ºN, 24-34 ºW; top left), north-east box (46-51 ºN, 14-24 ºW; top right), middle-west box (41-46 ºN, 27-37 ºW; middle left), middle-east box (41-46 ºN, 17-27 ºW; middle right), south-west box (36-41 ºN, 30-40 ºW; bottom left) and south-east box (36-41 ºN, 20-30 ºW; bottom right). See Figure 4 for geographic location of the boxes.

The major feature observed in Figure 3-2 is a warming trend in the southern and eastern boxes, both at surface and deep waters. Deep waters are characterized by a cold period between 1993-2000 and a warm period after 2001. Surface waters tend to follow this trend, although with higher variability and a peak in 2005 that is not observed in deeper waters. In the south-east box, the transition between the cold and warm periods in 2001 was marked by a slight decrease in 1999-2000, which is observed observed both at surface and deep waters. The middle-east box shows similar patterns of the south-east box, indicating similar water masses. The north-east box shows an earlier increase (around 1997), when compared to the other regions. The middle-west and north-west boxes do not

show any particular trend, with alternating periods of warming and cooling. The warming periods in these two regions are around 1995, 2000 and 2005.

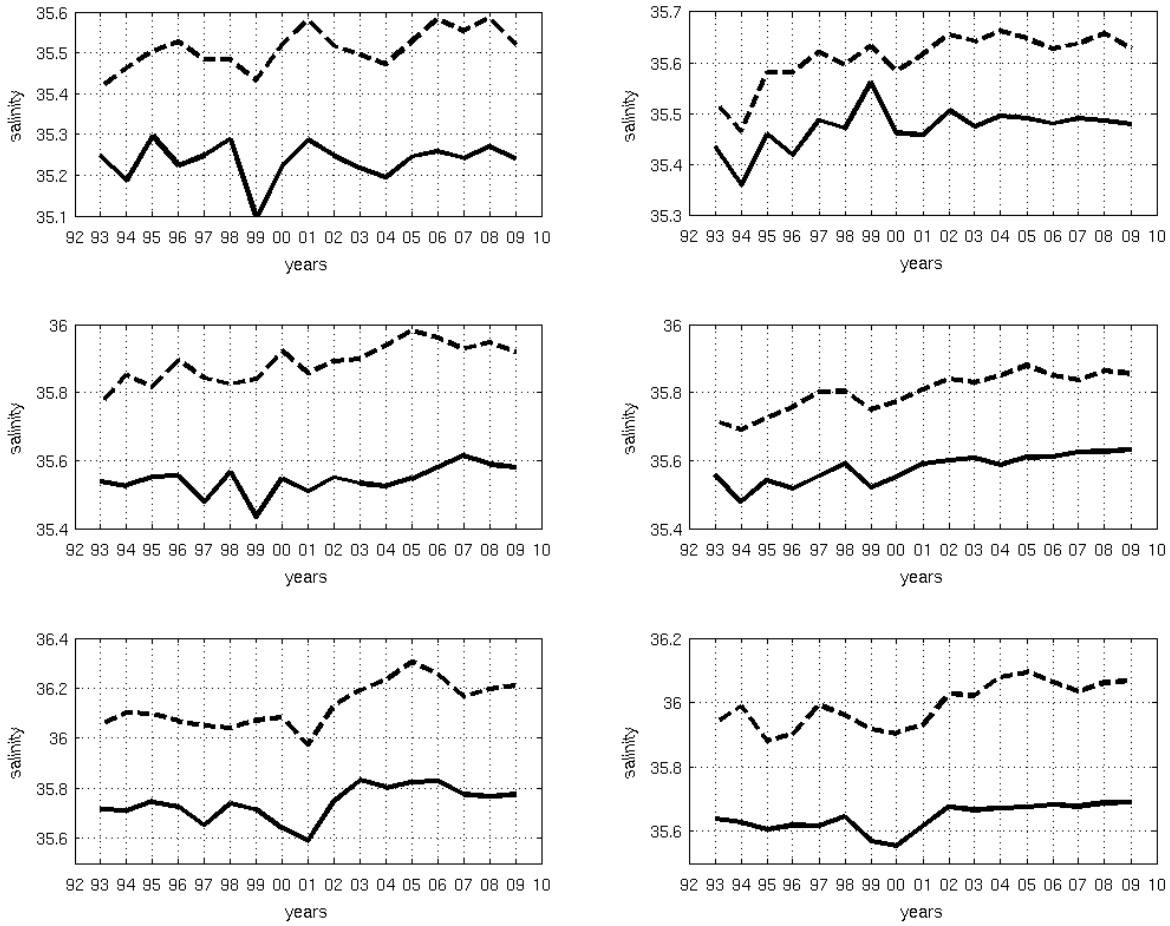

Figure 3-3 The same as Figure 3-2, but for salinity.

In Figure 3-3 is shown the same analysis of Figure 3-2, but for salinity. Salinity shows similar trends to temperature, in particular for the southern and eastern boxes. The southern boxes shifted from a fresh to salty period after 2001, while in the north-east box the increase in salinity occurred earlier. In the middle-west and north-west boxes the warm periods coincide with saltier periods, but there is an increasing trend in salinity at the surface, which is not so well observed in temperature. It should be noted that salinity signals are more stable in the ocean, while temperature is more easily damped from air-sea interactions and mixing with other water masses. Thus, if a mechanisms such as advection or air-sea fluxes increases salinity and temperature, the signal in salinity will persist longer in time.

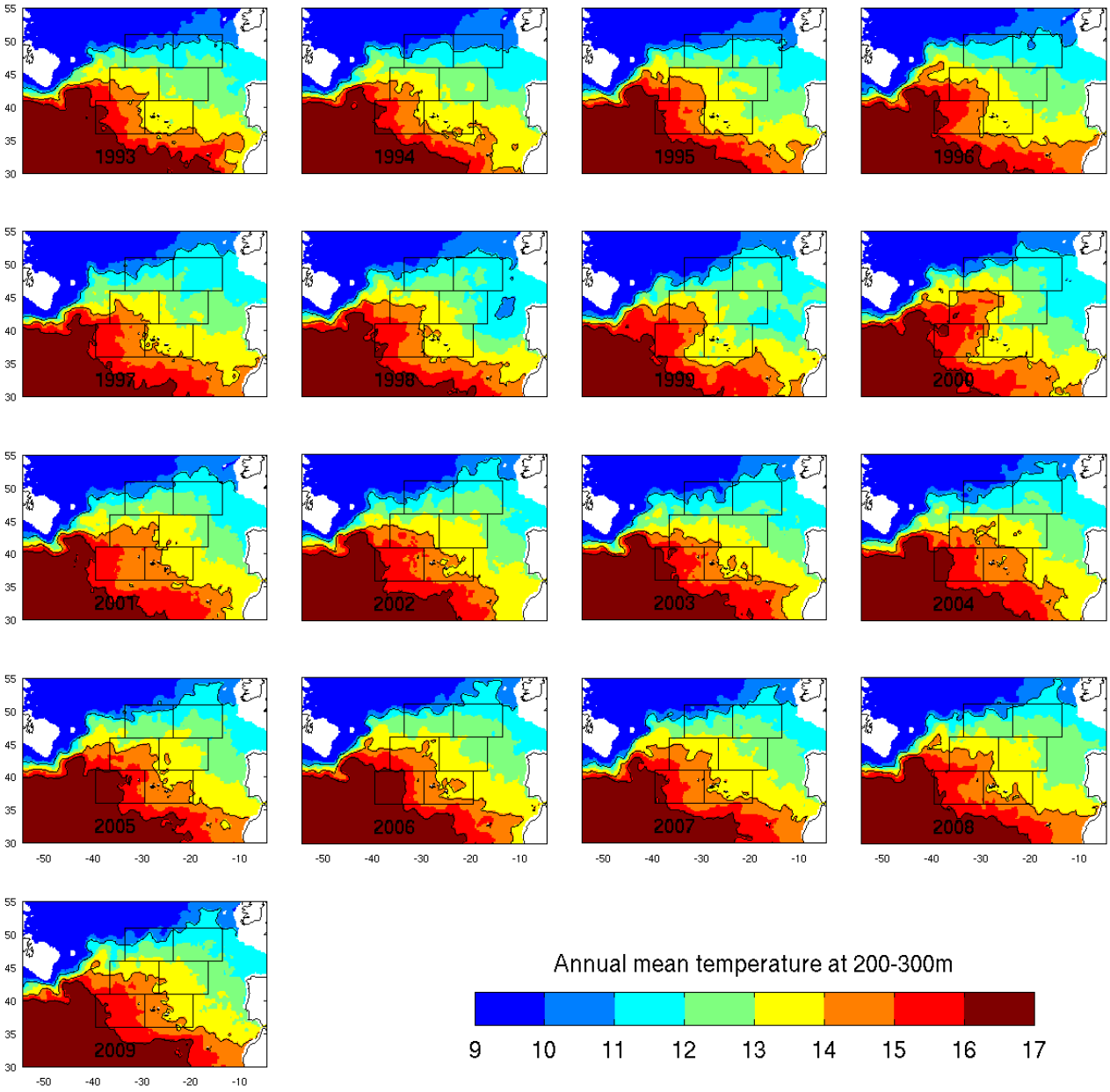

Figure 3-4 Annual average of temperature (ºC) at 200-300 m from MERCATOR monthly fields. The isotherms of 16 ºC, 14 ºC and 11 ºC are highlighted by a black contour. The location of the boxes where temperature and salinity were averaged is shown.

Figure 3-4 shows the spatial changes of temperature (ºC) in the region of interest. Temperature between 200 and 300 m was averaged in each grid point for a year. The major differences are found in the eastern boxes, where there is a one degree warming between the first and last years (compare for example 1993, 1999 and 2001 in the middle-east box). In the first years the waters in the eastern basin were relatively cold and stable. The warm and saline period appears to have started early in

the north-east box (1999) than in the middle-east and south-east boxes (2001-2002). In 2000, there was a shift in the position of 14 ºC isotherms, when there was an intrusion of warmer waters to the north of Azores with a simultaneous decrease in temperature around the archipelago. After this event the waters started to warm, with maximum temperatures in 2004-2005. In 2006 there is a temperature decrease in the south-east box, while in the middle-east box it remains unchanged. To the west of the Azores, the 16 ºC isotherm does not shows a significant displacement until 2004, where it almost reaches the archipelago. To the north, in the north-west box, near the subpolar front, it is not observed any particular change. The penetration of warmer and saltier waters to the subpolar region (Hatun et al., 2005) can be observed in a narrow region between the subpolar front and the British islands. The increase is particular observed in 2002, when the 11 ºC isotherm reached 55 ºN, remaining there until 2009. Finally it is noted that the subpolar front did not show any particular change in temperature during the observed period (compare the top left corner of the north-west box between years in Figure 3-4).

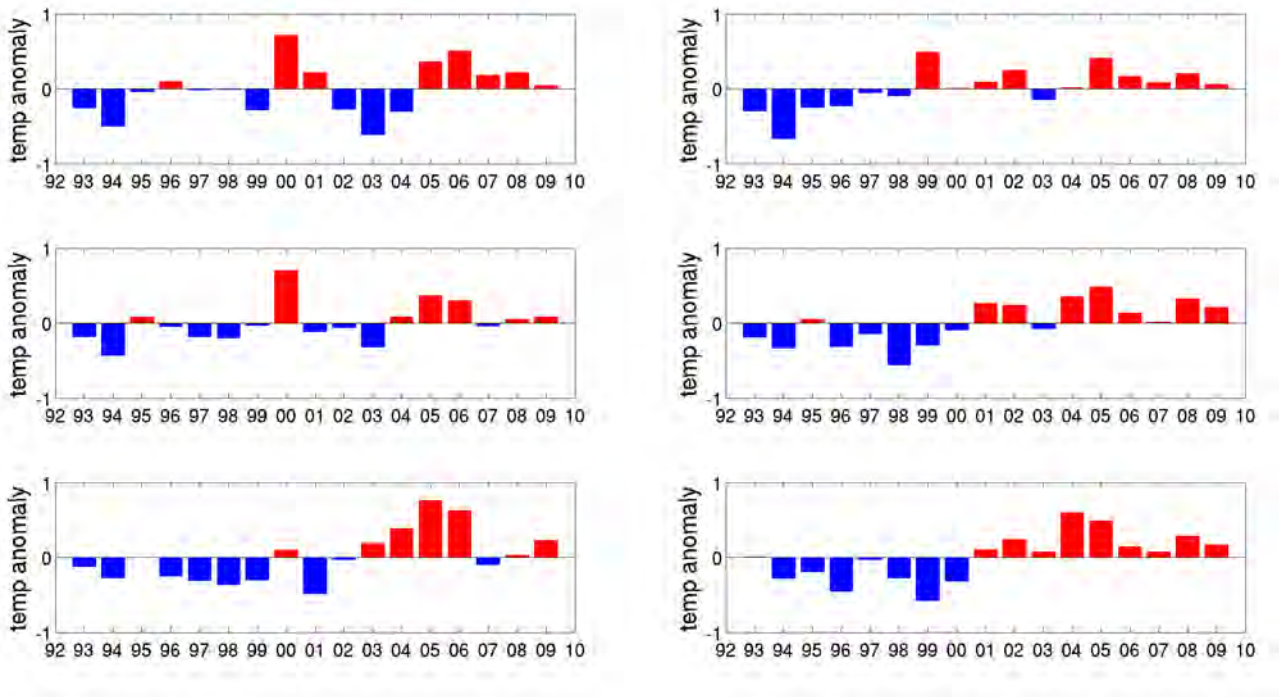

Figure 3-5 Annual anomaly (1993-2009) of temperature (ºC) at 100-200 m from MERCATOR monthly fields, at the: north-west box (46-51 ºN, 24-34 ºW), north-east box (46-51 ºN, 14-24 ºW), middle-west box (41-46 ºN, 27-37 ºW), middle-east box (41-46 ºN, 17-27 ºW), south-west box (36-41 ºN, 30-40 ºW) and south-east box (36-41 ºN, 20-30 ºW).

Figure 3-5 and Figure 3-6 show the annual anomalies of temperature and salinity at 100-200m, respectively. These anomalies are determined from the time series in Figure 3-2 and Figure 3-3, using the climatological mean between 1993-2009. Therefore, the changes are exactly the same as previously discussed, but allow for a better visualization of the increasing trends. The following conclusions can be drawn from this analysis: 1) changes at the surface follow changes at depth, 2) there was an increase in temperature and salinity at all eastern boxes, both at the surface and deep waters, between 1993-2009; 3) the southern boxes and the middle-east box show a particular rapid increase around 2001, while in the north-east box the increase occurred earlier; 4) after 2002, all southern and eastern boxes showed systematically higher surface salinity than in the first years before; 5) in the middle-west and north-west box, there is no clear trend in temperature, but surface salinity shows an increasing trend, overlapping three warm and saline periods around 1995, 2000 and 2005.

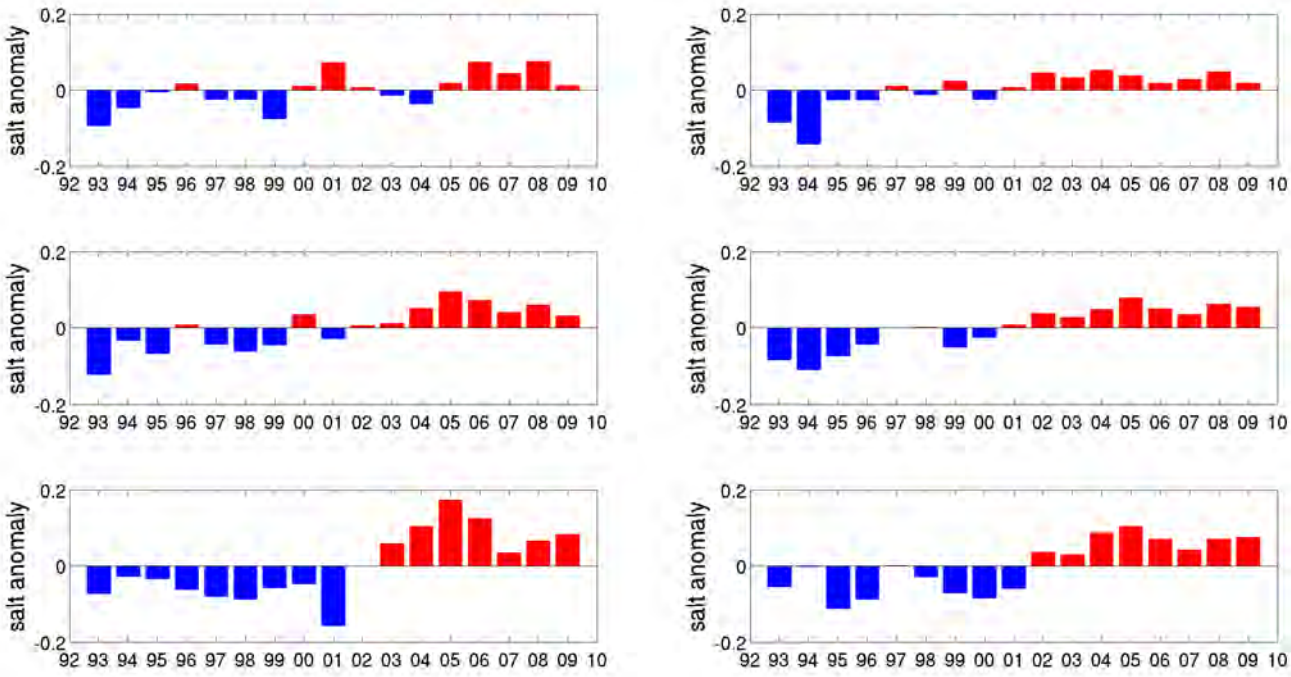

Figure 3-6 The same as Figure 3-5, but for salinity.

In-situ profiles of temperature from the Global Temperature-Salinity Profile Program (GTSPP) were analyzed in the region of the Azores Archipelago (36-41 ºN, 23-33 ºW) during the same time period. The box were the profiles were analyzed is shown in Figure 1-1 and Figure 1-2, and corresponds nearly to the south-east box (36-41 ºN, 20-30 ºW). The average annual temperature was computed in the Azores box from a total of 2995 temperature profiles (see Chapter 2 for number of profiles per year). Annual temperatures were also derived for the Azores box, from MERCATOR

and CMCC CGLORS models. The CMCC CGLORS (Storto et al., 2012) model provides the same variables as MERCATOR, but includes one more year (2010).

Figure 3-7 shows the temperature changes in the Azores Archipelago derived from in-situ data and the MERCATOR and CMCC models. Overall, there is an agreement between the three datasets. Regarding the two models there is an overall agreement, although the MERCATOR as higher values. The in-situ data compares particular well with the MERCATOR model at 400-500 m. The only period with differences is in 1999 and 2000, where the in-situ data shows an increase in temperature while the models show a decrease, followed by a rapid increase in 2001. It is difficult to consider the in-situ data as the "true" dataset, since the Azores Archipelago covers a considerable large region with distinct water masses and an heterogeneous spatial distribution of the profiles in one year could easily introduced a bias. Whether the transition to a warm salty period was smooth between 1999 and 2001, as the in-situ data suggests, or an abrupt increase in 2001 as seen in the models, it is unclear. One of the most important results of this figure, is a noticeable decrease in temperature between 2006 and 2011, specially in the upper layers (0-300 m). A sharp cooling-down is observed in the upper ocean in 2010, with temperatures returning to the values in the cold period. This highlights the importance of interpretation the trends carefully. Finally, the warming in the Northeast Atlantic after 2001 is illustrated in Figure 3-8 with the averaged temperature at 200-300 m from all in-situ profiles in the region of interest, during the periods 1998-2000 and 2004-2007.

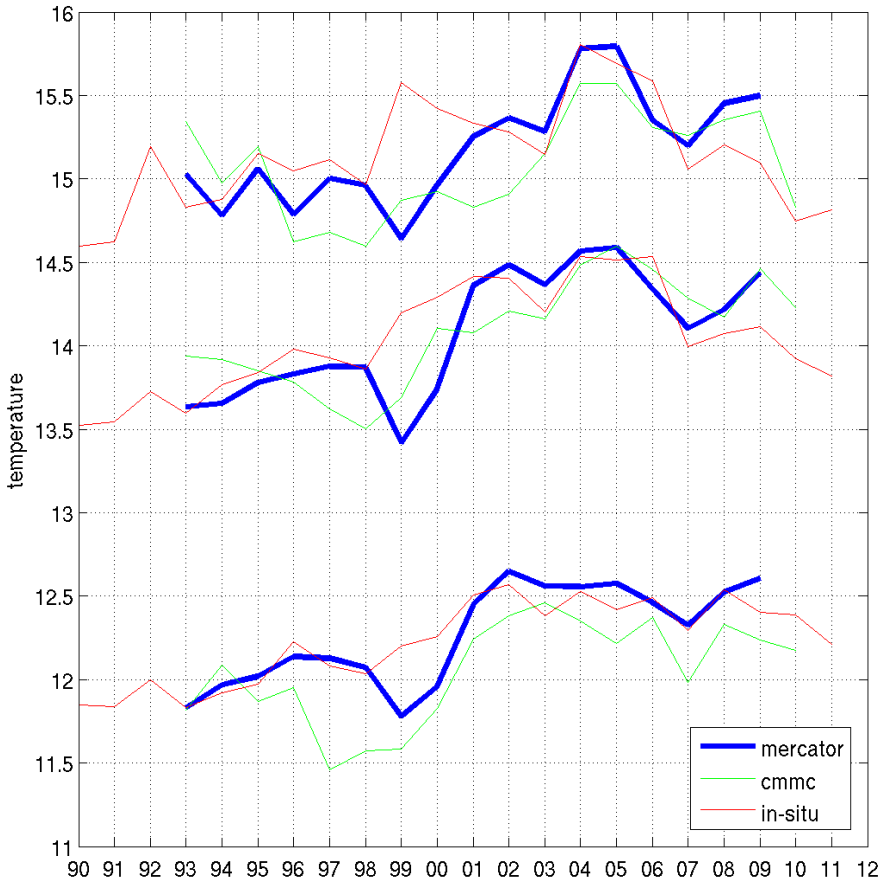

Figure 3-7 Averaged temperature (ºC) in the Azores Archipelago (36-41 ºN, 23-33 ºN), at 100-200 m, 200-300 m and 400-500 m, from GTSPP in-situ profiles (red lines), and models MERCATOR (blue lines) and CMCC(green lines).

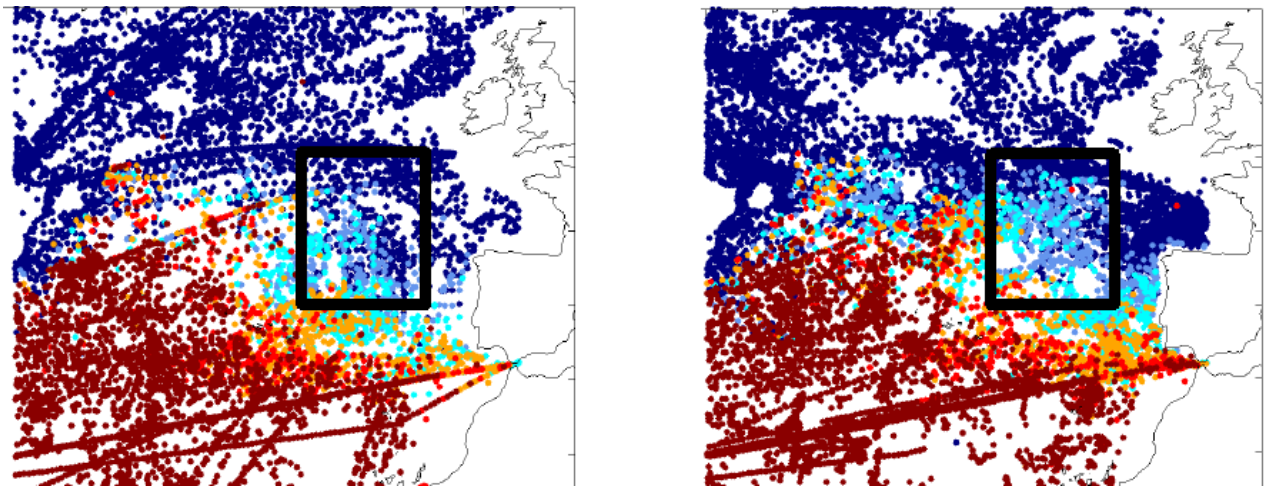

Figure 3-8 Averaged temperature (ºC) at 200-300 m from in-situ profiles (GTSPP) in the periods 1998-2000 (left) and 2004-2007 (right). Red dots represent profiles with temperatures greater than 14.5 ºC and blue dots less than 12.5 ºC. The four colors in between represent changes of 0.5 ºC.

3.3. Mixed layer depth changes

Interannual variability of mixed layer depth between 1998 and 2012 is analyzed from the model outputs of the Simple Ocean Data Assimilation (SODA) model and the Fleet Numerical Meteorology and Oceanography Center (FNMOC) high-resolution ocean analysis for the Global Ocean Data Assimilation Experiment (GODAE). It is followed the approach available at the “Ocean Productivity site“, where it is proposed a methodology to make a time series of MLD between 1998-2012, from different models, based on their comparison and temporal coverage (see Chapter 2 for more information). From 1998 to 2004 is used SODA model outputs (Carton et al., 2000), while from 2006 to 2012 is used the FNMOC model outputs (Cummings, 2005). The annual maximum MLD in each box is shown in Figure 3-9. The location of the boxes are shown in Figure 3-4. Each annual point in the time series represents the average MLD in the box, during the week of maximum averaged MLD for that year. The results are identical for an average MLD between February and March, the typical period with deeper mixed layers.

Figure 3-9 shows that mixed layer depths are shallower in the south-east box (~100-200 m) and deeper in the north-east box (~250-400 m). This suggests that, at least in the southern boxes, the changes in temperature and salinity at depths between 400-500 m are a result of horizontal advection, since the influence of the mixed layer is minimum at these depths. In the south-east box, MLD was never deeper than 250m and ranged around 150m. The shallower MLD occurred in 1999 and only was deeper than 200m in 2002, 2009, 2010 and 2011. In the south-west box, MLD was typically deeper than in the south-east box and the maximum mixing occurred in 2001 and 2002. The highest variability is found in the middle-east box, where MLD ranged between 120 m in 1999 and 350m in 2007, 2010 and 2011. A trend appears to present in the northern boxes and to some extent in the middle boxes, with weak mixing in the first years. In 1999 a shallow MLD is found in all boxes.

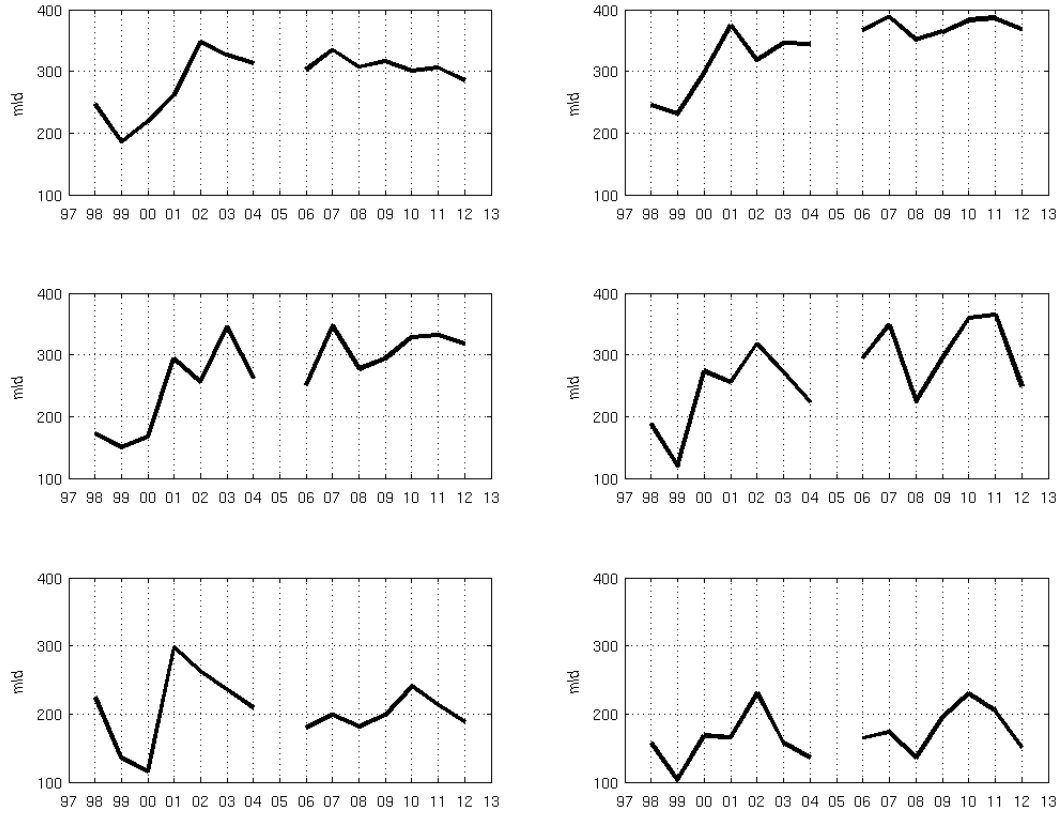

Figure 3-9 Annual changes in the annual maximum MLD (m) derived from SODA (1998-2004) and FNMOC (2006-2012) models, at the: north-west box (46-51 ºN, 24-34W), north-east box (46-51 ºN, 14-24W), middle-west box (41-46 ºN, 27-37W), middle-east box (41-46 ºN, 17-27 ºW), south-west box (36-41 ºN, 30-40W) and south-east box (34-41 ºN, 20-30 ºW).

3.4. Changes in current patterns

The previous analysis shows that the influence of the mixed layer depth at depths of 400-500 m appears to be minimum in the southern boxes. Therefore, at least in the southern and middle-east boxes, the increase in temperature and salinity in deep waters around 2001 can have been due to the influence of lateral advection. To investigate the influence of north-south and west-east horizontal advection into the eastern boxes, geostrophic ocean currents derived from satellite altimetry (AVISO) were analyzed in four sections: two meridional (at 30 ºW, one between 40-45 ºN and another between 45-50 ºN) and two zonal (at 45 ºN and 50 ºN, between 16-30 ºW). In the meridional sections, the zonal component of the current velocity was averaged over each week. Conversely, in the zonal sections the meridional component of current velocity was averaged. The objective is to investigate the intensity of eastward currents that cross the Mid-Atlantic Ridge (30

ºW) and the intensity of southward/northward currents at 45 ºN and 50 ºN in the eastern basin. The changes relate to eddies, to NAC branches and other narrow jet-like features such as meanders and recirculations. Both eastwards and northwards velocities across these sections have the capability of increasing temperature and salinity because of the meridional and latitudinal gradients in the region (Figure 1-5). The results are shown in Figure 3-10. A running mean of 1 year was performed in each time series.

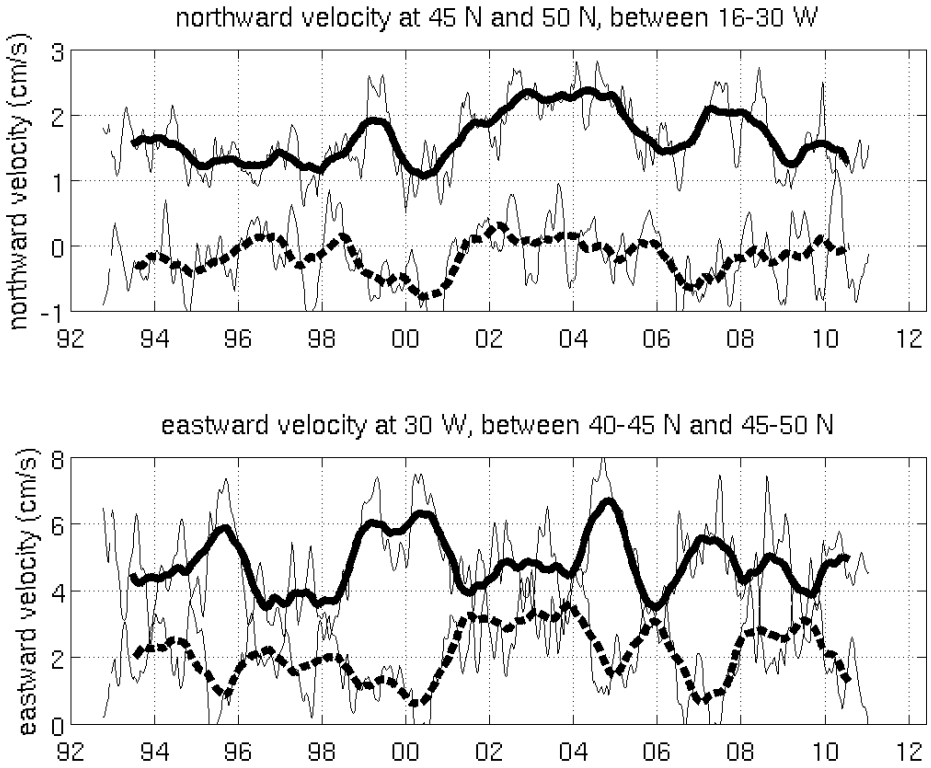

Figure 3-10 Averaged intensity (cm/s) of: the meridional component of current velocity in two zonal sections (top) and the zonal component of current velocity in two meridional sections (bottom). The zonal sections are at 50 ºN (solid line) and 45 ºN (dashed line) between 16-30 ºW. The meridional sections are at 30 ºW between 45-50 ºN (solid line) and 40-45 ºN (dashed line). Thin lines show the weekly average and thick lines the running mean over a year. Ocean currents are from satellite altimetry (AVISO).

Figure 3-10 shows the northward flow (top figure) at 50 ºN between 16-30 ºW (solid line) was always northward with a maximum between 2002 and 2004 and smaller peaks in 1999 and 2007. Further analysis showed that the anomalous northward flow during 2002-2004 occurred at other latitudes between 45 and 50 ºN. At 45 ºN (dashed line), the flow switches between periods with a southward flow and periods with weak meridional component in current velocity. The periods with

weak meridional component are 1996-1998 and 2001-2005. The periods of southward flow are 1999-2000 and 2006-2007. The eastward flow at 30 ºW (bottom figure) at latitudes of 40-45 ºN (dashed line) and 45-50 ºN (solid line), corresponds to the southern branches of the NAC. The southernmost branches of the NAC (i.e. 40-45 ºN, dashed line) had the strongest speeds between 2001 and 2004. A remarkable feature is the simultaneous change of eastward speeds at 30 ºW, between the southern (45-50 ºN) and southernmost (40-45 ºN) NAC branches. Another important result is that in the southernmost sections of the region (dashed lines) the periods of weak eastern flow tend to coincide with periods of southward flow and vice-versa.

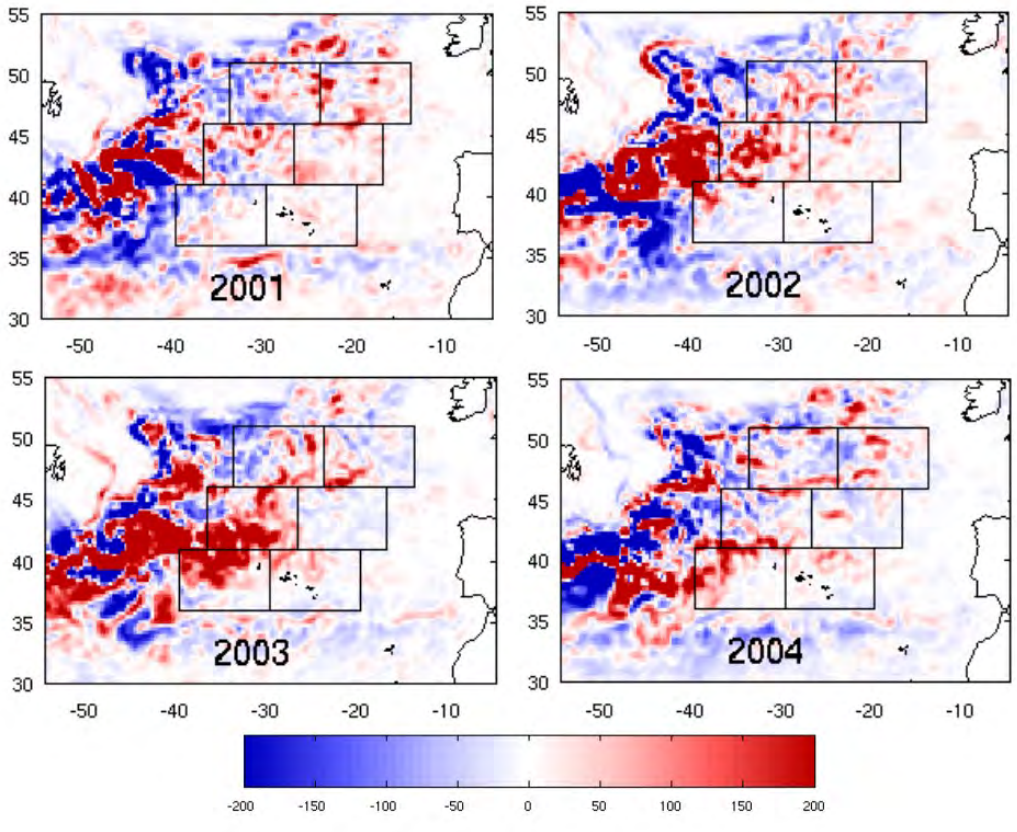

Figure 3-11 Anomaly of EKE (cm²/s²) calculated from the 1998-2011 climatological pattern. The annual means of EKE were computed from the weekly EKE fields, which in turn were computed from the weekly geostrophic currents derived from satellite altimetry (AVISO).

The previous analysis revealed that in 2001-2004 there was an anomalous northward flow at 50 ºN (between 16-30 ºW) and an anomalous eastward flow at 30 ºW (between 40-45 ºN). These changes can be traced to an anomalous event of southern branches of the NAC. This event is show in Figure 3-11 from the annual anomaly of Eddy Kinetic Energy (EKE) during 2001, 2002, 2003 and 2004. EKE was computed from weekly fields of satellite altimetry (AVISO) and the annual anomaly was

calculated on the basis of 1998-2011 climatological annual value for each pixel. Figure 3-11 shows a southern branch of the NAC around 45 ºN in 2001, evolving to an extreme event in 2002 and 2003, rich in meanders and mesoscale features, with several northeastward jets reaching 50 ºN. Figure 3-12 shows the *hovmoller* diagram of EKE at 34 ºW, further illustrating this event. At this longitude, it appears that the event started in 2000 and propagated to the south. The field of EKE started to increase in 2002 at the latitudes 40-45 ºN and reach the lowest latitudes in 2003-2004.

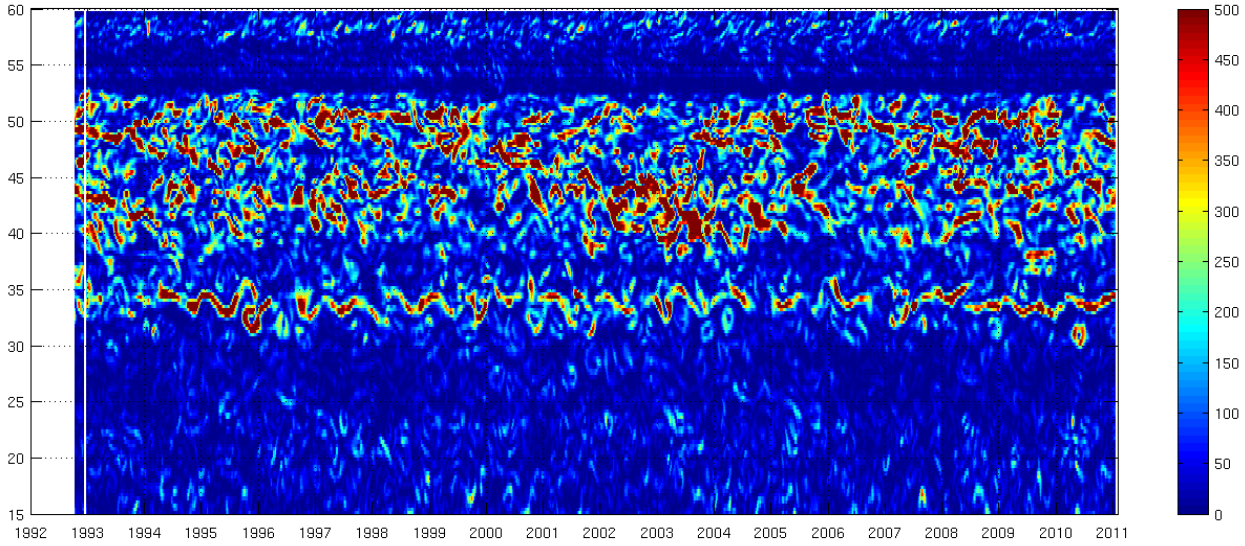

Figure 3-12 *Hovmoller* diagram of the EKE field (cm²/s²) at 34 ºW. EKE computed from satellite altimetry (AVISO).

The shift towards a more northeastward flow in 2001-2004 can be observed in other datasets such has the Ocean Surface Current Analysis - Real Time (OSCAR). Figure 3-13 shows differences in surface currents between the period 2001–2005 and the 1997-2000. Note that this figure does not show the currents, but an anomaly field. The signal is strongly dominated by the anomaly northeastward event in 2001–2005.

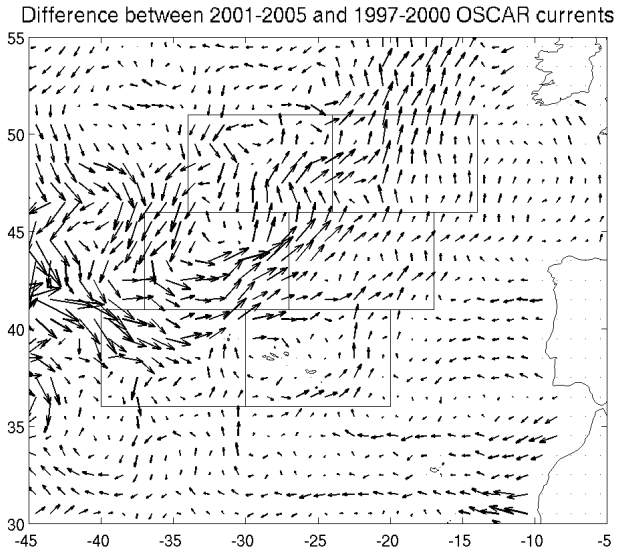

Figure 3-13 Changes in surface currents between the period 2001–2005 and 1997-2000. The surface currents were averaged for both periods and the 2001-2005 average was subtracted by the 1997-2000 average. Surface currents were obtained from the OSCAR currents, which combine the geostrophic currents and Ekman drift. (similar to Figure 9 of Häkkinen and Rhines, 2009)

3.5. Effect of currents on temperature and salinity

The effect of currents on temperature and salinity in the eastern basin south of 45 ºN are now illustrated with the changes in salinity in the middle-east box (41-46 ºN, 17-27 ºW). In Figure 3-14 the temperature at 100-200 m in the middle-east box is compared with satellite-derived geostrophic (AVISO) and total (OSCAR) ocean currents. The geostrophic currents are the same as the dashed lines in Figure 3-10, with a section at 30 ºW (between 40-45 ºN) and a section at 45 ºN (between 16-30 ºW), where the eastward and northward averaged annual speed is computed, respectively. Additionally, it is also shown the northward total current (OSCAR) averaged over the middle-east box between December and February of each year. The latter is more related to northward Ekman drift during the winter months, although it also contains the signal of the northward geostrophic flow. Relevant interpretations of Figure 3-14 include: 1) in 1996-1998 an increase in salinity and reduced southward flow at 45 ºN (Figure 3-14, middle); 2) in 1999-2000 a decrease in salinity and southward flow (Figure 3-14, middle); 3) in 2001-2002 an increase in salinity and a northeastward flow (Figure 3-14, top and middle); 4) in 2005 the increase in salinity appears related to Ekman drift since it was the maximum value (Figure 3-14, bottom).

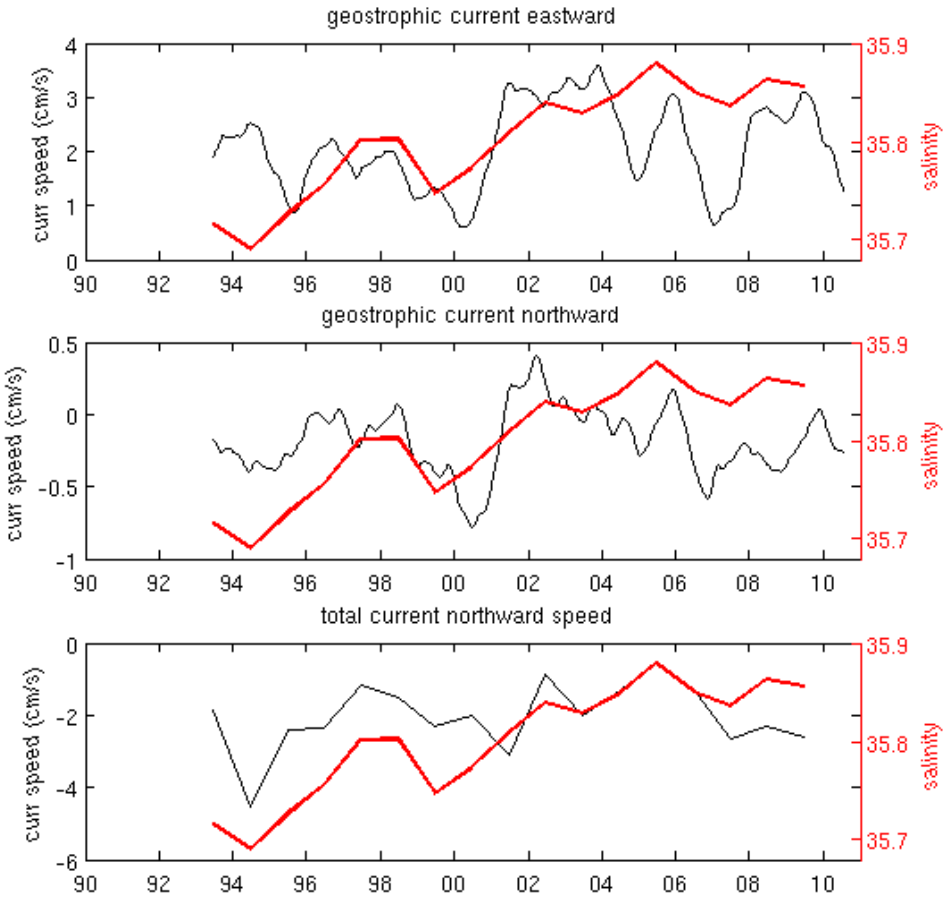

Figure 3-14 Ocean currents and salinity at 100-200 m in the middle-east box (41-46 ºN, 17-27 ºW). Top figure: eastward geostrophic current (AVISO) at 30 ºW, between 40-45 ºN (same as Figure 3-10, bottom dashed line). Middle figure: northward geostrophic current (AVISO) at 45 ºN, between 16-30 ºW (same as Figure 3-10, top dashed line). Bottom figure: northward total current (OSCAR) average over the middle-east box between December and February of each year.

The link between the abnormal eastward and northward flow in 2001-2004 with the increase in temperature and salinity, suggest that the fresh and cold waters found in the eastern basin during the early 1990's, were gradually replaced by episodes of warm salty northeastward pulses of subtropical waters. This in agreement with previous works with drifters and models at northern latitudes (e.g. Häkkinen and Rhines, 2009; Häkkinen et al., 2011a; Holliday, 2003). Additionally, years with anomalous northward Ekman transport (e.g. 2005) contribute to a further warming and years with southward flow tend to reduce the temperature and salinity (e.g. 1999-2000). It is possible that in addition to the anomalous northeastward flow along 30 ºW in 2001-2004, the intrusion of warm waters to the north of Azores in 2000 (see Figure 3-4) may have also contributed to the warm and saline period of the eastern basin.

In conclusion, the following mechanisms are proposed to explain the salinity changes after 2000. It is proposed that in 1999-2000 an anticyclone-like feature could have transported warm waters to the north of Azores and west of the MAR (see Figure 3-4, year 2000), and at the same time advecting the early-period cold and fresh water mass to the Azores latitudes (southward period 1998-2000 in Figure 3-10, top dashed line). In the following years these northern warm waters may have spread southeastward and warmed the region of the middle-east and south-east boxes, accomplished also by the increase in northeastward flow along 30 ºW. These warm water masses have then remained in the region, possibly even moved northward, and since 2005 have been been laterally replaced/mixed by other flows (such has the southward flow in 2006-2007) or vertically mixed by deep winter MLD (such as the deep winter mixing in 2010). The latitudes of 40-45 ºN and 45-50 ºN, correspond to the southern branches of the NAC and it is shown that they alternate in their strength. The periods of weaker eastern flow at 30 ºW, between 40-45 ºN tend to coincide with periods of increased southward flow at 45 ºN (Figure 3-10, dashed lines), which may indicate that when the NAC successively crosses the MAR in the south, the southward flow is reduced and more warm saline waters enter the region.

3.6. Effect of wind on currents

Figure 3-15 shows annual patterns of wind circulation (based on NCEP wind product). The climatological pattern is characterized by strong westerlies around 50 ºN and easterlies to the south of 30 ºN (this pattern can be observed in 1993-1995, 1999-2000, 2007-2009). Different climatological wind patterns are visually identified in years of 1996-1998, 2001-2006 and 2010-2011. Changes in the wind patterns can have an effect on the ocean circulation through several mechanisms. Here it is discussed the effect of wind stress curl in the geostrophic currents. In the Northern Hemisphere open ocean, regions of negative (positive) wind stress curl have a convergence (divergence) of Ekman drift at the surface which is compensated by a southward (northward) geostrophic current. In the eastern basin south of 45 ºN there is a region of decreased winds, characterized by a climatological negative wind stress curl and southward flow.

Figure 3-16 illustrates the link between wind stress curl and the eastward and northward geostrophic flow (from AVISO ocean currents) at 30 ºW (between 40-45 ºN) and 45 ºN (between 16-30 ºW), respectively. Figure 3-16 (top) shows a remarkable relation between wind stress curl in the eastern basin (40-50 ºN, 15-30 ºW) and northward geostrophic speed at 45 ºN, between 16-30 ºW. Periods of negative (positive) wind stress curl are followed by an increase (decrease) in southward flow.

Regarding the eastward flow (Figure 3-16 bottom) the relation is more complex. A reason for a major shift in the eastward currents between 40-45 ºN, might actually be related to changes in the wind stress curl in the north. Figure 3-16 (bottom) shows the wind stress curl in the northwestern region of the basin (44-54 ºN, 30-45 ºW) and the eastward geostrophic speed at 30 ºW, between 40-45 ºN. The region here considered for the wind stress curl, lies exactly above the main core of NAC (52 ºN), where the wind stress curl is zero. The years of 2001-2003 had a positive wind stress curl which implies a southward shift of the zero wind stress curl line and a northward geostrophic response in the north. It is possible that the increase in eastward currents in 2001-2003, have been a consequence of a southward displacement of the zero wind stress curl line as suggested by Häkkinen and Rhines (2009), but also to an increase in northward geostrophic currents induced by a positive wind stress curl (at 44-54 ºN, 30-45 ºW). Despite the mechanisms at play it is interesting to observe how the anomalous eastward currents in 2001-2004 can be related to an equally anomalous wind stress curl.

In resume, results show that the temperature and salinity increase in the eastern basin during the last two decades, shows fluctuations coincident with the currents which in turn are related to the wind circulation patterns. Southward inflows, during periods of negative wind stress curl in the eastern basin, transport cold and fresh water masses from northern origins, which decreases temperature and salinity in the region. During positive (and weak negative) wind stress curl the southward flow is reduced and the eastward flow transports warm and saline waters into the region, which increase temperature and salinity in the region. In 2001-2003, an anomalous positive wind stress curl in the northwest basin was observe to coincide with an anomalous northeastward flow along 30 ºW, which further transported warm and saline waters to the eastern basin. These fluctuations can be part of a multi-decadal cycle of wind stress curl with relations to the Atlantic Multidecadal Oscillation (Knight et al., 2009; Häkkinen et al., 2011b). Here we explored the role of horizontal advection, but is likely that the warm, saline periods can have multiple causes including air-sea fluxes, depth of the mixed layer, Ekman pumping and downstream water masses changes.

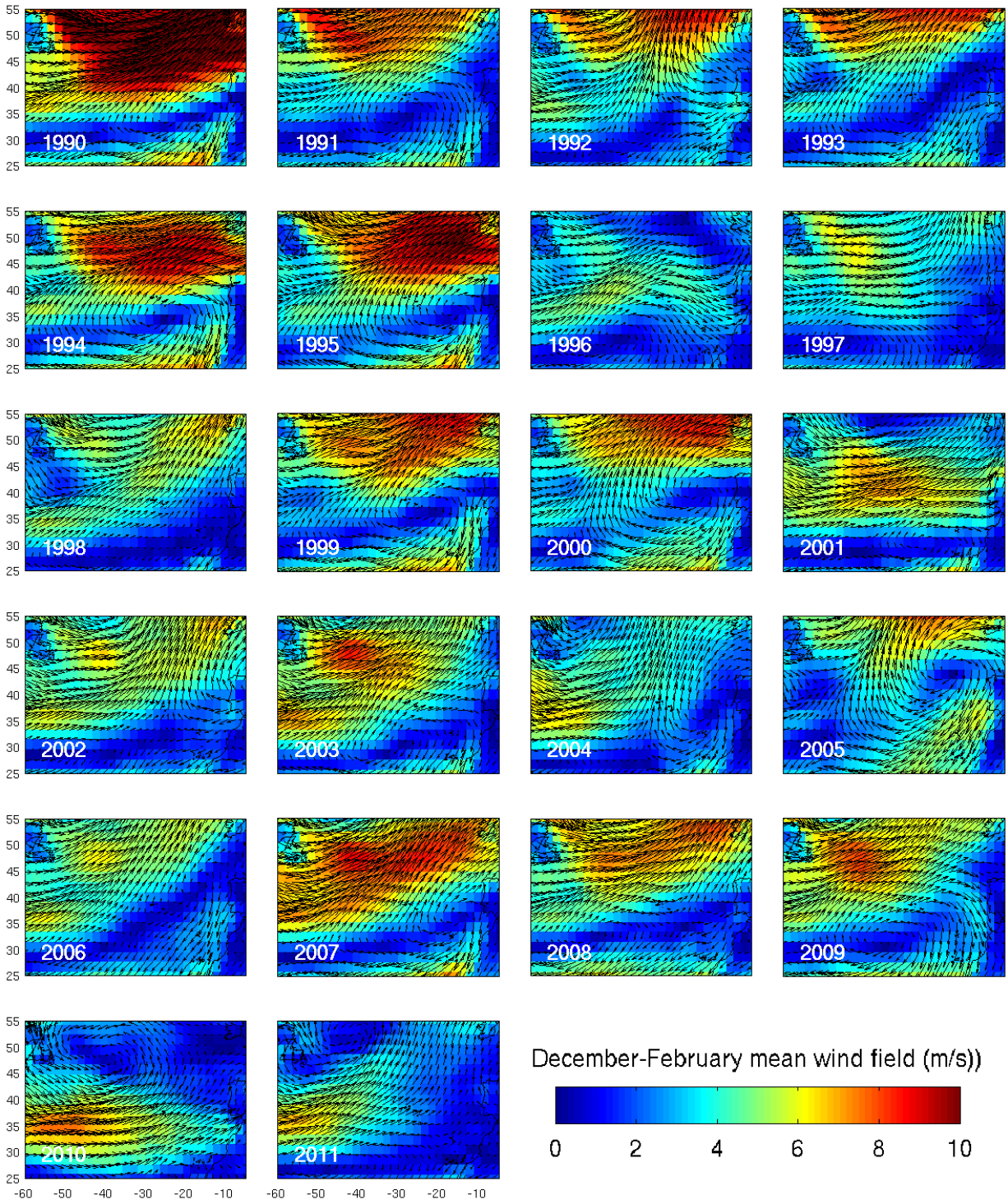

Figure 3-15 Wind patterns (m/s) between December and February. The mean wind field was computed from daily means from the NCEP reanalysis.

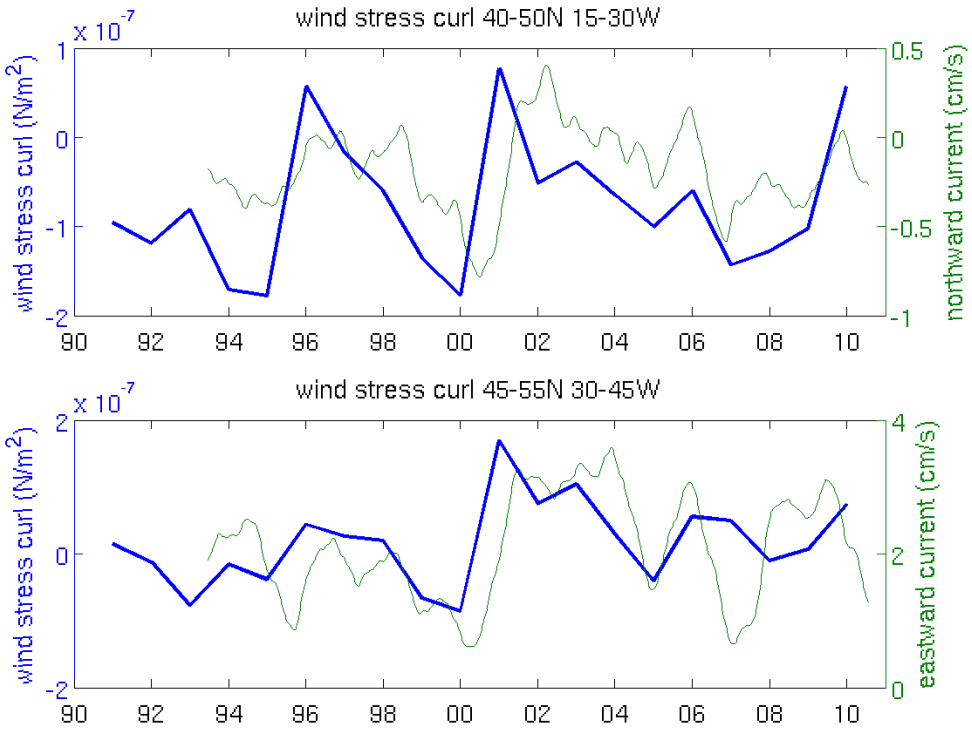

Figure 3-16 Wind stress curl and ocean currents. Top: wind stress curl averaged in the eastern basin (40-50 ºN, 15-30 ºW) between December-March and the northward geostrophic current (AVISO) at 45 ºN, between 16-30 ºW (same as Figure 3-10, top dashed line). Bottom: wind stress curl averaged in the northern western basin (45-55 ºN, 30-45 ºW) between December-March and eastward geostrophic current (AVISO) at 30 ºW, between 40-45 ºN (same as Figure 3-10, bottom dashed line).

CHAPTER 4: UNDERSTANDING THE EFFECTS OF PHYSICAL FORCES ON THE DISTRIBUTION OF CHLOROPHYLL-A IN THE NORTHEAST ATLANTIC FROM SATELLITE DATA

4.1. Introduction

Seasonal changes in mixed layer depth (MLD) play an important role over biological production in the North Atlantic. The MLD regulates annual phytoplankton growth through the nutrients it supplies to surface waters during winter (Siegel et al., 2002; Longhurst, 2006). In temperate latitudes, without a deepening of the mixed layer in winter, surface waters would be permanently stratified as in summer and oligotrophic conditions would prevail. Siegel et al. (2002) made a distinction between phytoplankton seasonality to the north and south of 40 °N. To the north of 40 °N, deep winter mixing elevates surface water nutrient concentrations, but it also reduces the average irradiance available to phytoplankton community and production is inhibited. Once the mixed layer depth shallows to a critical depth, the spring bloom occurs following Sverdrup's hypothesis (Sverdrup, 1953). South of 40 °N, especially in the eastern basin, winter mixing is less vigorous and the ecosystem is likely to be limited by nutrients rather than by light. Hence, the spring bloom in the south is initiated by the supply of nutrients from winter mixing and the conditions required by Sverdrup's hypothesis (1953) do not hold. Based on these concepts, the role of MLD in dictating light and nutrients available for phytoplankton growth, is invoked to explain chlorophyll-a concentration variability at seasonal and interannual time scales in the North Atlantic. For example, it has been shown that in years with deep mixed layers, chlorophyll-a concentration increases in the subtropics due to a higher nutrient supply, but decreases in the subpolar region due to the light limitation (Follows and Dutkiewicz, 2001; Levy et al., 2005; Henson et al., 2006; Henson et al., 2009). These findings are explored in the Azores region through the analyses of SeaWiFS and MODIS AQUA ocean color satellite images of chlorophyll-a concentration (SCHL) and complementary meteorological and oceanographic data. In the following sections it is provided an investigation over the physical mechanisms responsible for: 1) the large-scale climatological patterns, 2) the couple effect of the mixed layer depth and the subsurface nutrient field, 3) the seasonal dynamics in the Azores Archipelago, 4) the interannual variability of the spring bloom, 5) the island mass effect in the Azores Archipelago.

4.2. Climatological patterns

The climatological monthly mean SCHL in the midlatitude intergyre region of the North Atlantic (30-50 °N, 10-45 °W) is shown in Figure 4-1. The monthly climatology was derived from SeaWiFS weekly data (1998-2007). The climatological annual maximum MLD isoline of 180 m, typically achieved in February-March, is plotted repeatedly for the months between January and May. The MLD was derived from the climatology of De Boyer Montégut et al. (2004). The main features, away from continental margins, is the very low SCHL during summer and a rapid increase in spring that starts around 40 °N and propagates to the north in the following months. In winter, different patterns can be observed to the south and north of the annual maximum MLD 180 m isoline. To the north of this line SCHL decreases or maintains after December and only increases again in April. These are waters where production is interrupted during winter due to deep mixed layers accordingly to Sverdrup (1953) theory. In contrast, to the south of this line there is no interruption and production continues throughout winter.

A more detailed description of the different patterns is now presented. The summer months (July-September) are characterized by very low surface SCHL concentrations (0-0.2 µg/L). From October to December there is a progressive increase in SCHL, which can be observed by the southward movement of 0.2 µg/L SCHL isoline. In the following months (January-March) three different patterns can be observed. First, to the north of the 180 m isoline, SCHL decreases or maintains after December, and only increases in March-May. Second, south of ~37 °N, SCHL continuous to increase (southward migration of the 0.2 µg/L isoline), reaches its maximum in March and in April starts do decrease (the 0.2 µg/L SCHL isoline retreats northward). Third, between the 180 m isoline and ~37 °N, in a band between the Azores and Western Iberia, SCHL continuous to increase after December, but in April, unlike the southern waters which start to decrease, there is an increase during April-May. Other interesting patterns include the higher SCHL in February-March, in the Azores region and northwest of Western Iberia. The patch of higher chlorophyll around the Azores in February is discussed in a later section.

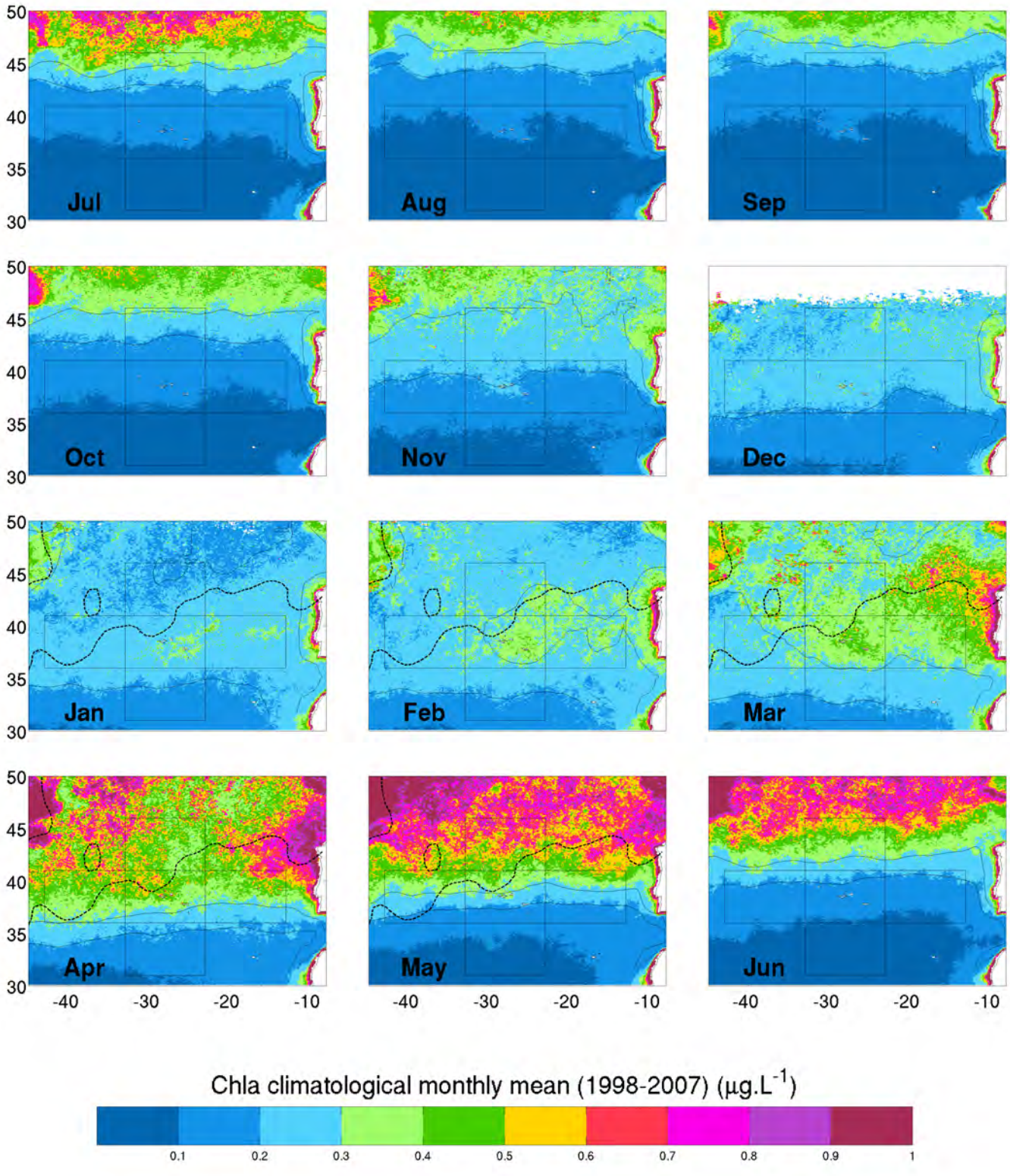
Jul
Aug
Sep
Oct
Nov
Dec
Jan
Feb
Mar
Apr
May
Jun
50
45
40
35
30
-40
-30
-20
-10
Chla climatological monthly mean (1998-2007) (µg.L-1)
0.1
0.2
0.3
0.4
0.5
0.6
0.7
0.8
0.9
1

Figure 4-1 Monthly climatology of SCHL derived from SeaWiFS weekly data for the period 1998-2007. The 0.2 μg/L and 0.4 μg/L are shown in black contours. The annual maximum MLD 180 m isoline (derived from the monthly climatological fields of De Boyer Montégut et al., 2004) is shown in dotted contour between January and May. The black squares correspond to the: subpolar box (41-46 °N, 23-33 °W), midlatitude box (36-41 °N, 23-33 °W), subtropical box (31-36 °N, 23-33 °W), midlatitude-west box (36-41 °N, 33-43 °W) and midlatitude-east box (36-41 °N, 13-23 °W).

The climatological seasonality of SCHL inside each box represented in Figure 4-1 is shown in Figure 4-2 and Figure 4-3. The boxes are named as follows: subpolar (41-46 °N, 23-33 °W), midlatitude (36-41 °N, 23-33 °W), subtropical (31-36 °N, 23-33 °W), midlatitude-east (36-41 °N, 13-23 °W) and midlatitude-west (36-41 °N, 33-43 °W). In Figure 4-2, the subpolar box is shown to have higher mean SCHL in all months, except between January and March, where the midlatitude box has higher SCHL. The spatial pattern of this feature can be observed in Figure 4-1 as a band with values 0.3-0.4 μg/L between Azores and Western Iberia. Other features are the subpolar box being characterized by a strong spring bloom, while the midlatitude and subtropical boxes are characterized by a gradual increase from summer to winter. The previously described differences after March, to the south and north at 37 °N, can be observed in the subtropical box, where SCHL decreases after March, and in the midlatitude box, where SCHL increases until April. Overall, four different major SCHL seasonal changes can be identified: 1) low concentrations in summer, 2) an increase during fall, 3) a decrease or increase during winter, and 4) an increase or decrease in spring.

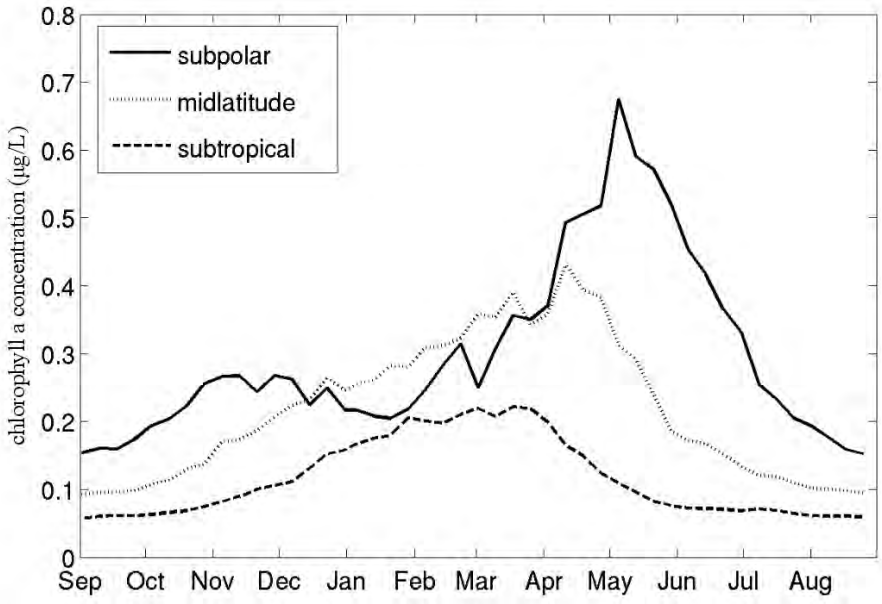

Figure 4-2 Time series of weekly climatological SCHL derived from SeaWiFS between 1998-2007. The time series were averaged over the subpolar box, midlatitude box and subtropical box shown in Figure 4-1. These time series are similar to the production regimes of Levy et al. (2005) in the region 30-50 °N, 16-22 °W.

In a nearby region (30-50 °N, 16-22 °W) the three patterns showed in Figure 4-2 were described and summarized by Levy et al. (2005), referred as LEV05 from now onwards. LEV05 defined three production regimes: subpolar, midlatitude and subtropical. The subpolar regime is characterized by deep MLD (>200 m) during winter which repeatedly sunk phytoplankton populations to deeper and darker depths, where light levels are minimum, resulting in low production during winter, despite high nutrient availability. In spring there is a restratification of the water column trapping phytoplankton in surface waters. The availability of light and nutrients, leads to an explosion of phytoplankton population, the so-called spring bloom (Sverdrup, 1956). The subtropical regime is characterized by shallow mixed layer depths (<120m) which result in low nutrients and low SCHL throughout the year, despite the light availability. Seasonality of SCHL is characterized by a gradual increase that starts in autumn and peaks in winter when the mixed layer depth is deeper. The subtropical and subpolar regimes are well known in the North Atlantic (Follows and Dutkiewicz, 2001; Henson et al., 2009), but LEV05 introduced the concept of a third regime: the midlatitude regime. In this regime, located between the subpolar and subtropical regimes, phytoplankton is both light and nutrient limited, due to mixed layer depths between 100-200m. The midlatitude regime differs from the subpolar regime because there is no interruption of production in winter (i.e. it is

not light limited) and it differs from the subtropical regime because there is a small spring bloom around April, during the restratification (i.e. it is not nutrient limited). Although LEV05 does not discuss the spatial extension of the midlatitude regime it can be related to be the band of high SCHL between the Azores and Western Iberia observed in Figure 4-1 during February.

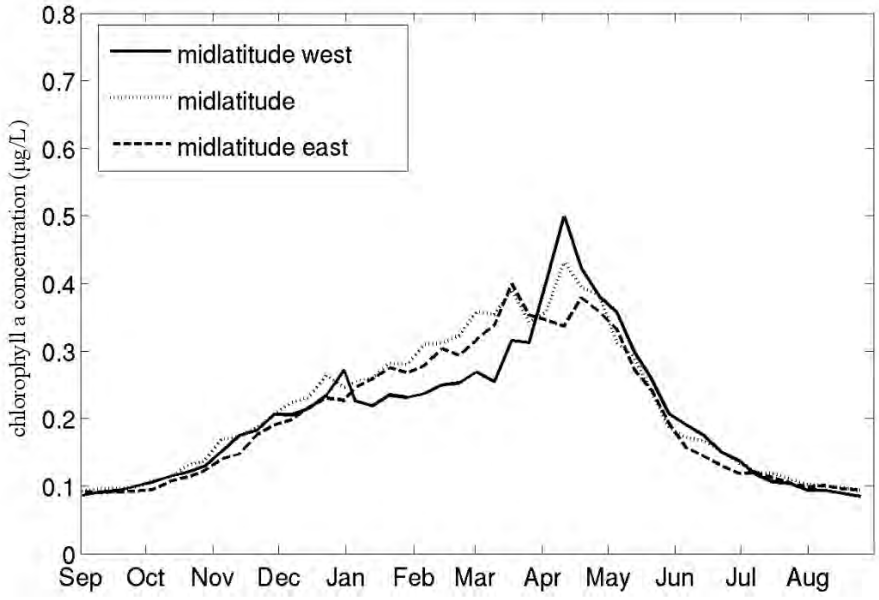

Figure 4-3 Time series of weekly climatological SCHL derived from SeaWiFS data between 1998-2007. The time series were averaged over the midlatitude-west box (36-41 °N, 33-43 °W), midlatitude box (36-41 °N, 23-33 °W) and midlatitude-east box (36-41 °N, 13-23 °W), which are shown in Figure 4-1.

To analyze the seasonality of SCHL at midlatitudes (36-41 °N), the seasonal climatology is computed in three boxes: midlatitude-west (36-41 °N, 33-43 °W), midlatitude (36-41 °N, 23-33 °W) and midlatitude-east (36-41 °N, 13-23 °W). The time series are shown in Figure 4-3 and the geographic location of the boxes are illustrated in Figure 4-1. It can be observed from Figure 4-3, that both the midlatitude-east box (corresponding to the original midlatitude regime of LEV05) and the midlatitude box have a gradual increase during winter and spring. In contrast, the midlatitude-west box SCHL seasonality has resemblances to the subpolar regime; i.e. SCHL does not increase during winter and has a bloom in April. Therefore, although with a smaller bloom magnitude, it shares the same characteristics of the subpolar regime described by LEV05. The nomenclature of “subpolar”, does not seems appropriate for the midlatitude-west box, since its latitude is at 36-41 °N, but the same characteristics apply, i.e. interrupted production during winter

due to light limitation as a result of deep MLD and a bloom in spring when the MLD shoals. Extrapolating the regimes of LEV05 to a broader area, the Azores region is surrounded by different seasonal cycles of phytoplankton growth. To the north and west, production is light limited during winter (MLD>200 m) with a spring bloom in April when stratification is established. To the east, production can be both light and nutrient limited during winter (MLD~100-200 m) with a weak spring bloom in April as a result of stratification. To the south, production is nutrient limited throughout the year and the maximum production is found in March during the maximum MLD (~120m).

The LEV05 regimes are intrinsically related to different nutrient regimes as a function of the MLD. A deep MLD (subpolar regime, MLD > 200 m) leads to high nutrient concentration at surface during winter and a strong spring bloom (SCHL >1 μg/L). An intermediate MLD (midlatitude regime, MLD~100-200 m) results in a SCHL spring peak with values ranging between the subtropical and subpolar regime (SCHL~0.4-1 μg/L). A shallow MLD (subtropical regime, MLD<120 m) results in low nutrient concentration at surface and SCHL peaks when MLD is deeper (SCHL < 0.4 μg/L).

These concepts lead to the idea that MLD alone determines the annual supply of nutrients and by consequence the annual mean SCHL. A puzzling pattern than emerges when comparing the spatial pattern of MLD and SCHL. This is illustrated in Figure 4-4 with the climatological maximum MLD 180 m isoline superimposed on the fields of the climatological SCHL annual mean (left) and maximum (right). The mean and maximum SCHL have similar patterns, because the maximum SCHL (spring bloom magnitude) is the main contributor for the annual SCHL mean. Figure 4-4 shows that the MLD isoline has a southwest-northeast orientation, while the SCHL has a zonal distribution. Therefore the magnitude of the bloom cannot be explained solely on MLD in all regions. Along the 180 m MLD isoline there are considerable differences in SCHL and along a given latitude (e.g. 40 °N) the SCHL is the same, but the MLD decreases to the east. This suggests that MLD is not the only factor controlling the distribution of SCHL. An alternative mechanism is highlighted in the following section.

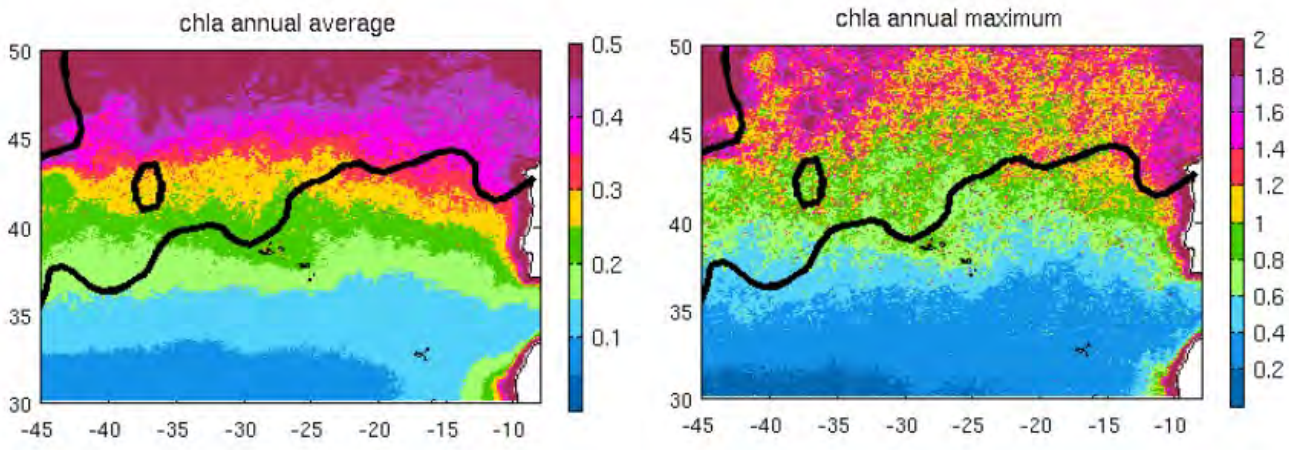

Figure 4-4 Annual mean climatology (left) and annual maximum climatology (right) of SCHL derived from the SeaWiFS weekly data between 1998-2007. The annual maximum MLD 180 m isoline (derived from the monthly climatology of De Boyer Montégut et al., 2004) is shown in the black contour.

4.3. The coupled effect of the mixed layer depth and the subsurface nutrient field

This section aims to explain the differences in the spatial distribution of SCHL and MLD in the midlatitude intergyre region of the North Atlantic. It will be argued that the same MLD to the north and south of Azores can supply different amount of nutrients to the surface and as a consequence SCHL present lower/higher values in the south/north. An explanation is provided based on the latitudinal changes of the subsurface nutrient field (or nutricline depth). It is shown that the subsurface nutrient field is considerably different at latitudes between 32-44 °N, therefore the same MLD cannot supply the same amount of nutrients. The latitudinal changes in subsurface nutrient field provide an explanation for the different latitudinal biological responses, therefore being equally important as the MLD itself. Therefore the MLD is not the main factor controlling SCHL variability in all regions and the nutrient subsurface field also plays an important role in the amount of nutrients winter MLD can provide to annual phytoplankton growth.

First, is shown in Figure 4-5 three nitrate sections from the AMT cruises (2010, 2011, and 2012) in the central region of the Northeast Atlantic during September-October. These months are characterized by shallow MLD (<50m) and correspond to a period before any substantial winter mixing. In addition, at the end of summer, nutrient supply from the remineralisation of organic matter produced during the previous spring is likely to achieve its maximum levels. Overall, Figure 4-5 can be interpreted as the nutrient subsurface field available for phytoplankton growth at given

latitude. In the following months, winter will arrive and the deepening of MLD will start to entrain the subsurface nutrients. The major feature in Figure 4-5 is a latitudinal decrease in the concentration of nitrate at all depths. At 35 °N, in the subtropical front, there is a sharp change in the nitrate concentration. These nitrate sections clearly demonstrate that the same MLD of 200 m would provide considerably different amounts of nitrate to the surface at 32 °N, 38 °N and 44 °N.

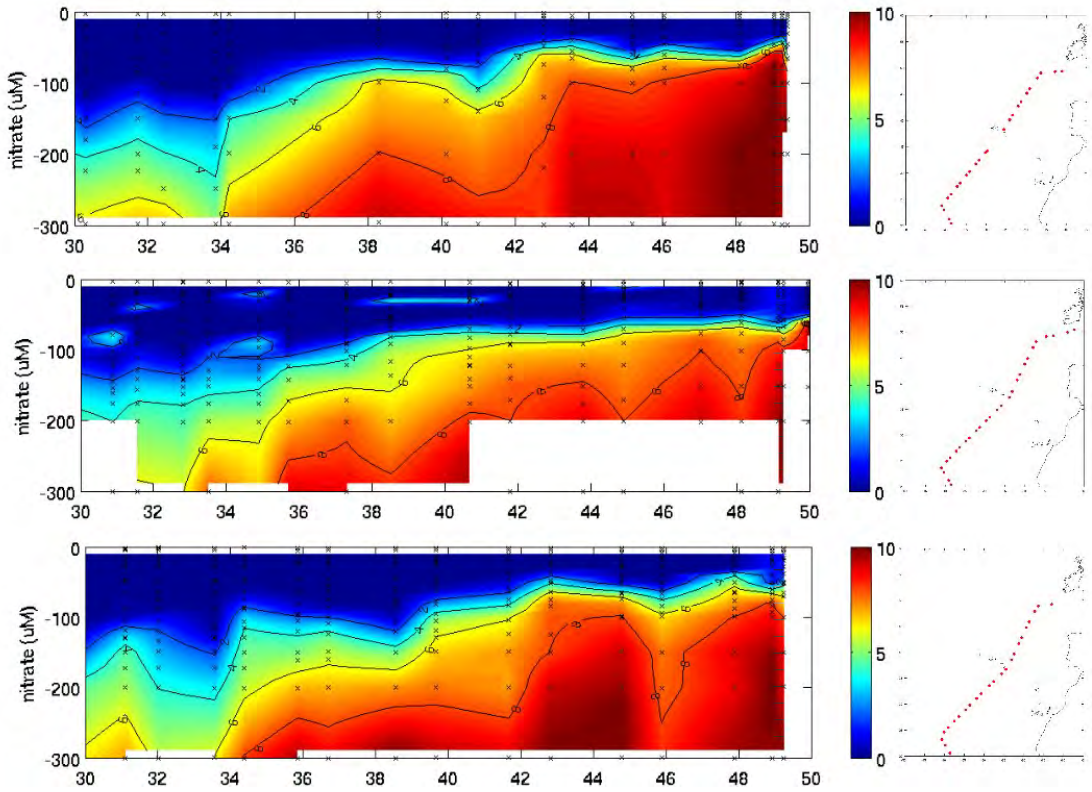

Figure 4-5 Meridional sections of nitrate concentration (µM) from the AMT cruises of 2010 (top), 2011 (middle) and 2012 (bottom). All cruises were between September and October.

Interannual variability of MLD between 35 and 45 °N ranges between 100 m and 400 m. To the south of the Azores islands (~38 °N), MLD is typically shallow, but winters with MLD of 150-200 m were observed in model and in-situ data. However, SCHL rarely reached 0.4 µg/L. Only in some years, when the MLD was greater than 200 m did SCHL reached 0.4-0.6 µg/L. Conversely, to the north of 38 °N, a MLD of 200 m can result in SCHL greater than 1 µg/L and shallower MLD are rare. In 1999, there was an exceptional shallow MLD of 100-150 m and SCHL maximum was greater than 0.8 µg/L. In Figure 4-6 is shown the annual maximum MLD (from the SODA model) and annual mean SCHL (SeaWiFS) in 1998 and 1999. In 1998, note the deep MLD between 35-40 °N to the southwest of Azores and the lower SCHL, while at 40 °N the MLD is shallower and

SCHL is higher. In 1999, there was an exceptional shallow MLD of 100-150 m to the north of 40 °N and SCHL still was higher. This indicates that the effect of MLD on SCHL is geographically different.

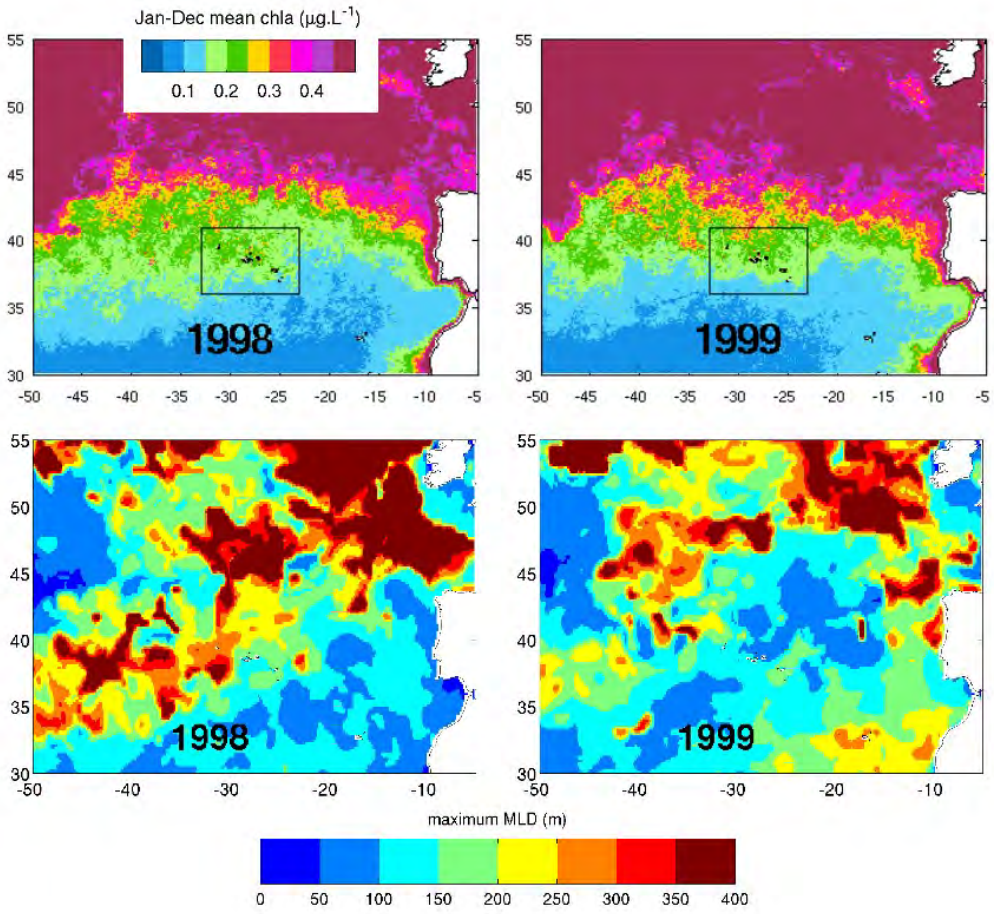

Figure 4-6 Annual mean of SCHL in 1998 (top left) and 1999 (top right) from SeaWiFS data. In the bottom, annual maximum MLD in 1998 (bottom left) and 1999 (bottom right) from SODA model.

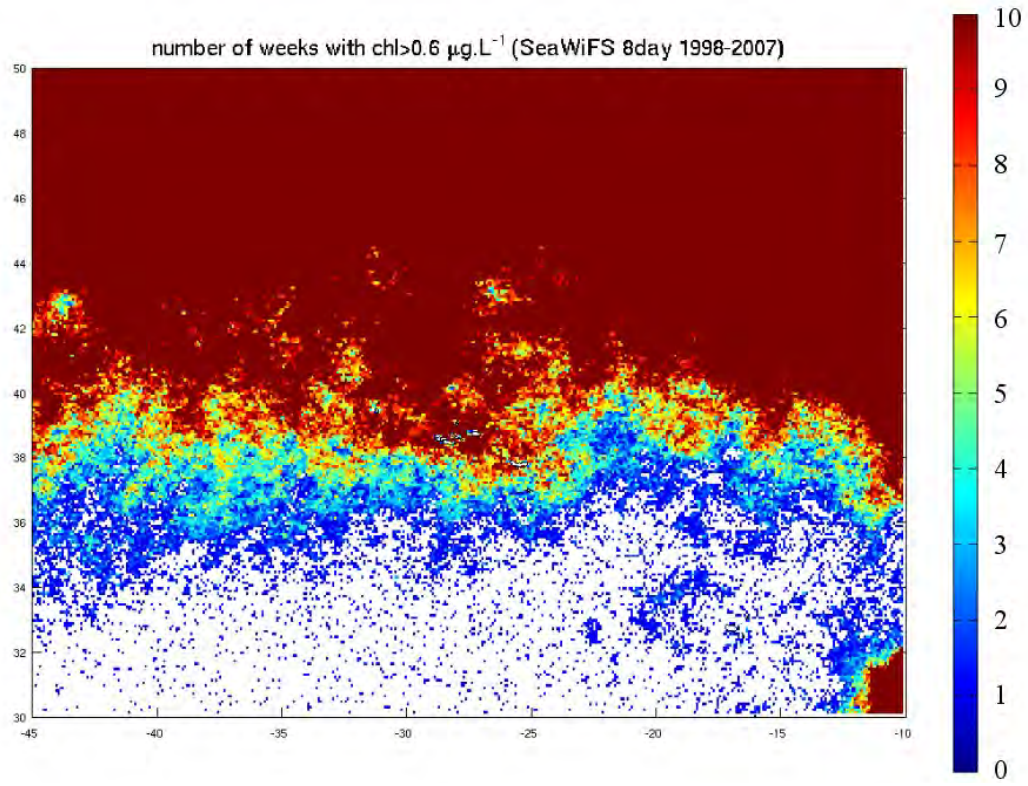

Figure 4-7 Number of weeks between 1998-2007 a given pixel had SCHL higher than 0.6 µg/L. Derived from SeaWiFS weekly data.

The number of weeks a given pixel was higher than 0.6 µg/L during 10 years (1998-2007) of weekly satellite SCHL maps from SeaWiFS is shown in Figure 4-7. Pixels that never reached 0.6 µg/L are masked. To the south of 34 °N the value of 0.6 µg/L was never reached in 10 years, while to the north of 38 °N it was commonly reached. There is a remarkable match with the location of the subtropical front at 34 °N. The changes in the subsurface nutrient at 34 °N are shown in Figure 4-5. Even at latitudes between 34-37 °N, the number of weeks a pixel was higher than 0.6 µg/L are considerably lower than at 38 °N. Although there is a rapid change in MLD at these latitudes, it is possible that the nutrient subsurface field is also low between 34 and 38 °N, related to the mixing with waters to the south of the subtropical front. In fact the abrupt changes around 40 °N, with waters easily reaching 0.6 in each year, are more closely related to the short spatial scales of oceanic fronts that separate different water masses, than the larger spatial scales of MLD variability. Another interesting feature to the southwest is the southwest-northeast tilt in the pattern of pixels higher than 0.6 µg/L. This band is probably related the typical deep MLD of this region which are able to supply more nutrients to surface waters, despite the low subsurface nutrient field.

The questions that now arise are: 1) why is the subsurface nutrient field higher north of 40 °N, 2) what is the spatial distribution of the subsurface nutrient field, and 3) why along a given latitude (e.g. 40 °N) annual SCHL is the same, despite the maximum MLD decreases to the east. To investigate the spatial distribution of the subsurface nutrient field it is shown in Figure 4-8 the WOA05 climatological nitrate field of the summer months (July-September) averaged over 200-300 m (left) and 0-200m (right). As in Figure 4-5, summer months were chosen for the analysis. The contours of summer temperature averaged at 200-300 m from the WOA05 climatology are superimposed in the nitrate field.

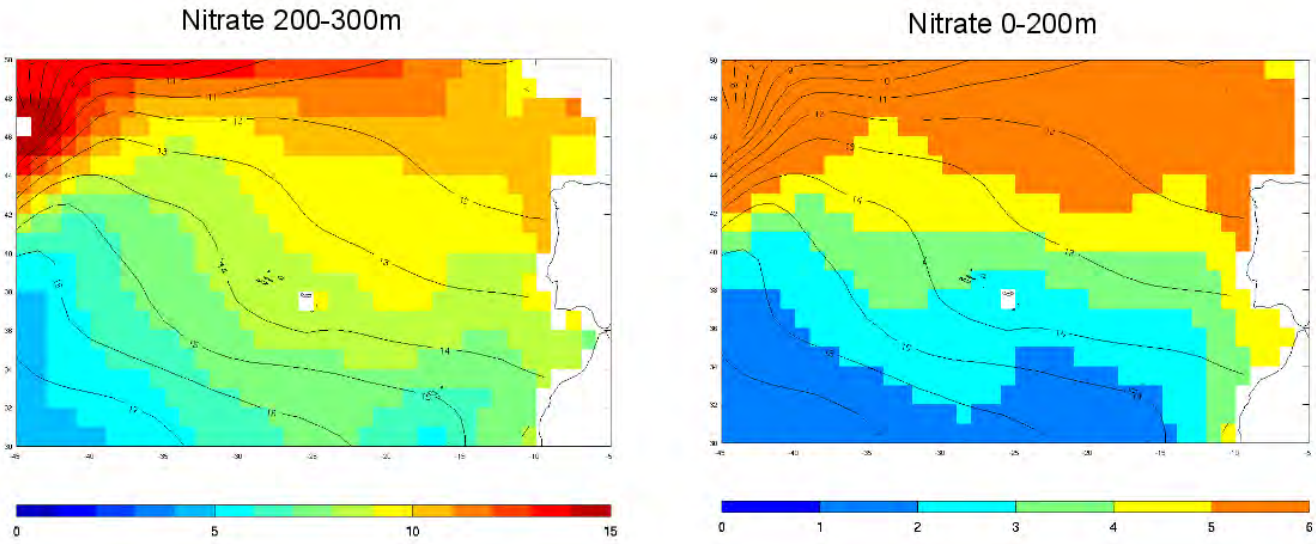

Figure 4-8 Climatological nitrate concentration (µM) during the summer months (July-September) between 200-300 m (left) and 0-200 m (right). The climatological isolines of temperature (at every 1 °C) during the summer months at 200-300 m are superimposed in the nitrate filed. Both nitrate concentration and temperature fields were computed from the WOA05 monthly climatology.

In the nitrate field at 200-300 m (Figure 4-8 left) there is a northwest-southeast orientation of the nutrient field, which is likely a consequence of the mixing that occurs in Gulf Stream (Palter et al., 2004; Pelegri, 2006; Williams et al., 2011). The mixing occurs between the warm, saline and low surface nutrient subtropical water masses and the cold, fresh and high surface nutrient subpolar waters. The nutrient-enriched mixed waters are than advected by the NAC southern branches southeastward or northeastward, and irrigate the region with nutrients. The direction of the average flow can be seen in the contours of temperature at 200-300 m. The nitrate field in the first 200 m (Figure 4-8 right) as similar patterns, but the northwest-southeast tilt is less present. In fact, at 40 °N, at depths of 200-300 m, the eastern basin as a higher nitrate concentration, but in the first 200 m

the nitrate is similar in both basins. This is discussed in the following paragraphs. The average nitrate in the first 200 m (Figure 4-8 right) can be interpreted as the available nitrate for production if all the North Atlantic had a winter maximum MLD of 200 m. Although it illustrates the control of the subsurface nutrient field, a MLD of 200 m is unrealistic for some parts of the ocean.

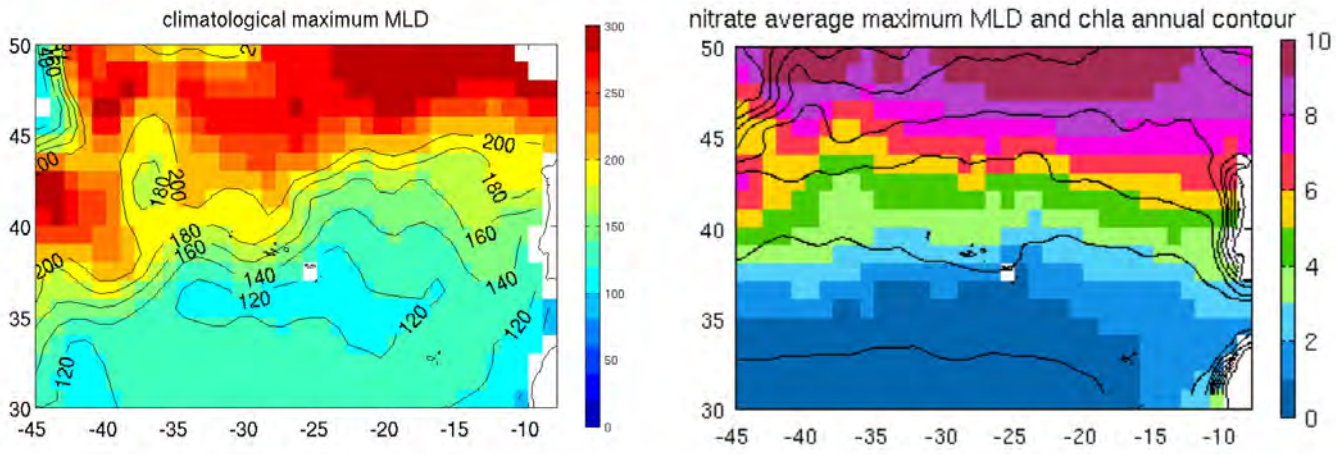

Figure 4-9 Left: climatological annual maximum MLD derived from the climatology of De Boyer Montégut et al (2004). Right: maximum winter surface nitrate concentration (µM) superimposed with the annual mean SCHL climatology isolines every 0.1 µg/L. The maximum winter surface nitrate concentration was computed by averaging the annual nitrate concentration climatology during the summer months at the depths of the annual maximum MLD climatology (this figure, in the left side). The annual mean SCHL climatology was derived from SeaWiFS data between 1998-2007 (and the map is shown Figure 4-4).

For a more realistic analysis of the nutrient supplied to the surface by winter mixing, the climatological fields of MLD and nitrate are combined. In Figure 4-9 (left) it is shown the climatological maximum MLD calculated from De Boyer Montegut (2004) monthly climatology. The band with high MLD indicates the track of the midlatitude depressions. Interestingly, the northwest-southeast orientation of the nutrient subsurface field at 200-300 m (Figure 4-8 left) is nearly perpendicular to the southwest-northeast orientation of the spatial field of maximum MLD (Figure 4-9 left). The combination of these two fields, provide the climatological winter surface nitrate available for phytoplankton growth in each year. This is shown on Figure 4-9 (right), by averaging the summer climatological nitrate field over the depth of maximum climatological MLD which occurs in winter (Figure 4-9 left). The contours of the climatological annual SCHL between 1998-2007 (shown in Figure 4-4 left) are superimposed in the nitrate field. The nearly match of

both SCHL and nitrate (as a function of subsurface nutrient field and MLD), supports the hypothesis that these two factors are important in regulating the spatial patterns of biological production in the midlatitude region of the North Atlantic. It provides an explanation for why in the southwest part of the region despite deep MLD, SCHL is lower (Figure 4-6, see 1998). That is, in the southwest region, although MLD is deeper, there are less nutrients at depth than at 40 °N.

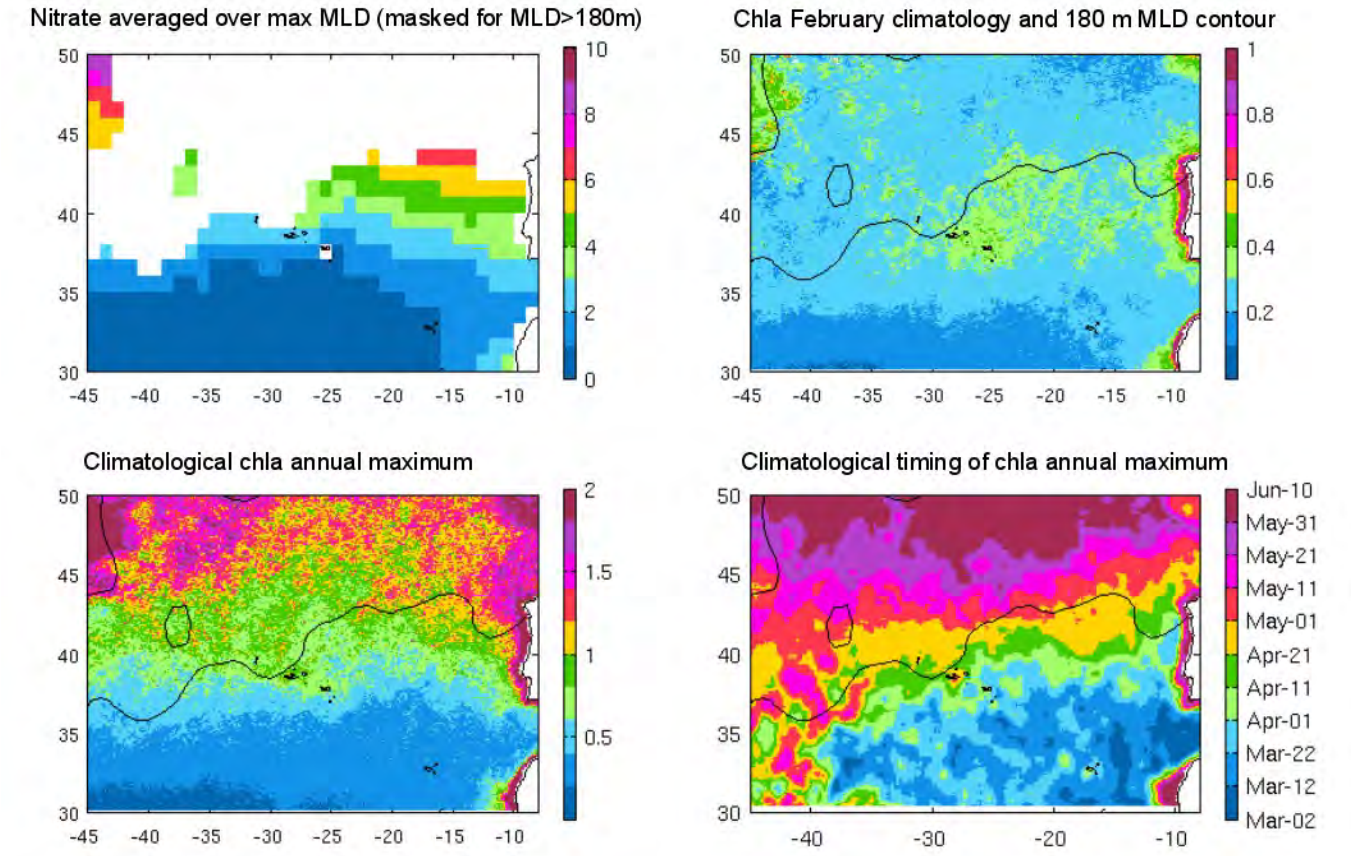

Figure 4-10 Top left: maximum winter surface nitrate concentration (μM) (as in Figure 9 right), but the area with MLD greater than 180 m was masked. Top right: monthly climatology of SCHL in February. Bottom left: annual maximum climatology of SCHL. Bottom right: climatology of the timing of the annual maximum of SCHL. All the three fields of SCHL (top right, bottom left and bottom right) were derived from SeaWiFS data between 1998-2007 and are superimposed by the climatological annual maximum MLD 180 m isoline derived from the monthly climatology of De Boyer Montégut et al (2004).

The band with high SCHL between the Azores and Western Iberia, which appears to correspond to the midlatitude regime of LEV05, is discussed in the context of the subsurface nutrient field. In Figure 4-10 (top left) it is shown the nitrate averaged over the maximum MLD (same as Figure 4-9, right) with all MLD greater than 180 m masked. In Figure 4-10 it is also shown the SCHL February climatology (top right), the SCHL annual maximum climatology (bottom left) and the timing of SCHL annual maximum (bottom right). The fields of SCHL are superimposed by the climatological annual maximum MLD 180 m isoline derived from the climatology of De Boyer Montégut et al (2004). The interpretation can be as follows. First, during winter to the north of the MLD 180 m isoline; production is inhibited, which results in a lower SCHL (top right). To the south of the MLD 180 m isoline, production continues throughout the winter. The region between Azores and Western Iberia shows higher SCHL in comparison to the south (top right). To the south, the lower SCHL is likely to be influenced by shallower MLD (as seen in Figure 4-9, left), but also have a contribution from a poorer subsurface nutrient reservoir. The higher SCHL between 40 °N and the 180 m MLD isoline (Figure 4-10, top right), can be related to a deeper MLD (~120-150 m, Figure 4-9 left), but also a consequence of a higher subsurface nutrient field (Figure 4-8). The pattern of the spring bloom timing (Figure 4-10 bottom right) matches the pattern where the MLD was deeper than 180 m, therefore production can only start later during spring stratification.

In Figure 4-11 and Figure 4-12 two patterns are shown: 1) the decrease of SCHL during the winter months in regions where the MLD is deeper, and 2) the midlatitude regime (band with higher SCHL between Azores and Western Iberia). These patterns are illustrated by SCHL February averages superimposed with the MLD from in-situ (Figure 4-11) and model data (Figure 4-12). Regions with deep MLD (200 m in in-situ data and 160 m in model data) show less SCHL. As previously suggested, in regions with MLD lower than 200 m, the pattern of SCHL is controlled by the couple effect of MLD and the subsurface nutrient field.

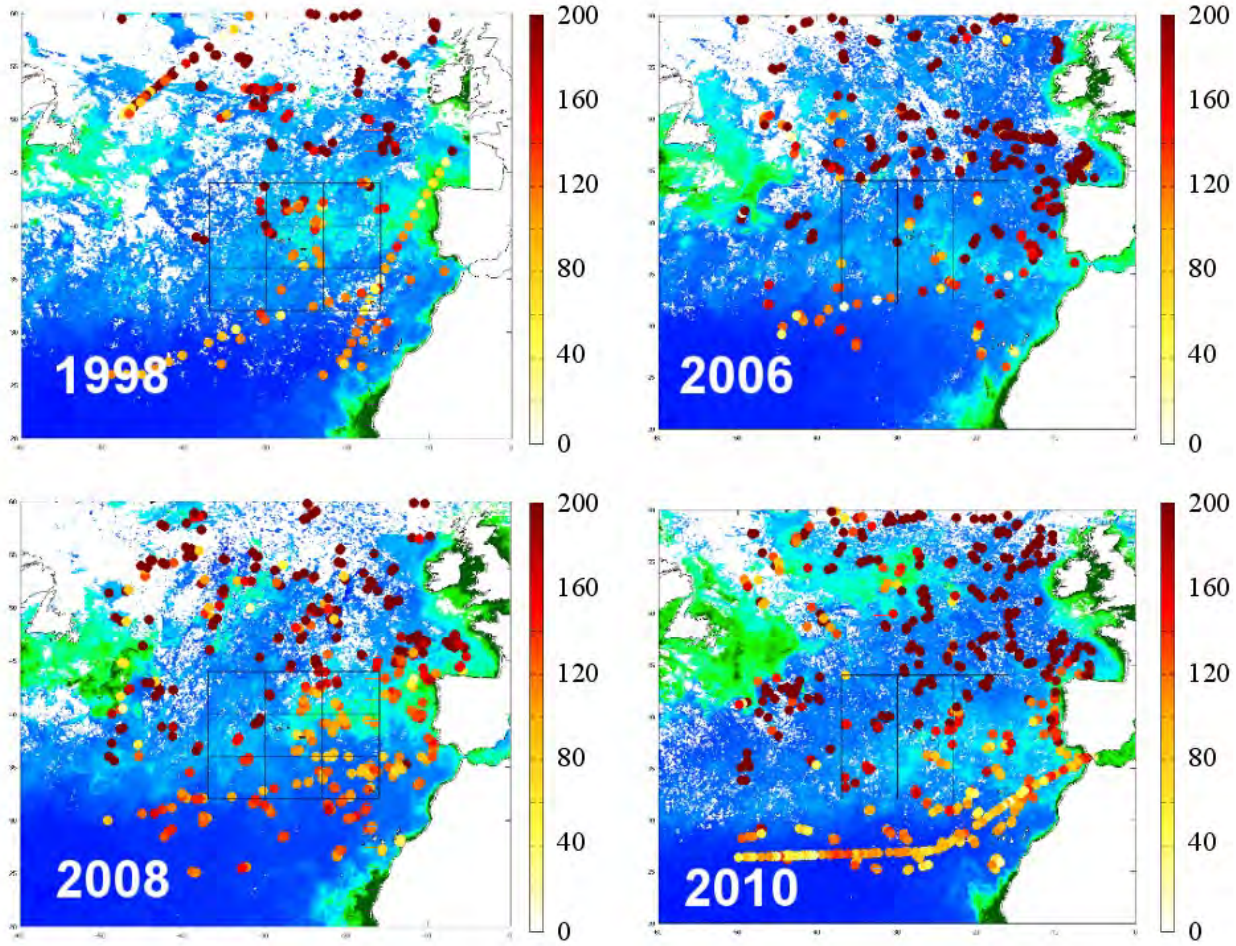

Figure 4-11 Monthly mean SCHL during February derived from SeaWiFS (1998) and MODIS AQUA (2006, 2008, and 2010). The dots correspond to MLD derived from the temperature of in-situ profiles available during February of each year in the GTSPP dataset. The MLD was calculated by the depth at which the temperature varied by 0.3 °C from the surface temperature.

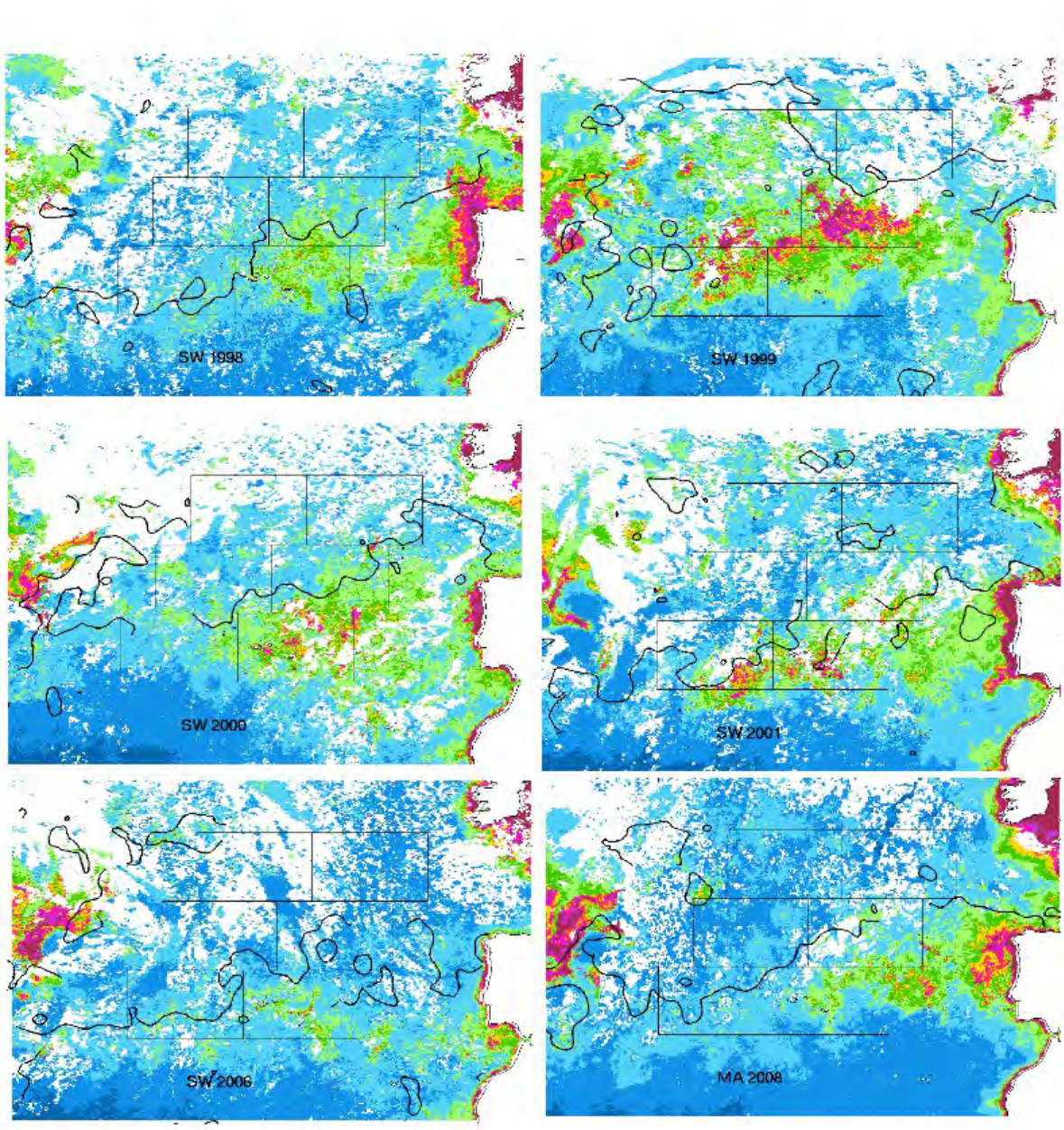

Figure 4-12 Monthly mean SCHL during February derived from SeaWiFS in 1998, 1999, 2000, 2001 and from MODIS AQUA in 2006 and 2008. The black line is the MLD contour of 160 m derived from the the temperature field in the MERCATOR model. The MLD was calculated as in Figure 4-11.

In resume, the subsurface nutrient content is regulated by mixing in the Gulf Stream and advected by the NAC and AC (Pelegri, 2006; Williams et al., 2011). Consecutive winters of deep MLD characteristic of the regions surrounding the Gulf Stream combine with the subsurface nutrient field to define the nitrate in the top 200 m. This way, waters found at 40 °N, have been moderately mixed in the Gulf Stream, maybe reached latitudes of 45 °N, underwent severe surface mixing during following winters, and then followed a south-eastward route to 40 °N. To the south of 34 °N, water masses have not been properly mixed in the Gulf Stream, remaining nutrient-poor waters, and the consecutive winters of deep mixing in the southwestern area are not efficient in increasing surface nutrient (0-200 m). The subtropical front and its associated current system Azores Current (AC), than efficiently separates these water masses, the subpolar rich in nutrients and the subtropical poor in nutrients. Other horizontal advective sources of nutrients include westward advection of nutrients from the Western Iberia upwelling system by mesoscale features (Le Cann et al., 2005) and by the counter current of AC (Alves et al., 2002). This section provided evidence that the MLD alone does not explain the annual SCHL pattern in the region and that the pattern can be explained by the coupled effect of MLD and nutrient subsurface field, being the latter defined by the ocean circulation.

4.4. Seasonal dynamics in the Azores region

The seasonal cycle of SCHL in the Azores is a result of the low and high rates of phytoplankton growth in summer and winter-spring, respectively. According to the ecological models of Longhurst (2006), biological production in the Azores can vary between the “Winter–Spring Production with Nutrient Limitation” and “Nutrient-Limited Spring Production” cases. The first case describes a seasonal cycle in regions of the ocean where production is not limited in winter due to a shallow MLD. The second case is related to regions where production is interrupted during winter as a result of a deep MLD.

The seasonality of SCHL in the region can be better understood starting in summer. In late summer (August-September), to the south of 45N, the open ocean is characterized by a shallow mixed layer depth (~30 m), very low surface SCHL concentrations (0-0.2μg/L) and nearly zero surface nitrate concentration (climatological end of summer nitrate concentration at surface is ~0.001 μM). During autumn and winter, the mixed layer deepens and a limited stock of nutrients (from Figure 4-9 right side, less than 1 μM in the southeast and up to 3 μM in the northwest) is supplied to surface waters from the mixing of deeper nutrient-rich waters. If the winter mixed layer depth is shallow (< 200 m)

production continues through winter. If the mixed layer depth is deep (> 200 m) production can be limited by light and it is interrupted during this period. During spring, weaker winds and stronger solar irradiance, form a shallow thermally stratified layer at the surface of the ocean (the “seasonal thermocline”). This stratification at the surface provides the ideal conditions for primary production, by trapping phytoplankton populations in very illuminated waters, with moderated-high concentration of nutrients. Phytoplankton than starts to grow and multiply, consuming the available nutrients. As summer advances, the seasonal thermocline gets progressively stronger and shallower, acting like a barrier between deeper and surface waters. During summer, this surface layer is never mixed with deeper waters, therefore never refilled with nutrients from below. Even during strong winds the thermal stratification strongly constrains any significant (>50 m) vertical wind-induced mixing. Without any nutrient supply from below, phytoplankton eventually consumes all available nutrients, diminishing the stock of nutrients to nearly zero. The initial content in nutrients is therefore completed depleted by late summer due to biological consumption and phytoplankton starves, decreasing their biomass to minimum values in late summer. These conditions are called “oligotrophic conditions”, resulting in clear blue waters. Interestingly, as surface phytoplankton biomass decreases, a simultaneous increase in chlorophyll a concentration occurs bellow the seasonal thermocline around 50-100m, denominated the deep chlorophyll maximum (DCM). Since satellite only observes the first tenths of meters, it is not possible to observe this feature from the space. The DCM constitutes a widespread phenomenon in the world oceans and may be formed through a variety of mechanism including accumulation of cells from overlying waters, differential sinking rates, physiological photo acclimation and enhanced in situ growth sustained by nutrient diffusion through the thermocline (e.g. Cullen, 1982; Gould, 1987). As for the minimum SCHL during summer, it is higher to the north, which can be explain in terms of a higher stock of nutrients and a later initiation of the consumption. Another explanation is that the light levels in northern latitudes are too low to force a full consumption of the available nutrients in summer. In late summer the oligotrophic conditions come to an end, when the first storms and convective mixing start to erode the seasonal thermocline and the annual cycle starts again.

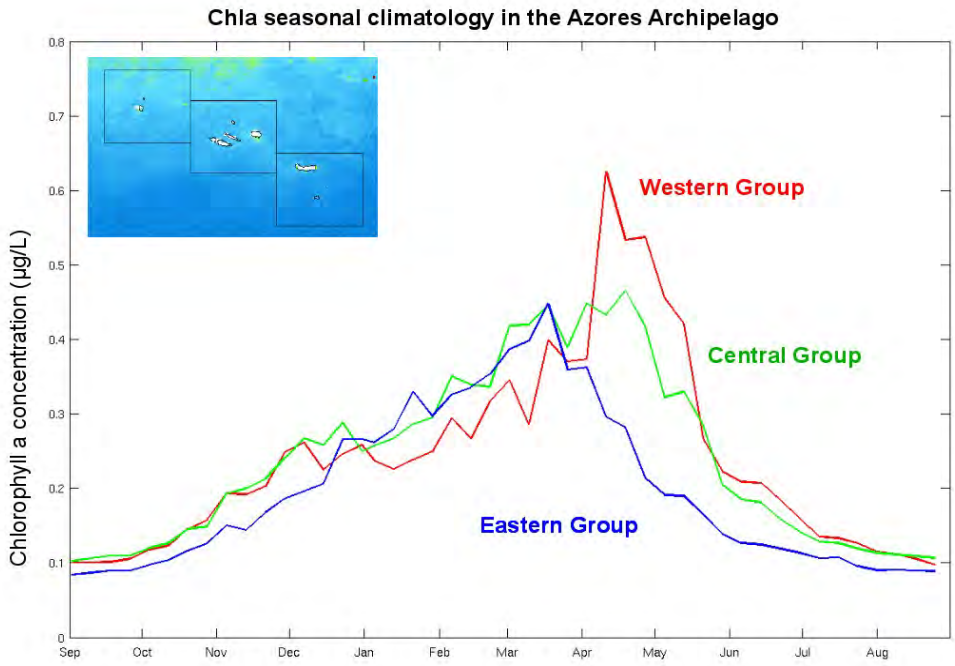

Figure 4-13 Climatology of the seasonal cycle of SCHL in the Azores region. Computed from SeaWiFS weekly data between 1997-2007. The boxes for the Western Group (38.5-40.5 °N and 29.5-32.5 °W), Central Group (37.65-39.65 °N, 26.5-29.5 °W) and Eastern Group (36.2-38.2 °N, 23.5-26.5 °W) are illustrated in the top left map.

The seasonal cycle of SCHL in each group of the Azorean islands is shown in Figure 4-13. In the Western Group, the SCHL during winter is lower than in the other groups, but have a strong bloom in April. From the previous section, it is clear that the MLD just to the west of islands is sufficiently deep to decrease SCHL during winter (Figures 4-10, 4-11, 4-12). In the Central and Eastern Group, SCHL increases from summer to winter, without a decrease in winter. In spring the Central Group as higher SCHL than the Eastern Group, which might be related to differences in MLD and ambient water masses with different subsurface nutrient fields.

Starting in autumn, the first storms, through convection and wind stirring cause a deepening of the mixed layer and an increase in surface chlorophyll-a concentration. This autumn increase is described in the literature as the “fall”, or “entrainment” bloom, and is typically related to the input of nutrients from bellow the seasonal thermocline (e.g. LEV05). One other reason, rarely mentioned, is the upward transport of phytoplankton cells from the DCM, by the autumn vertical mixing, and therefore not necessarily related to an increase in primary production. The southern propagation of the autumn bloom is illustrated in Figure 4-1 by the southward displacement of the

0.2 µg/L SCHL isoline between October and December. The timing of the fall bloom is proposed by LEV05 as the time when the mixed layer reaches the nutricline depth. In addition it was also suggested by LEV05 that this propagation is driven by the nutricline meridional gradient (the nutricline being shallower in the north than it is in the south), and not so much by the southward propagation of the mixed layer deepening (which is much more rapid). Again, these authors do not mention the close coupling between the nutricline and the DCM (e.g. Teira et al 2005), and that the DCM also has a meridional slope (e.g. Strass and Woods, 1991). Despite the possibility of increase in SCHL in autumn might actually be related to the mixing of the DCM and therefore not necessarily a result of phytoplankton growth from the injection of nutrients, the terminology of "fall" bloom will be used.

The exact timing of the SCHL increase in autumn is illustrated in Figure 4-14. In this figure it is shown the Qnet, SCHL and MLD. Qnet is calculated from the daily air-sea fluxes from NCEP reanalysis. A negative Qnet represents a loss of heat from the ocean. SCHL is from the weekly fields of SeaWiFS (year 2001) and MODIS AQUA (year 2011) data. Weekly MLD is from the models SODA (for 2001) and FNMOC (for 2011). The black dots are MLD calculated from in-situ profiles in the GTSPP dataset. The area corresponds to the northwest (38.5-41 °N, 28-33 °W) quadrant of the Azores Archipelago. It is shown in Figure 4-14 that the SCHL increases simultaneously with the loss of heat from the ocean and that this is accompanied by a small increase in MLD. The year of 2001 was anomalous because the autumn was very mild, with a very late decrease in Qnet. In 2011, the decrease in Qnet occurred earlier and there was also a fast response in SCHL. The years of 2001 and 2011 serve as an example, but almost all years show the same match between Qnet, SCHL and MLD. This shows an agreement between SCHL and the erosion of the seasonal thermocline, through heat loss at the surface.

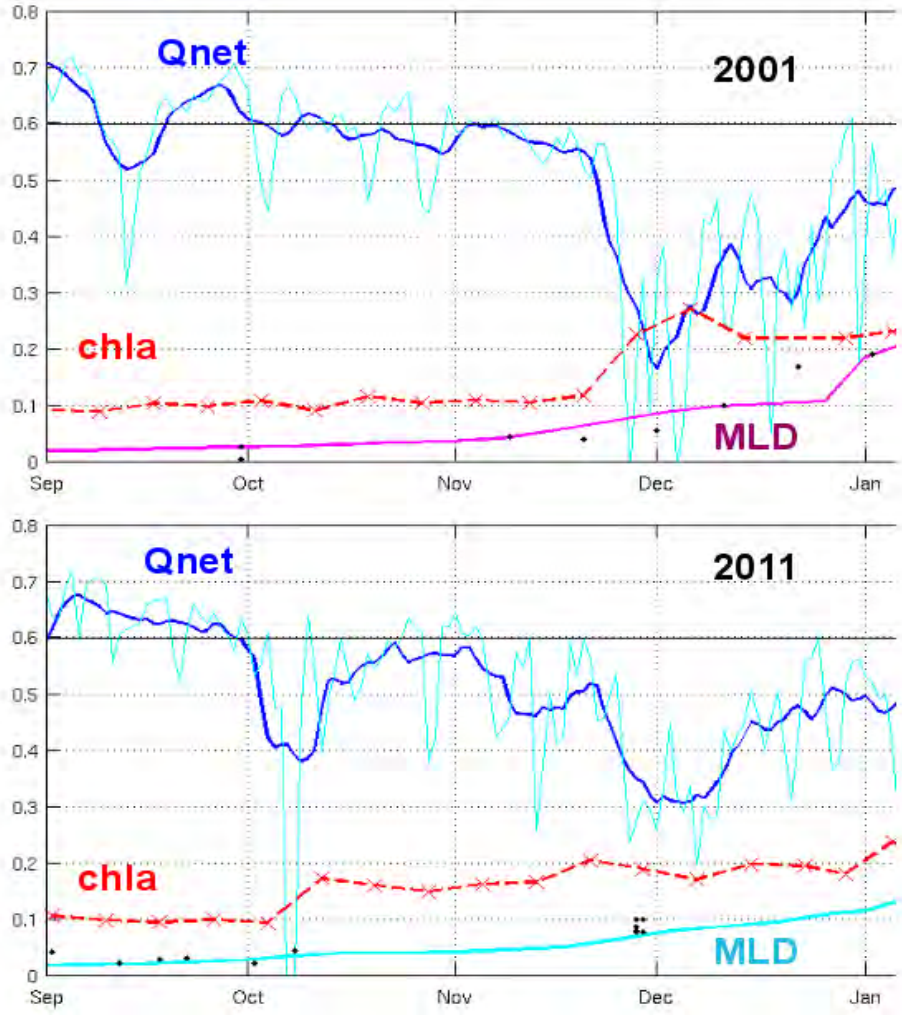

Figure 4-14 Timing of the "fall" bloom for 2001 (top) and 2011 (bottom) in the northwest (38.5-41 °N, 28-33 °W) quadrant of the Azores Archipelago. The red line is the weekly SCHL (only weeks with more than 10 % valid pixels are shown) derived from SeaWiFS in 2001 and from MODIS AQUA in 2011. The blue and cyan lines are the 8-day running mean and daily time series of Qnet, respectively. Qnet was computed from NCEP reanalysis data interpolated to a 0.5 ° grid. Positive Qnet indicates ocean heat gain. The black line represents Qnet=0. The weekly MLD from SODA in 2001 (magenta line) and FNMOC in 2011 (cyan line) is also shown. The black dots are MLD calculated from in-situ profiles in the GTSPP dataset. The MLD was calculated by the depth at which the temperature varied by 0.3 °C from the surface temperature. The y axis represents the units of SCHL in µg/L, of Qnet in [(yaxis*1000)-600] W/m2 and MLD in [yaxis*1000] m.

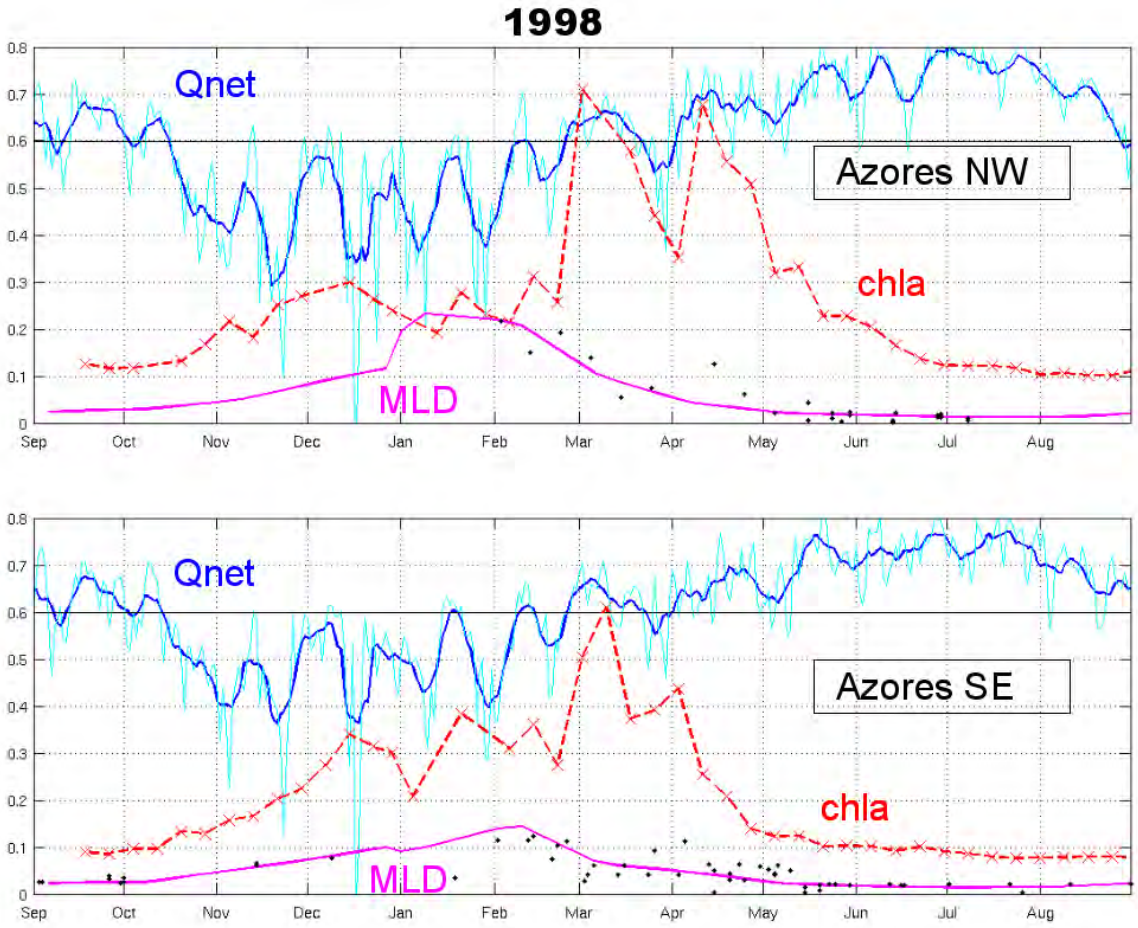

Figure 4-15 Seasonal cycle of SCHL for 1998 in the northwest (38.5-41 °N, 28-33 °W) and southeast (36-38.5 °N, 23-28 °W) quadrants of the Azores Archipelago. The SCHL from SeaWiFS (red line), Qnet from NCEP (blue and cyan lines), MLD from SODA model (magenta line) and MLD from GTSPP in-situ data (black points) were computed as in Figure 4-14.

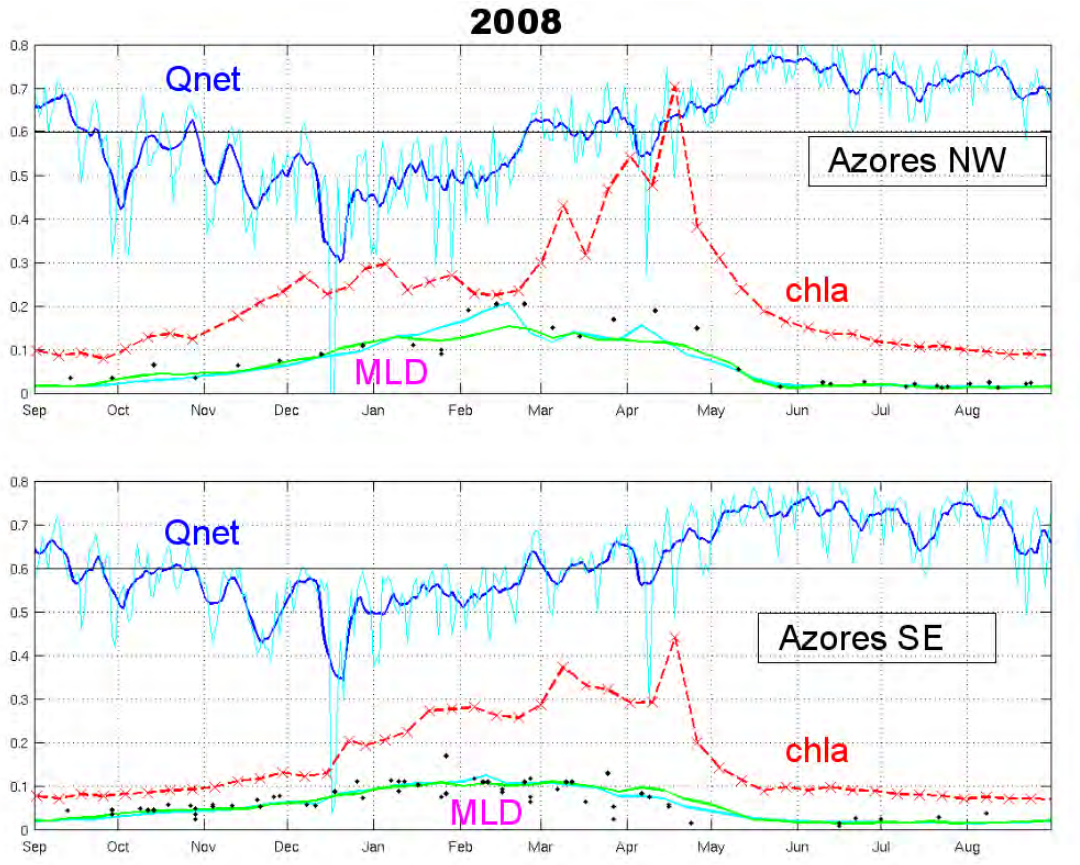

Figure 4-16 The same as Figure 4-15 but for 2008. The exceptions are that SCHL was derived from MODIS AQUA and the MLD was derived from TOPS (green line) and FMOC (cyan line) models.

The full seasonal cycle for 1998 and 2008, is show in Figure 4-15 and 4-16, respectively. In each figure, the top and bottom corresponds to the northwest and southeast quadrants of the Azores Archipelago region, respectively. Both years show similar patterns and are given as examples since all years show similar patterns. After autumn SCHL gradually increases to a platform around 0.3 µg/L. In winter, if MLD exceeds 150-200 m SCHL will tend to decrease/maintain, if it is shallower SCHL continues to increase until spring. In the southeast region, the MLD is shallower (~100m) and SCHL increases gradually, with the episodic increases of SCHL matching the periods of zero Qnet. In contrast, the northwest region decreases its SCHL during a deeper MLD (>200 m) and the spring increase occurs when Qnet is largely positive. The response of SCHL in the northwest region to Qnet appears to be not so fast as in the southeast, possibly because of the dilution of phytoplankton in the water column. The overall relation between the timing of the spring bloom and the timing Qnet changes to positive values is resumed in Figure 4-17, where the time series of SCHL in the entire Azores Archipelago is overlaid with the timing Qnet switches from negative to positive values (vertical line). The dates of this change are shown in the top of the figure.

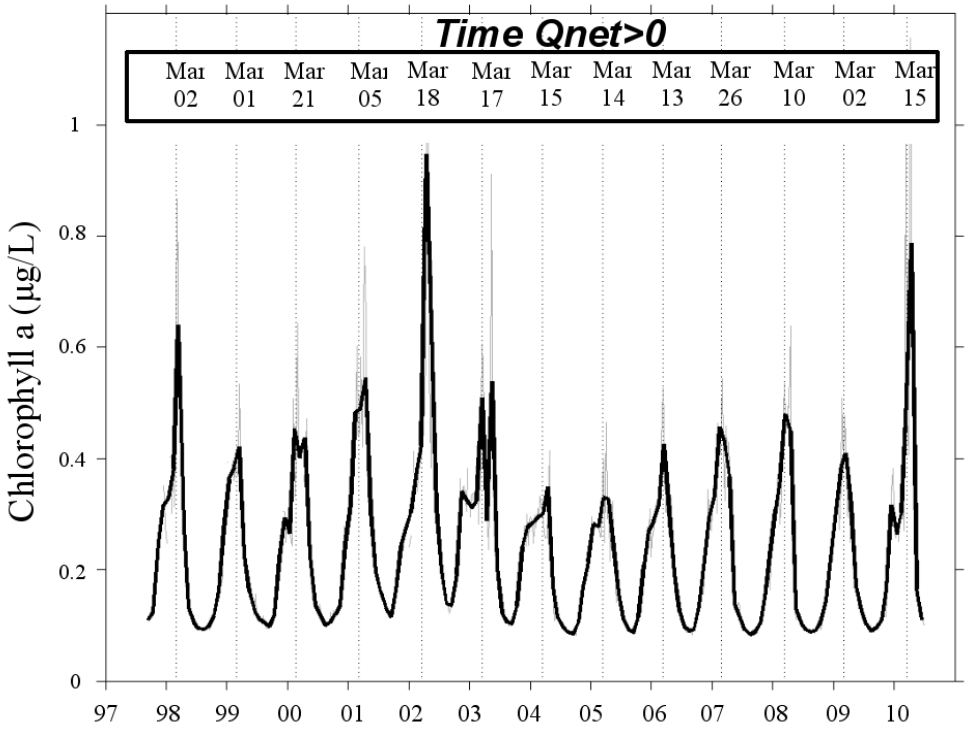

Figure 4-17 The time Qnet switches from negative to positive values (vertical line) and the time series of SCHL (monthly in black line and weekly in grey line) in the Azores Archipelago (36-41 °N, 23-33 °W) from weekly SeaWiFS (1997-2002) and MODIS AQUA (2003-2010). The daily Qnet data is averaged over 7 days and a running mean over 4 weeks is applied. The date when Qnet> 0 is shown in the top.

The decrease in SCHL during winter is typically observed in the western group, but other regions can also have MLD higher than 200m. Accordingly to Sverdrup (1953), in regions with deep MLD, to occur a bloom, it requires the MLD to get shallower than a critical depth, which in the Azores is between 30 and 50 m (see Figure 4 of Follows and Dutkiewicz, 2001; and Figure 6 of Townsend et al., 1994). Other hypotheses for the initiation of spring blooms do not require a mixed layer shoaling, such has when the mixed layer turbulence decreases, allowing phytoplankton to grow within a deep, but weakly mixed layer (Townsend et al., 1992; Taylor and Ferrari, 2011). This mechanism occurs in the absence of convective mixing, such as in end of winter, when the daily average heat flux across the air-sea interface tends to zero (Qnet=0). During this period, apart from nocturnal periods of convective mixing, the only other source of energy for deep vertical mixing is the wind. Taylor and Ferrari (2011), do not even account for wind mixing (which the depth of influence is a topic of debate) and suggests that the transitional period of Qnet=0, is sufficient to

trigger an increase in phytoplankton population. In this work, it is found a match between periods of no convection (Qnet=0) and spring SCHL increases. These results are in agreement with the turbulence hypothesis (e.g. Taylor and Ferrari, 2011) since the MLD appears to be around 100 m during the episodic SCHL increases. As stated by LEV05, the euphotic depth of around 100 m in this region, allows phytoplankton populations to stay near the euphotic depth. Although several years show identical patterns, it is not possible to discard the Sverdrup hypothesis, which would require that the observed increases in SCHL are a result of short periods with shallower MLD not captured by the model and in-situ data used in this work.

In the previous section it was discussed the role of the subsurface nutrient field and MLD in shaping the pattern of annual SCHL. There might be differences in the subsurface nutrient field associated with water masses in the region. In fact is common to say that northern waters are colder, fresher and nutrient-richer than southern waters. The nutrient content has been previously discussed and it was suggested to be linked to different levels of mixing in the Gulf Stream and winter mixing. Therefore it is possible that a same MLD could supply different amounts of nutrients to the surface resulting in different levels of biological production. The proximity of the islands to the Azores Current makes the region prone to these effects. In Figure 4-18 it is shown the vertical profile of temperature and salinity for three ARGO floaters dispersed around Azores in the first week of February of 2008. The profiles are part of the GTSPP in-situ dataset. The MLD was calculated for the three profiles and two of them have a MLD of 100 m while a third one to the west has a MLD of 200 m. This is a typical pattern of the region, with shallow (< 200 m) and deep (> 200 m) MLD to the southeast and northwest, respectively. The different water masses in the region can also be observed with two main clusters of data: the cold and fresh profiles from the northeastern floater, and the warm and saline profiles from the southern and western profiles. The meander emerging from the AC is an occasional feature that brings, particularly warm and salty, subtropical waters close to the south of the islands. The southernmost floater is being transported by this meander and shows the drastic differences between water masses in the region. At 150 m there is an almost 2 °C difference between the two profiles in the eastern part of the area. The distance between these two profiles is minimal, but the water masses are completely different. Interesting the MLD is the same, but the SCHL signal is different. Furthermore, the following increases in SCHL (not shown) were higher in the northern waters which resulted in higher annual SCHL in northern side of the islands (Figure 4-19 and 4-20, year 2008). This further supports the role of the subsurface nutrient field. Differences in nutrient supply may create the changes in plankton community structure observed between the two domains (Silva et al., 2013).

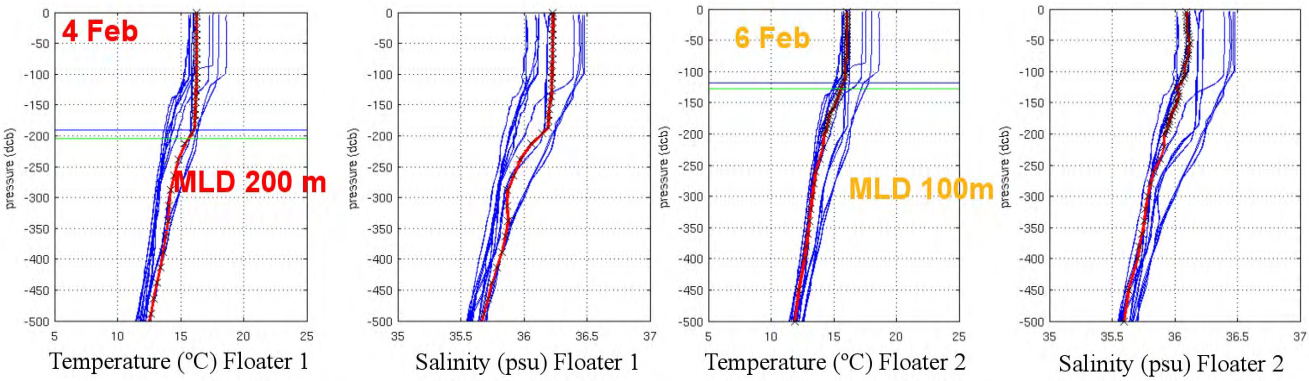

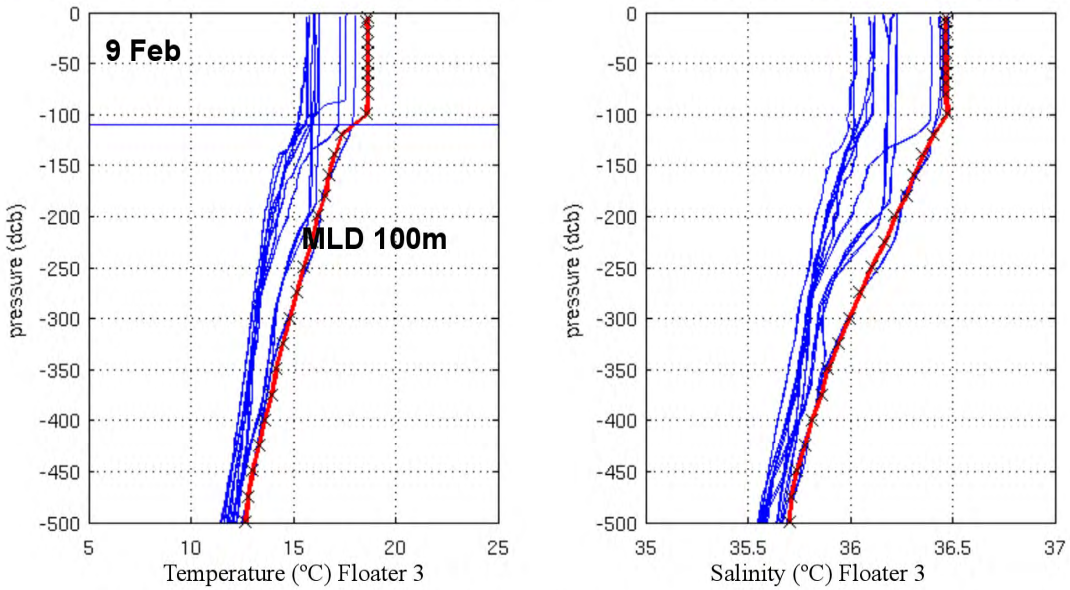

Weekly average of chla and AVISO geostrophic currents in 6 February 2008

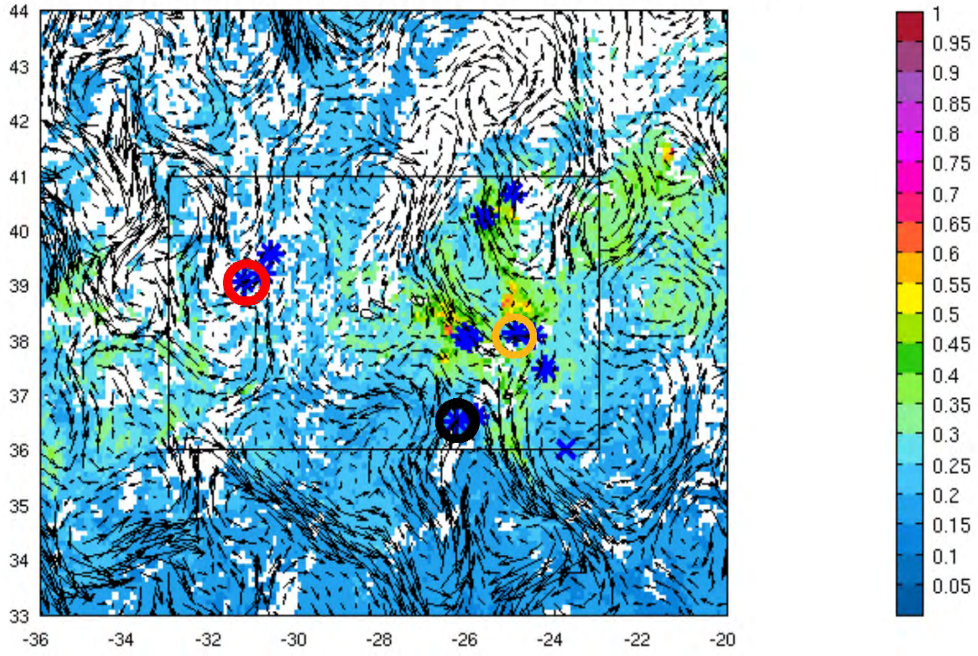

Figure 4-18 Vertical profiles of temperature and salinity from three ARGO Floaters and the weekly average of SCHL from MODIS AQUA superimposed with the currents from AVISO altimetry. The satellite weekly averages are centered on the 6th of February 2008. The Floater 1 (top left profiles and red circle in map), Floater 2 (top right profiles and yellow circle in map) and Floater 3 (enlarged center profiles and black circle in map) are from 4, 6 and 9 of February 2008. The blue and green horizontal lines in each temperature profile shows the MLD, which was calculated by the depth where the temperature varied by 0.3 and 0.5 °C from the surface temperature. The approximate MLD value is shown for interpretation of the figures. The ARGO profiles were available in the GTSPP dataset. All profiles available during February in the box (36-41 °N, 23-33 °W) are shown in blue asterisks in the map.

4.5. Interannual variability in the spring bloom magnitude

In Figure 4-19 is shown the average SCHL in each pixel over the weeks of the first 6 months of the year. In Figure 4-20 is shown the maximum SCHL in each pixel over each year. In Figure 4-21 is shown the average of the previous variables, in the four quadrants of the Azores Archipelago region: northwest (38.5-41 °N, 28-33 °W), northeast (38.5-41 °N, 23-28 °W), southwest (36-38.5 °N, 28-33 °W) and southeast (36-38.5 °N, 23-28 °W). The spatial patterns of the annual maximum (spring bloom magnitude, Figure 4-20) match closely the spatial patterns of the semi-annual mean (Figure 4-19). The reason for such relation is that SCHL has weak interannual variability except for the spring period. Therefore any mean of SCHL over a period that includes the week of the maximum SCHL (spring), will be strongly related to the maximum value achieved in that week. The fact that the average over the first 6 months is well related to the SCHL annual maximum indicates that both methods are appropriate to describe the spring bloom. The mean was favored rather than the median, and the SCHL values were not logarithmic normalized, because the interest is on the spring bloom pattern, and such methods would attenuate the maximum value.

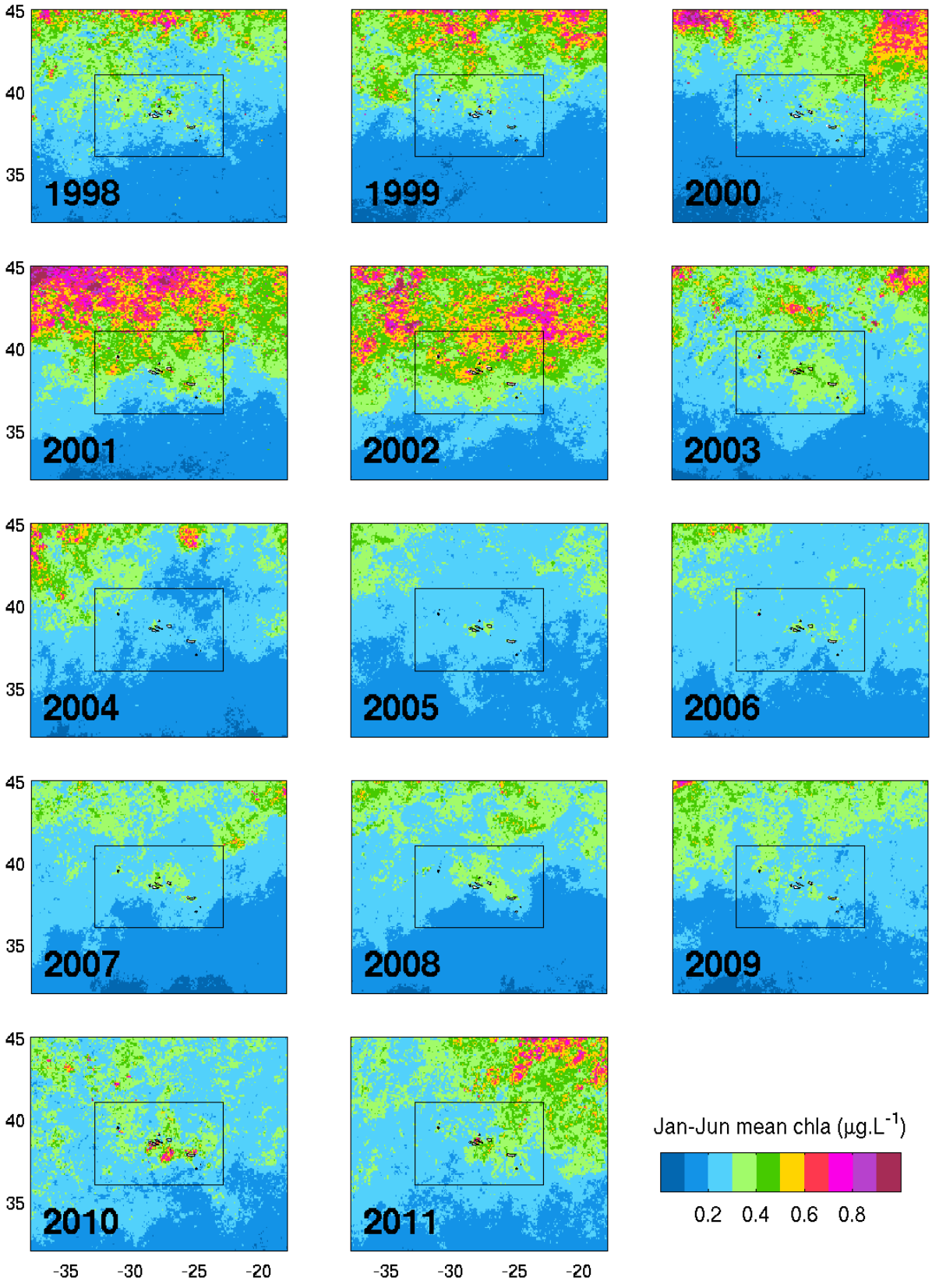

Figure 4-19 Average SCHL between January and June for each year between 1998 and 2011. The fields were derived from SeaWiFS (1997-2002) and MODIS AQUA (2003-2010) weekly data.

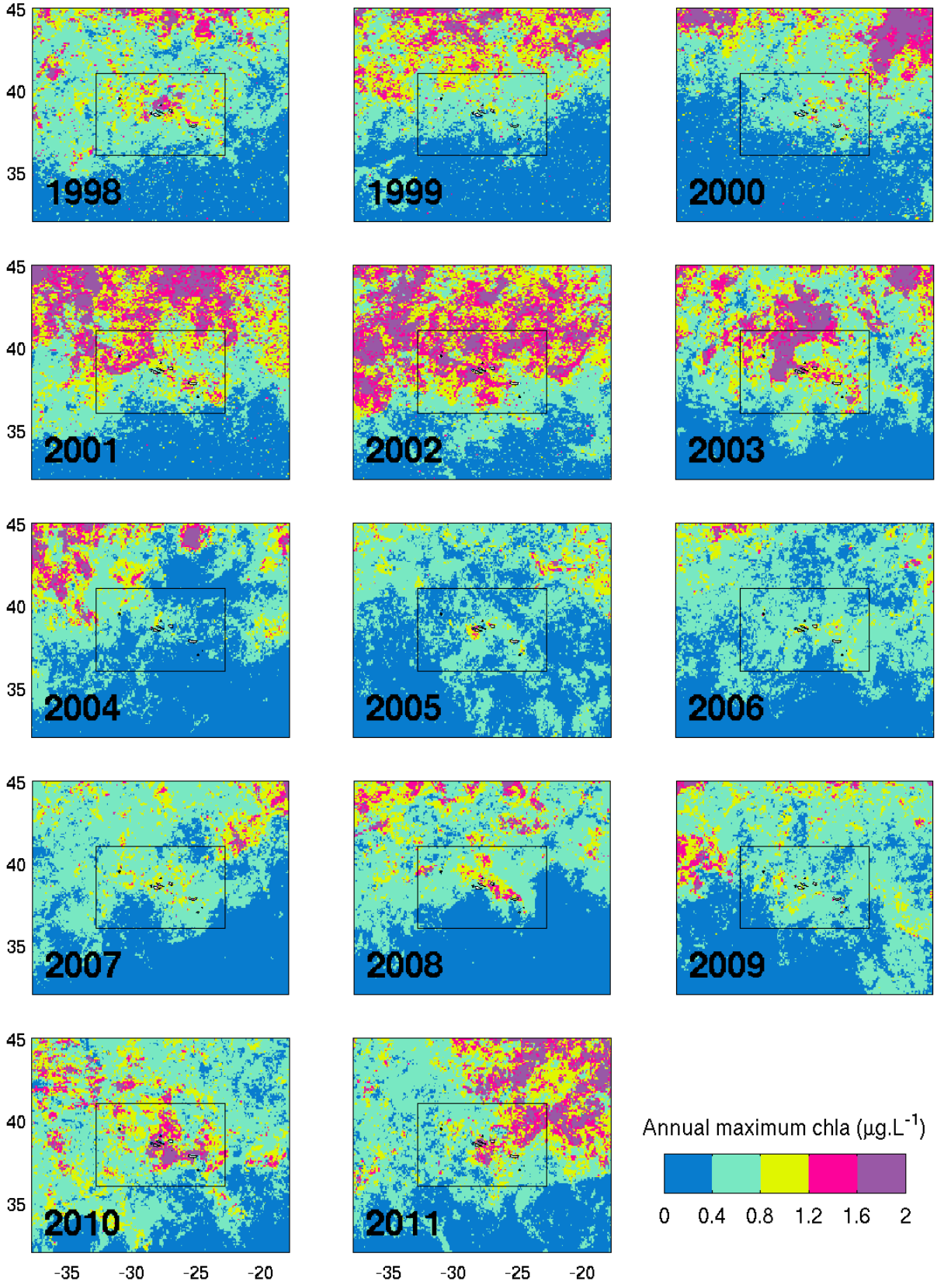

Figure 4-20 Annual maximum SCHL for each year between 1998 and 2011. The fields were derived from SeaWiFS (1997-2002) and MODIS AQUA (2003-2010) weekly data.

Many patterns can be observed from Figure 4-19 and Figure 4-20. First, in all years SCHL is lower to the south than to the north and near the Azores waters there is a sharp transition in the maximum annual value, with some areas not reaching 0.4 µg/L, while others higher than 0.8 µg/L (Figure 4-20, e.g. 2001, 2008, 2010, 2011). In addition, there is also much less interannual variability to the south than to the north. Second, the year of 2001 and 2002 had notorious strong spring bloom. Third, the years of 2004-2006 did not have any spring bloom. Fourth, to the north of ~ 40 ºN the SCHL was higher in 1998-2000 than in 2004-2009 (better seen in Figure 4-19). Fifth, there appears to be evidence of increase SCHL around the Azores islands (e.g. 2010).

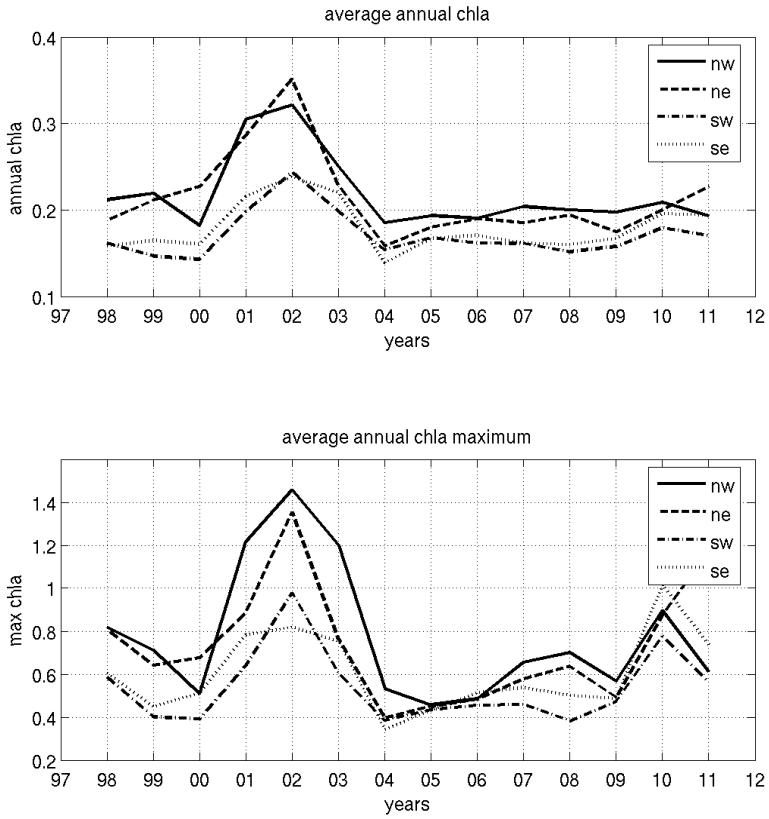

Figure 4-21 Annual mean SCHL (top) and annual maximum SCHL (bottom) in the Azores Archipelago. Each time series represents a quadrant inside the region shown in Figure 4-20. The four quadrants of the Azores Archipelago are: northwest (38.5-41 °N, 28-33 °W), northeast (38.5-41 °N, 23-28 °W), southwest (36-38.5 °N, 28-33 °W) and southeast (36-38.5 °N, 23-28 °W). Each annual value was averaged from the fields shown in Figure 4-19 and Figure 4-20. The units are µg/L.

To understand if the observed patterns were related to the depth of mixed layer and therefore nutrient limitation, the weekly SCHL and MLD are compared in one box between 40-45 °N and 20-30 °W. The MLD time series is calculated from three different models: SODA (Carton et al., 2000) in 1998-2004, TOPS (Cummings, 2005) in 2005 and FNMOC (Cummings, 2005) in 2006-2011. Information about the models and time series is given in Chapter 2. The SCHL time series is from SeaWiFS and MODIS AQUA, after and before 2003, respectively. The results are shown in Figure 4-22. The years of stronger MLD were 2001, 2002, 2003, 2007, 2010, with depths reaching 300 m. The year with lowest MLD (<150m) was 1999, followed by 1998, 1999, 2004, 2005 (~200 m). The remaining years, 2006, 2008, 2009 had intermediate MLD (~250 m). If the MLD is the only factor regulating nutrient supply to surface waters and by that, controlling the spring bloom magnitude (Levy et al 2005), than the SCHL time series should match the MLD. However, the time series of SCHL shows different patterns. For example, a shallow MLD occurs in 1998, 1999, 2000, 2004, 2005, but the SCHL values are higher in the first three years of the time series. On the other hand a deep MLD is observed in 2001, 2002, 2003, 2007, 2010 but the SCHL is considerably higher in the first three years (2001-2003). In addition there is a slow decreasing trend from 2000 to 2005 in the minimum value achieved during summer.

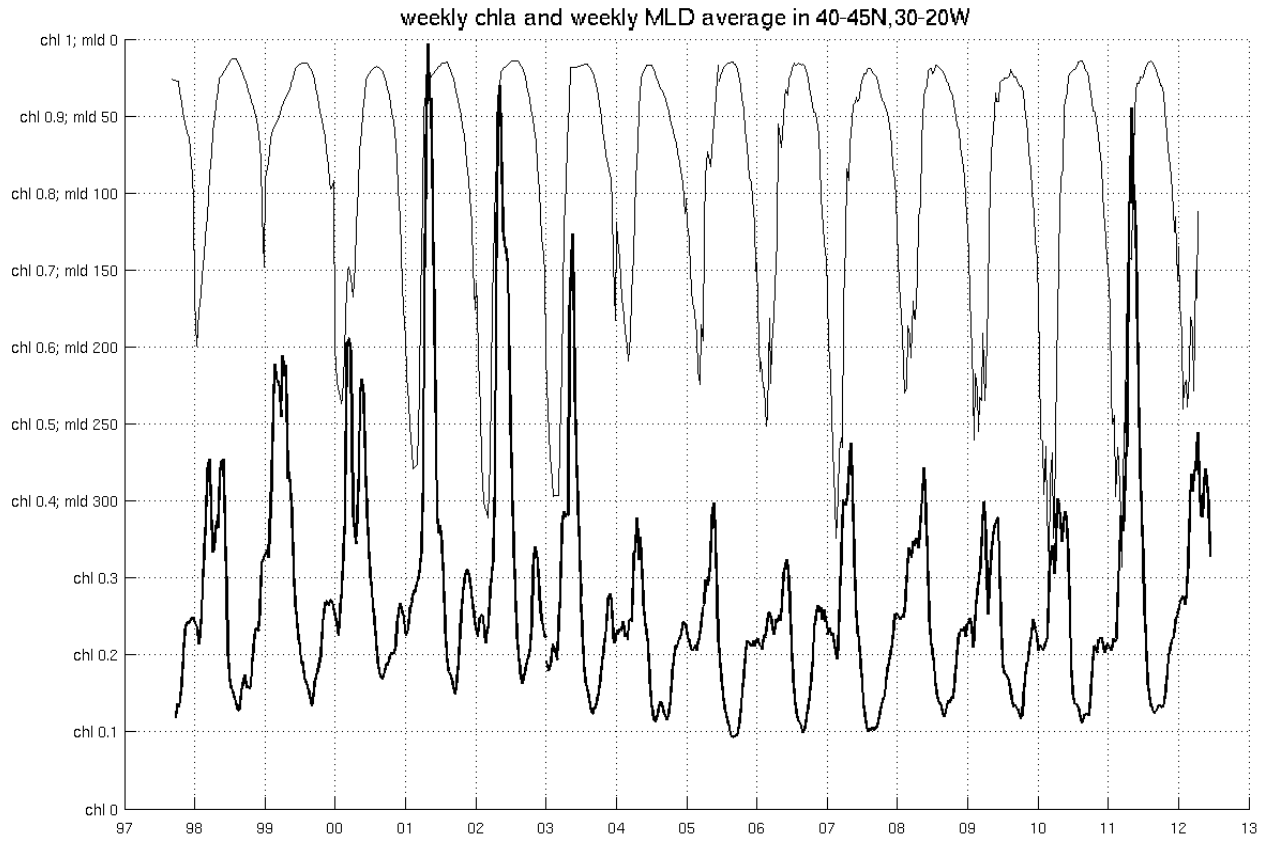

Figure 4-22 Weekly SCHL (µg/L) and MLD (m) averaged in one box between 40-45 °N and 20-30 °W. The MLD data is from the SODA and FNMOC models, after and before 2005, respectively. For 2005 it is used the TOPS model. SCHL is derived from SeaWiFS and MODIS AQUA weekly data, after and before 2003, respectively. A 2 week running mean is applied to SCHL time series.

Several factors may have played a role in the observed changes. One aspect is that the shallow MLD in the first three years occurred early in the year (January). Therefore SCHL could have been higher in those years, because phytoplankton would have more time to growth, but the supply of nutrients would still have been less than years with deeper MLD. Also, a very deep MLD provides more nutrients, but it can also decrease the probability of a bloom because it decreases the time phytoplankton stay in the euphotic depth and allows zooplankton population to grow creating a grazing forcing (Henson et al., 2006). This might have happen in 2007 and 2010. However, between 2001-2003 there was also a deep MLD, but high SCHL. The overall lack of relation between MLD and SCHL, suggest the influence of another mechanisms controlling the bloom.

The decreasing trend in SCHL observed between 1998-2007 in Figure 4-22 has been identified by many authors (e.g. Behrenfeld et al., 2006; Vantrepotte and Melin, 2009). Note that the SCHL decrease between 1998-2007 is observed both in the spring bloom magnitude and in the summer minimum (Figure 4-22). However until now, no study has been able to explain the responsible mechanisms. This trend can be found until latitudes of 50 °N. To illustrate the spatial patterns of the trend, the average SCHL between 1998-2000 is subtracted to the average of the following three years (Figure 4-23). The trend is also clear in the anomaly of annual of SCHL shown in Figure 4-24, for the six boxes showed in Figure 4-23. The SCHL used to make these plots are from SeaWiFS and MODIS AQUA weekly data, after and before 2003, respectively. It is noted that the sensors show the same variability during the period where both sensors were operational (2003-2007).

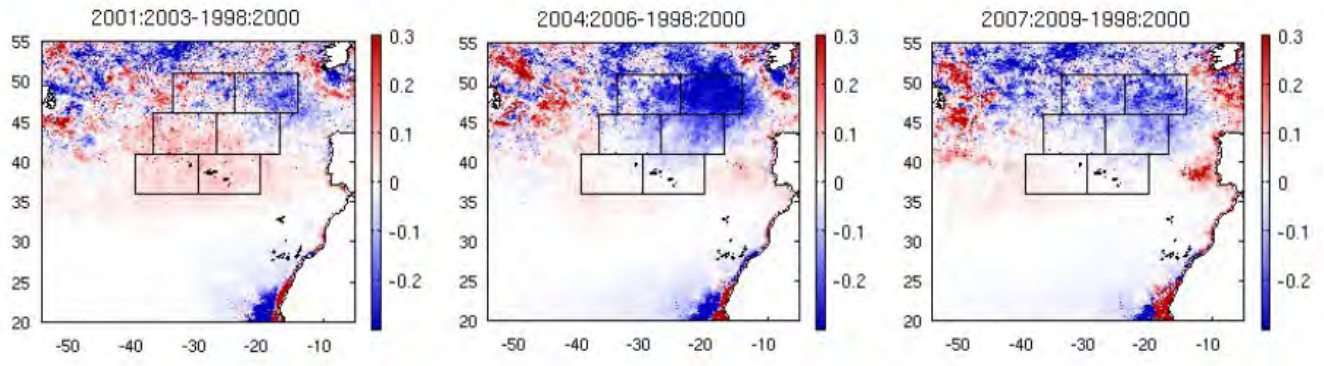

Figure 4-23 Spatial pattern of the decreasing trend of SCHL in the Northeast Atlantic (Vantrepotte and Melin, 2009). The three year average SCHL between 1998-2000 is subtracted to the three year average of 2001-2003 (left), 2004-2006 (middle) and 2007-2009 (right). Units are on µg/L. The boxes indicate the: north-west box (46-51 °N, 24-34 °W), north-east box (46-51 °N, 14-24 °W), middle-west box (41-46 °N, 27-37 °W), middle-east box (41-46 °N, 17-27 °W), south-west box (36-41 °N, 30-40 °W) and south-east box (34-41 °N, 20-30 °W). These are the same boxes used in Chapter 3.

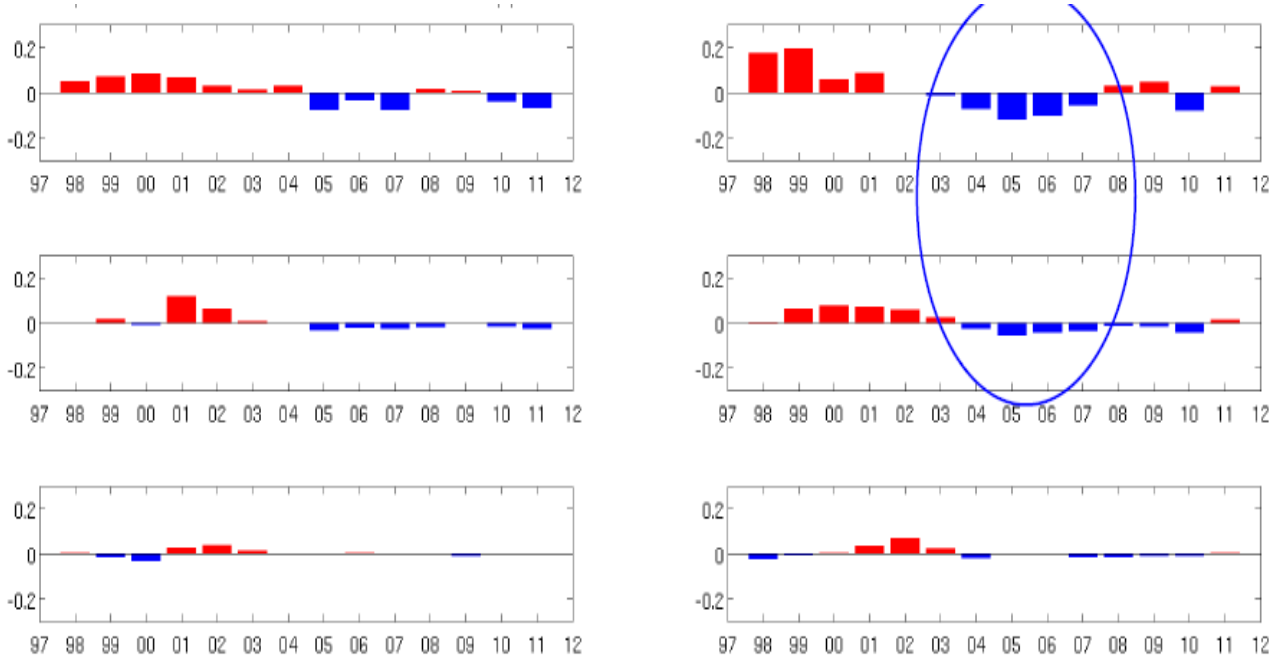

Figure 4-24 Time series of annual SCHL anomaly (µg/L) in 6 boxes on the Northeast Atlantic. The location of the boxes is shown in Figure 4-23. These are the same boxes used in Chapter 3. In each box, the anomaly is obtained by subtracting the mean annual SCHL between 1998-2011 to the annual mean in each year. The SCHL is derived from SeaWiFS and MODIS AQUA weekly data, after and before 2003, respectively.

To investigate the possible mechanisms for the decreasing trend in the Northeast Atlantic (see Vantrepotte and Melin, 2009), the winter wind mixing in February-March is plotted against the annual mean SCHL in each box (Figure 4-25). The response of SCHL to wind mixing agrees with previous studies (Follows and Dutkiewicz , 2001; Levy et al., 2005; Henson et al., 2006; Henson et al., 2009). In the northern boxes, deep mixing will entrain more nutrients into the euphotic zone; however, the controlling factor on subpolar blooms is likely to be light availability, so in the northern boxes, years with increased mixing result in a delayed, low-magnitude bloom. In the south-west box, where nutrient limitation of the phytoplankton bloom prevails, increased mixing results in increased bloom magnitude. In the south-east and middle boxes, the lack of a relationship between wind mixing and SCHL confirms what other studies (Follows and Dutkiewicz, 2001; Levy et al., 2005; Henson et al., 2009) have found: in the North Atlantic there is a transition region where SCHL interannual variability does not shows a consistent response to changes in the MLD. In this region, the bloom may have either subpolar or subtropical characteristics.

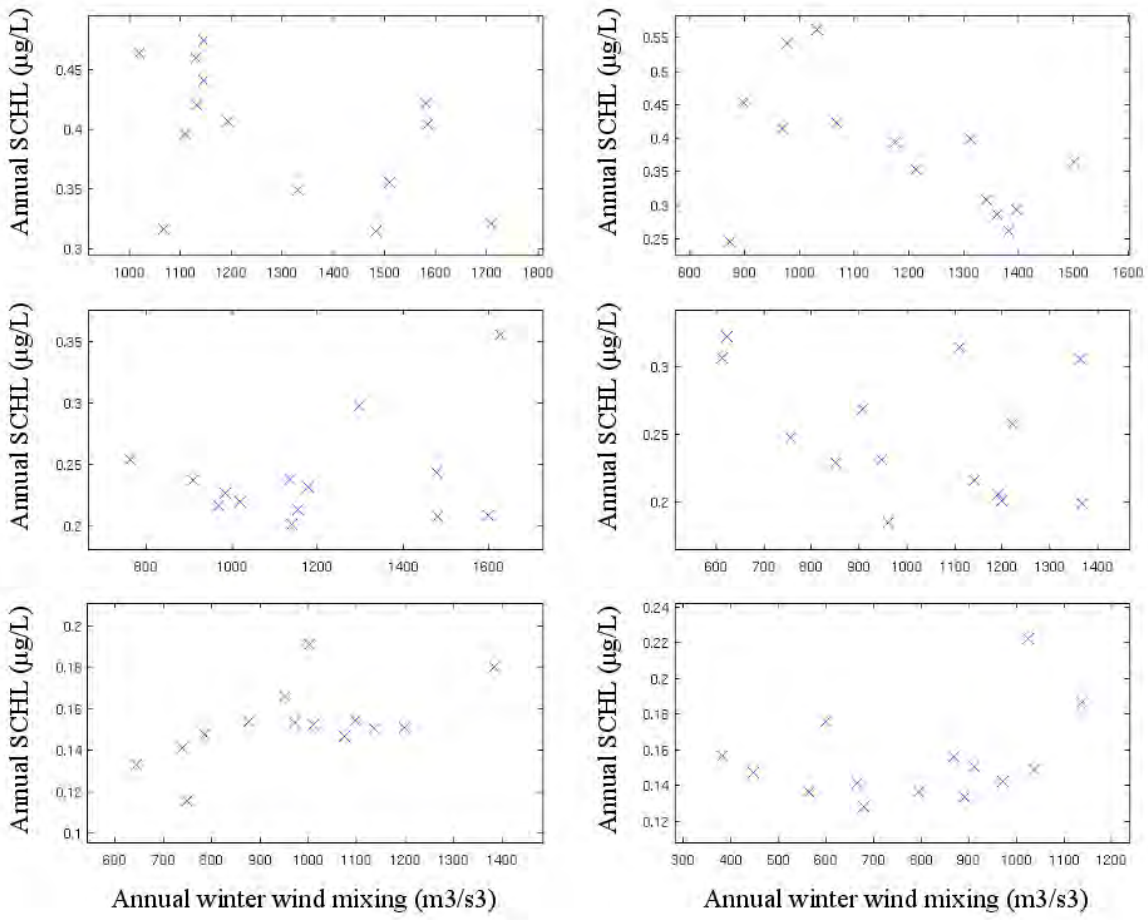

Figure 4-25 Annual mean SCHL plotted against the wind mixing during February-March, in 6 boxes in the Northeast Atlantic. The location of the boxes is shown in Figure 4-23. The SCHL is derived from SeaWiFS and MODIS AQUA weekly data, after and before 2003, respectively. The wind mixing is obtained by averaging the cubed wind speed during February and March.

Despite all the myriad factors that might have led to the decreasing trend in 1997-2007, the idea of nutrient limitation is further explored. In concrete, it is explored the hypothesis that interannual changes in the subsurface nutrient field, as a result of different ambient water masses, might have resulted in lower biological production. The typical assumption is that in the subtropics a shallow MLD results in less biological production due to nutrient limitation. Conversely, in the subpolar region a shallow MLD results in higher biological production, because the subsurface nutrient field is higher near the surface. The transition region is located between high and low subsurface nutrient fields. This can be well observed in the AMT sections of nitrate (Figure 4-5). Interannual variability in the subsurface nutrient field can be a result of spring biological productivity (that sinks and his decomposed in summer), of the previous winter mixed layer depth (that sets the physical and

biogeochemical properties of subsurface waters for the next winter) and of lateral advection (which transports waters from nearby regions with different subsurface nutrient concentrations). Unfortunately the available nutrient data has limited spatial and temporal resolution to analyze the interannual variability of the nutrient subsurface field. However, subsurface changes in temperature and salinity may indicate changes in the nutrient content.

In Figure 4-26 is shown the annual changes of temperature at different depths in the same region of Figure 4-22 where the SCHL was observed to decrease between 1998-2005, i.e. between 40-45 ºN and 20-30 ºW. The temperature at 100-200 m, 200-300 m and 400-500 m is computed from the MERCATOR model. In addition it is also shown the temperature from the CMCC model at 200-300 m and 400-500 m. The CMCC model is used, because its time series goes until December 2010, and provides an important insight to the strong mixing that occurred in the winter 2009-2010. During the following discussion the winter of a given year is the period including the first months of that year. For example, the winter of 2010 corresponds to the months of 2009/2010. In Figure 4-26, each year mean is representative of the temperature before any winter mixing occurs. In other words, the temperature of a given year was averaged between July and November of the preceding year. Therefore for each year, the values are related to the subsurface temperature before the MLD erodes depths greater than 100 m. It can be seen in Figure 4-22 that the MLD reaches 100m during December. The objective of such method is to analyze the structure of water column that would be available for the spring bloom of each year, independent of the atmospheric forcing and depth of the MLD. For depths of 400-500 m this analysis is not relevant because waters at these depths are typically isolated from winter mixing and their annual changes are more related to lateral advection. However, in upper waters, temperature changes with the deepening of the MLD. This method provides an independent analysis of the winter mixing that occurred in a particular year. Changes in annual values in upper layers are therefore influenced by both lateral advection and by the winter mixing in the previous year. In addition to the subsurface temperature from the MERCATOR and CMCC models, the SST from the AVHRR OI monthly dataset, were averaged between February and March for each year. Note the different averaging period of SST and temperature at depth.

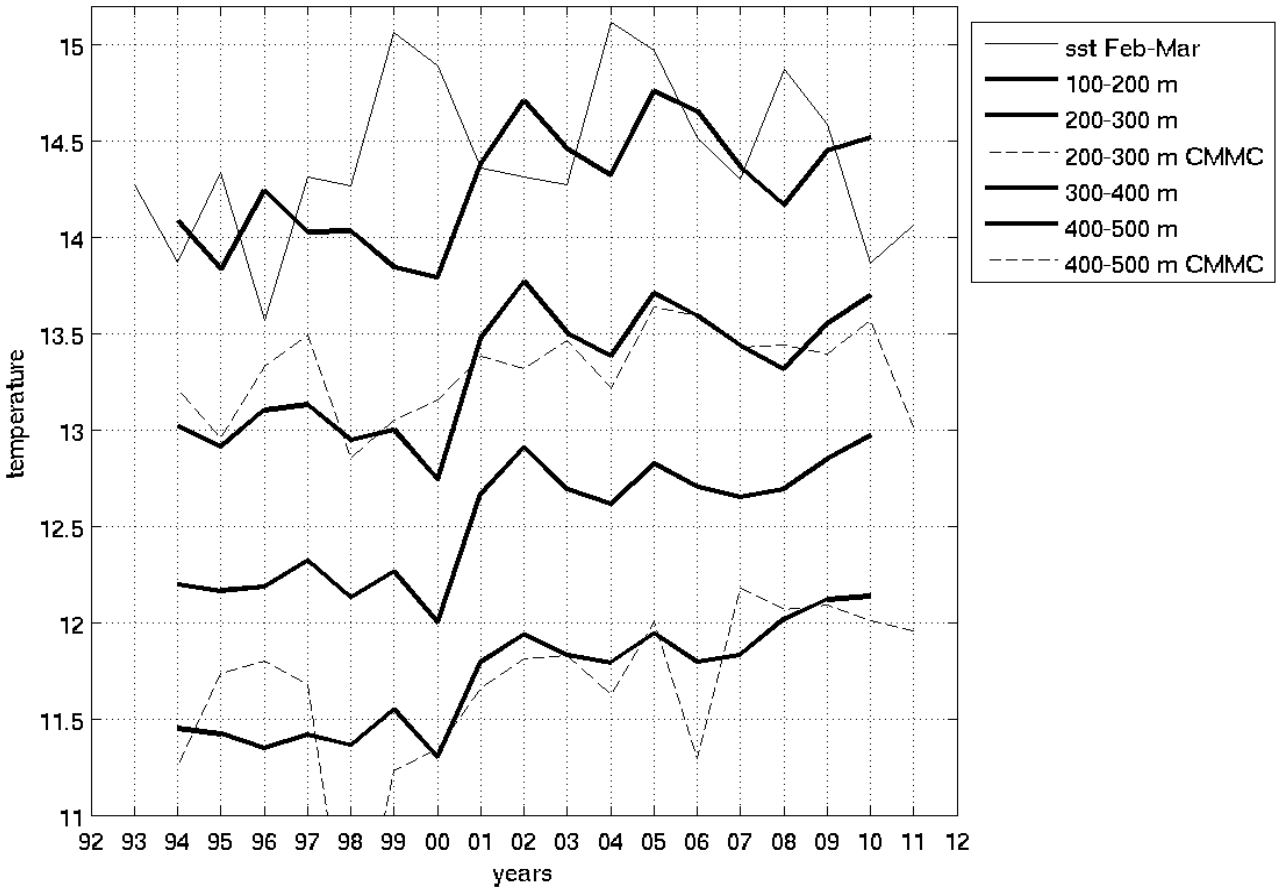

Figure 4-26 Annual changes of temperature at different depths in the region 40-45 °N, 20-30 °W. Data is from the MERCATOR model. The temperature from the CMCC model at 200-300 m and 400-500 m is also shown to examine the changes after the winter 2009/2010. SST from AVHRR OI monthly dataset is averaged in the same region between February and March for each year. Annual temperature from MERCATOR and CMCC corresponds to the averaged temperature between July and November of the year before.

Figure 4-26 can be interpreted in the following manner. From the MERCATOR data it can be observed an abrupt temperature increase in 2001 at all depths. In fact, because these values are measured from the year before, it means that the abrupt increase was observed in July-November of 2000. The CMCC model shows more variability, with a maximum around 1996 and a steady increase from 1998 to 2001. The following hypothesis is drawn. Before 2000 waters were cold and fresh, possibly from subpolar origin and with a higher nutrient concentration. From 2001 to 2006 pulses of saline and warm waters, changed the subsurface nutrient field which would supply less nutrients to the surface by the winter MLD. After 2006, consecutive winters of deep mixing and

typical southward flows (such has in 2007, see Figure 3-10 dashed line) started to change the water masses. Finally, in 2010, one of the coldest and windiest winters, severally mixed surface waters, decreased temperature and SCHL values returned to values of 1998-2000. These mechanisms are speculative and should be addressed in a future work. Nevertheless, the decrease in nutrients has been showed to occur between 2003-2005 at 50 °N, 20 °W, and lateral advection of subtropical waters was suggest to be the responsible mechanisms (Hartman et al., 2010). Other mechanisms related to changes in the ambient water masses are not excluded and include changes in phytoplankton community.

A change in the subsurface nutrient field as a result of changes in water masses in this region, provides an explanation for the 2000-2005 decrease in the transition region where previous studies did not find relation between vertical mixing and interannual variability of SCHL. The possible change of the subsurface nutrient field simultaneously with the temperature change are illustrated in Figure 4-27. It is shown the climatological nitrate field superimposed with the climatological contours of temperature at 200-300 m, derived from the WOA05 climatology. Additionally, is also shown the annual temperature contours in 2002 and 2005 at 200-300 m from the MERCATOR model. The chosen contours are 12.5 °C, 13.5 °C and 14.5 °C. The chosen years where 2002 and 2005 because it was when the annual contours from the MERCATOR model penetrated further into the central area of the intergyre region. If the subsurface nutrient field follows the temperature field at deeper waters, than the transition region was clearly influence by subtropical waters with less subsurface nutrients. The northward migration or expansion of the subtropical gyre (discussed in chapter 3), and the consequent flow of subtropical water into northern latitudes, are indicative of large advective changes, which can reduce the ambient nutrient concentration and the annual biological production in the intergyre region.

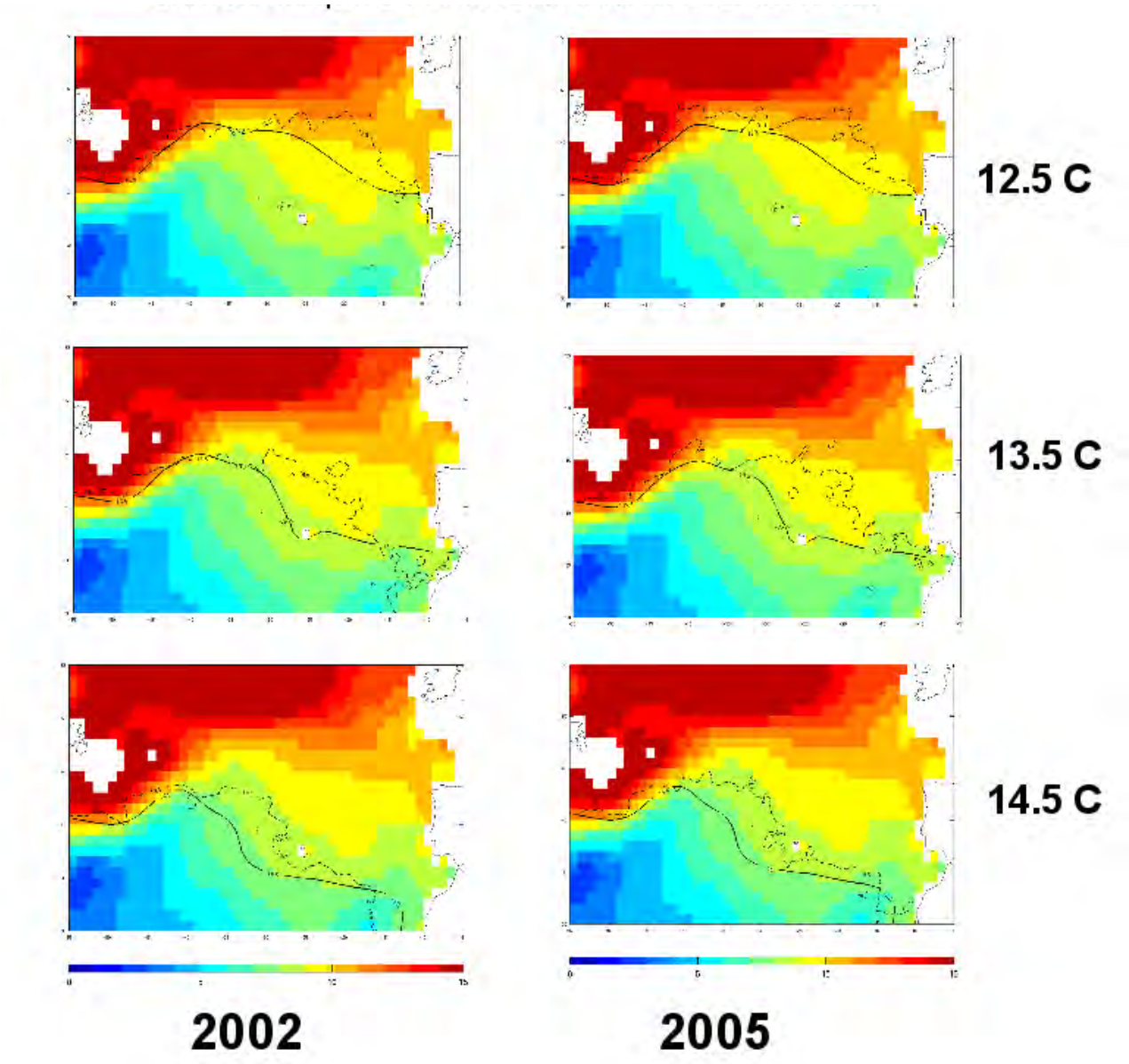

Figure 4-27 Climatological nitrate field (colors) superimposed with the climatological temperature contours (solid line). Both variables were averaged at 200-300 m during the summer months (July-September) from the WOA05 monthly climatology. In addition, it is shown the annual temperature contour (dashed line) at 200-300 m from the MERCATOR model. The chosen contours are 12.5 °C (top), 13.5 °C (middle) and 14.5 °C (bottom). The years 2002 (left) and 2005 (right), where chosen because it was when the annual contours from the MERCATOR model (dashed line) penetrated further into the central area of the intergyre region.

4.6. Island mass effect

The island mass effect is known as an increase in biological production around an islands. Ocean conditions around the Azores islands are poorly known. Using satellite and field data Lafon et al (2004) observed episodes of lower temperatures and higher chlorophyll concentrations, on the south coasts of S. Miguel and Sta. Maria islands, than in surrounding waters. The authors proposed the existence of wind-driven upwelling south of these islands. In other geographic regions, higher chlorophyll content and sea surface cooling in the vicinity of an island has been associated to a wide range of physical mechanism including tidal stirring in shallow waters (Simpson et al., 1982), internal waves on the shelf break (Sangra et al., 2001), island generated cyclonic eddies (Seki et al., 2001) and island-blockage of currents which can induce upward vertical motions and transport of nutrients from the island shores (Hasegawa et al., 2004; Palacios et al 2002).

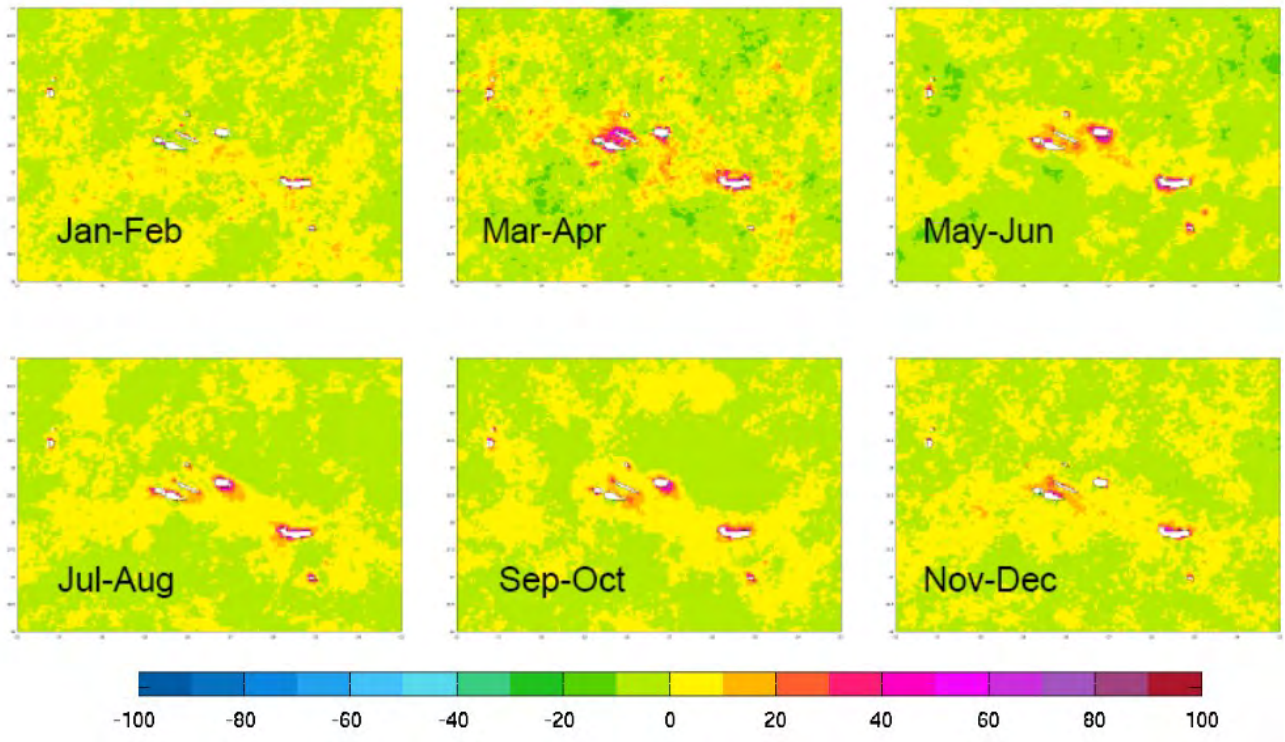

Figure 4-28 Climatological mean of the percentage a given pixel deviates from a 2x2 degrees box around that pixel. Calculated from weekly satellite maps of SCHL MODIS AQUA at 4 km resolution between 2002 and 2010.

The island mass effect is here studied using a climatological approach. In Figure 4-28 it is shown the climatological mean of the percentage a given pixel deviates from a 2x2 degrees box around that pixel. This method, firstly computes, for each weekly map of SCHL and for each valid pixel in that

map, the difference (in percentage) between a pixel value and the mean of a 2x2 degree box around that pixel. For example if the pixel value is 1.2 µg/L and the mean box around the pixel is 1µg/L, the pixel is awarded with the value 20 %. The climatological means in Figure 4-28 are than computed from the weekly maps. The weekly SCHL data was from MODIS AQUA 4 km resolution, between 2002 and 2010. High values in Figure 4-28 can than be interpreted as regions with higher probability of having higher SCHL than the surrounding area (2x2 degree).

During summer almost all islands produce an island-mass effect, although Terceira and S. Miguel show particular higher values. A more detailed analysis shows that the higher values are found at the east-west flanks of the islands. The higher SCHL found during summer is either a result of increase biological production or the mixing of the deep chlorophyll maximum (DCM) found typically during summer at depths 50-100 m. Additional analysis indicated that this increase around the islands coincides with lower sea surface temperatures. Moreover, they also coincide with the regions of stronger tidal currents, which are located in the east-west flanks of the islands. It is likely that regions of enhanced stirring from tidal currents disturb the typical seasonal thermocline and mix warm surface waters with deeper colder waters. These waters are than advected by the mean circulation. During visualization of satellite images it was also noted that the influence of southern waters from the AC suppressed the observed SCHL increase around the islands.

From November to February the island-mass effect appears to be weaker. From March to April there is an increase and it can be observed a plume of higher values originating from Terceira island. This provides evidence that the islands can effectively increase biological production. Nevertheless it is suggested that the primary mechanisms for the spring increase in SCHL is the deepening of the MLD. Without a sufficient deep MLD the spring bloom will be weak and also will be the island-mass effect. However the combined effect of island-mass effect and MLD could increase SCHL. It is plausible to think that a deep MLD would mix more nutrients from the rocky bottom of the islands coasts and together with an incident flow would be more effectively in irrigating waters downstream of the islands with nutrients. This appears to be the case of the spring bloom in 2010 (see Figure 4-20). The presence of other colored water constituents (suspended inorganic matter and “gelbstoff”) in coastal waters can introduce errors in the SCHL, nevertheless if this would be the reason for the higher SCHL near the islands, it would not disprove an effect of the islands in the surrounding ocean.

Finally a larger pattern of higher values around all the islands, as a band oriented west-east, can be

distinguished in Figure 4-28. This may be the result of the Azores region having permanently higher SCHL than the nearby regions, which in turn can be the result of a frequent input of nutrients from the island-mass effect, seamounts and mixing from different water masses.

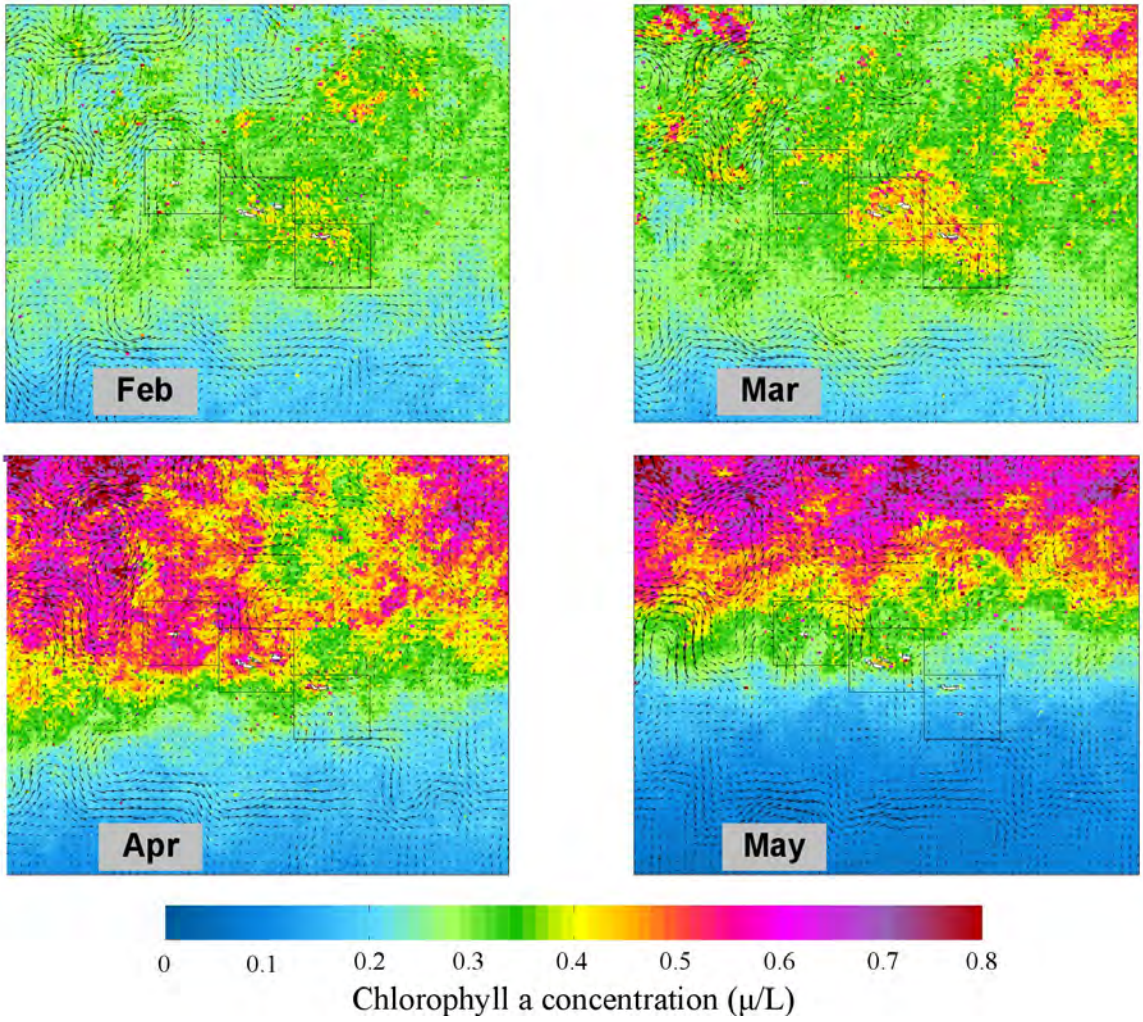

Figure 4-29 Monthly climatology of SCHL in the Azores Archipelago for the spring bloom months (February, March, April, May). Computed from SeaWiFS weekly data between 1997-2007. Superimposed is the monthly climatology of the ocean currents from satellite altimetry (AVISO) for the same months. The boxes the for the Western Group (38.5-40.5 °N and 29.5-32.5 °W), Central Group (37.65-39.65 °N, 26.5-29.5 °W) and Eastern Group (36.2-38.2 °N, 23.5-26.5 °W) are illustrated.

In Figure 4-29, a larger pattern is also observed around February and March, with a patch of high SCHL around the Central Group. In a first instance the pattern resembles an island-mass effect. However, in the following month (April), the regions immediate to the northwest of the patch have

a stronger bloom. The circulation patterns clearly show a southeastward current toward the islands. From the several years analyzed, the presence of a current interacting with the islands does not appear sufficient to cause a bloom. The major factor controlling the SCHL signal as previously discussed appears to be the MLD. Nevertheless in some years (e.g. 2005, 2010) the maximum of SCHL in the entire midlatitude intergyre region was near the islands (see 2005 and 2010, Figure 4-20) which clearly indicates the presence of island-mass effect. However, as indicated by Figure 4-28, the dimensions of the island mass effect are apparently smaller than the patch observed in Figure 4-29. From the analyses performed in this work it is not possible to give a clear answer on the mechanism responsible for the occurrence and non-occurrence of the large-scale patch around the Azores in different years, but the following hypothesis are suggested and can be investigated in future work: 1) southeastward advection of surface waters that have gained a higher nutrient content from deeper MLD to the northwest and find in the Azores favorable conditions for production (shallower mixed layer depths); 2) shallow (or weakly mixed) MLD in the region (due to milder atmospheric conditions) while the surrounding waters have deeper MLDs; 3) regional enrichment of nutrients as a result of mixing different water masses; 4) regional enrichment of nutrients derived by topographic disturbances; 5) a nutrient pool around the Archipelago derived from the continuously action of the previous two mechanisms.

CHAPTER 5: SYNTHESIS AND CONCLUSIONS

5.1. Physical changes during the last two decades

The recent increases in temperature and salinity in the Northeast Atlantic (Hatun et al 2005; Holliday et al., 2008; Häkkinen and Rhines, 2009; Häkkinen et al., 2011) were analyzed in a broad area that corresponds to the midlatitude intergyre region (35-50 ºN, 15-40 ºW) between 1993-2009. This large-scale analysis was done based on temperature and salinity model outputs from the MERCATOR GLORYS2V1 Global Ocean Reanalysis (Ferry et al., 2012). In a complementary regional analysis, the temperature changes in the Azores region were investigated between 1990-2011 using in-situ observations from the Global Temperature-Salinity Profile Program (GTSPP) project (Sun et al., 2010) and model outputs from the MERCATOR GLORYS2V1 (Ferry et al., 2012) and the CMCC CGLORS Global Ocean Reanalysis (Storto et al., 2012).

In the Azores regional analysis (Figure 3-7), there was an overall agreement between the temperature derived from in-situ observations and the MERCATOR modeled temperature. The only period with major differences between these two datasets was in 1999 and 2000, where the in-situ temperature shows an increase, while the modeled temperature shows a decrease. Regarding the two models (MERCATOR and CMCC) they show similar patterns, but there are some differences in the first half of the time series (1993-2001). The major finding from this analysis is a temperature increase at deep waters (400-500 m) between 1993 and 2001, followed by a more stable period between 2002-2008. After 2008 there is a decrease, but the temperature is still warmer than at the start of the time series. The same changes are observed at the surface (100-200 m), but with particular differences. First, in contrast to deep water, where temperatures remained stable between 2001-2005, at the surface there was a maximum in 2004 and 2005. Another major difference is the sharp cooling-down observed in 2010, which resulted in temperatures returning to the values of the early 1990's. In relation to the increase between 1993 and 2001, there are differences between the datasets. The in-situ dataset shows a gradual increase in temperature, but the model outputs show a decrease in temperature around 1997-1998 (CMCC) or 1999-2000 (MERCATOR). This decrease in modeled temperature is compensated by an abrupt increase in 2001. It is difficult to consider the in-situ data as the “true” dataset, since the Azores Archipelago covers a considerable large region with distinct water masses. An heterogeneous spatial distribution of the profiles in one year could easily introduced a bias. Whether the transition from a cold fresh period to a a warm saline period was smooth between 1999 and 2001, as the in-situ data suggests, or occurred as an abrupt increase

in 2001 as seen in the model data, it remains unclear.

Regarding the large-scale analysis, the changes in temperature and salinity were described for 6 boxes using the MERCATOR model outputs. In all eastern boxes, which correspond to the eastern basin (i.e. east of the Mid-Atlantic Ridge (MAR)), there was an increase in temperature and salinity between 1993 and 2009, both at the surface and deep waters. This increase, occurred mainly between 1993 and 2001 (Figure 3-2 and Figure 3-3). In the southern part of the eastern basin the main increase occurred in 2001, which marked the transition between a cold, fresh period (1993-2000) to warm, saline period (2001-2009). In the northeast region, the increase was more gradual and earlier (around 1997). It should be noted that the increase in temperature and salinity in the eastern basin between 1993 and 2001 was not smooth or continuous, but often interrupted by colder and fresher years. In the western basin, the southern region (south-west box) showed a similar pattern to the southern region of the eastern basin (south-east box). In contrast, the northern area of the western basin (north-west and middle-west boxes), showed high variability with alternating periods of warming and cooling. Only surface salinity showed a slight increase. The warm and saline events to the northwest were in 1992-1996, 1999-2001 and 2004-2006.

The changes can be summarized as follows. In the northwest part of the intergyre region variability is high, with alternating periods of warming and cooling. This is more noticeable in the time series of salinity, possibly because the salinity signals are more stable in the ocean, while temperature is more easily damped from air-sea interactions and mixing with other water masses. Thus, if a mechanism such as advection or air-sea fluxes increases salinity and temperature, the signal in salinity will persist longer in time. The variability found to the northwest is possibly related to the closeness of these boxes to the main core of North Atlantic Current (NAC). Latitudinal changes in the NAC branches that detach from the main current system and drift eastward, could result in increased transport of: warm, saline water masses of subtropical origin; or cold, fresh water masses of subpolar origin. In the eastern and southern part of the intergyre region (i.e. eastern and southern boxes), there is an increase in temperature and salinity between 1993 and 2009 at deep and surface waters, but the this increase occurred mainly between 1993 and 2001. After 2002 the temperature and salinity were relatively stable in deeper waters.

The changes in temperature and salinity at deeper waters in the eastern basin, below the influence of the winter mixed layer, indicate that horizontal advection may have played a role. This was investigated for the region between Azores and mainland Portugal (corresponding to the middle-east

box) using geostrophic currents derived from AVISO altimetry. The average circulation in this region is weak, with a southeastward component (Reverdin et al., 2003), which tends to transport cold and fresh water masses to southern latitudes. The resident water masses can than be slowly influenced by anomalies in ocean circulation (southeastward/northeastward pulses of subpolar/subtropical waters) and/or anomalies in the water masses transported by the currents (anomalies in the subpolar or subtropical gyre centers). In the early 1990's the region between Azores and mainland Portugal was characterized by colder (and fresher) waters at 200-300 m (Figure 3-4). The mechanisms responsible for these early conditions in the eastern basin, is out of the scope of this work, however relations can be made with the strong/expanded subpolar gyre of the early 1990's (Hatun et al., 2005; Häkkinen et al., 2004) and from succeeding the cold phase period (1970-1990) of the Atlantic Multidecadal Oscillation (Knight et al., 2009). After 1996, the temperature and salinity started to increase in the first 500 m. There are resemblances between the increases in salinity and the decrease in southward flow at 45 °N. The decrease in southward flow at 45 °N occurred in 1996-1998, 2001-2005, which matches the increases in salinity (Figure 3-14). According to Figure 3-14, it is possible that during these periods, there is a decrease in the southward transport of cold, fresh northern water masses and at same time an increased influence of the warm, saline eastward flows into the region. In addition, a major eastward flow at 30 °W, between 40-45 °N, occurred during 2001-2003 (Figure 3-14). This was a result of an anomalous northeastward flow along 30 °W that occurred during 2001-2003 (Figure 3-11). This anomalous event may have played a role in definitely replacing the resident, cold and fresh, water masses of the early 1990's. In addition, it is possible that the warm and saline periods in the northwestern region (Figure 3-3) also play a role by modifying the water masses that are subsequently transported into the eastern basin.

In conclusion, the following mechanisms are proposed to explain the salinity changes after 2000 in the eastern basin. It is speculated that in 1999-2000 an anticyclone-like feature transported warm waters to the north of Azores and west of the MAR (Figure 3-4, see year 2000), and at the same time advecting the early-period cold and fresh water mass to the Azores region (southward period 1998-2000 in Figure 3-10, top dashed line). In the following years these northern warm waters spread eastward and warmed the region between Azores and mainland Portugal, accomplished also by the anomalous increase in northeastward flow along 30 ºW (Figure 3-11). These warm water masses have then remained in the region, possibly even moved northward, and since 2005 have been been laterally replaced/mixed by other flows (such has the southward flow in 2006-2007) or vertically mixed by deep winter mixing (such as the deep winter mixing in 2010). The latitudes of

40-45 ºN and 45-50 ºN, correspond to the southern branches of the NAC and it is shown that they alternate in their strength at 30 °W (Figure 3-10, bottom). The periods of stronger eastern flow at 30 ºW, between 40-45 ºN tend to coincide with periods of decreased southward flow at 45 ºN (Figure 3-10, dashed lines), which suggests that when the NAC successively crosses the MAR in the south, the southward flow is reduced and more warm saline waters enter the region.

Changes in the wind patterns can have an effect on the ocean circulation through several mechanisms. Here it was discussed the effect of wind stress curl in the geostrophic currents. In the Northern Hemisphere open ocean, regions of negative (positive) wind stress curl have a convergence (divergence) of Ekman drift at the surface which is compensated by a southward (northward) geostrophic current. In the eastern basin, between Azores and mainland Portugal, there is a region of decreased winds, characterized by a climatological negative wind stress curl and southward flow. When the wind stress curl climatological pattern reverse the ocean response is such that the southward flow decreases and the northward penetration of subtropical waters is enhanced (Häkkinen and Rhines, 2009; Häkkinen et al., 2011). The results in this study agree with this mechanism. It was observed an increased southward flow at 45 °N, following periods of negative wind stress curl (Figure 3-16). Moreover it is shown that the anomalous northeastward flow along 30 °W in 2001-2003 (Figure 3-11), is coincident with an anomalous positive wind stress curl during the same period in a region exactly above the main core of NAC (44-54 ºN, 30-45 ºW) (Figure 3-16). These changes in wind stress curl in 2001-2003 can be related to the southward shift of the zero wind stress curl line showed by Häkkinen and Rhines (2009).

In resume, results shows that the temperature and salinity increase in the eastern basin during the last two decades, shows fluctuations coincident with the currents which in turn are related to the wind circulation patterns. Southern inflows, during periods of negative wind stress curl in the eastern basin, transport cold and fresh water masses from northern origins, which decreases temperature and salinity in the region. During positive (and weak negative) wind stress curl the southward flow is reduced and the eastward flow transports warm and saline waters into the region, which increase temperature and salinity in the region. In 2001-2003, an anomalous positive wind stress curl in the northwest part of the region was observe to coincide with an anomalous northeastward flow along 30 °W, which possibly further transported warm and saline waters to the eastern basin. These fluctuations can be part of a multi-decadal cycle of wind stress curl with relations to the Atlantic Multidecadal Oscillation (Knight et al., 2009; Häkkinen et al., 2011b). Here we explored the role of horizontal advection, but is likely that the warm, saline periods can have

multiple causes such as air-sea fluxes, depth of the mixed layer, Ekman pumping and downstream water masses changes.

5.2. Physical controls of chlorophyll-a

The physical mechanisms responsible for the temporal and spatial distribution of chlorophyll-a concentration in the Azores region were investigated using SeaWiFS and MODIS AQUA ocean color satellite images of chlorophyll-a concentration (SCHL) and complementary meteorological and oceanographic data. The work was divided in the analysis of: 1) the large-scale climatological pattern, 2) the couple effect of the mixed layer depth and the subsurface nutrient field, 3) the seasonal dynamics in the Azores Archipelago, 4) the interannual variability of the spring bloom, and 5) the island mass effect in the Azores Archipelago.

Seasonal changes in mixed layer depth (MLD) play a crucial role over biological production in the North Atlantic. The MLD regulates annual phytoplankton growth through the nutrient it supplies to surface waters during winter (Longhurst, 2006). However, the amount of nutrients a given mixed layer can provide to the surface also depends on the subsurface nutrient field (Yentsch, 1989; Longhurst, 2006). Accordingly, in this work is suggested that the distribution of SCHL in the Azores region is controlled by both the mixed layer depth (MLD) and the subsurface nutrient field. It is provided evidence that the same MLD to the south and north of the Azores results in lower SCHL to the south (Figure 4-4 and 4-6). An explanation is provided on the basis of the subsurface nutrient field. It is shown that the subsurface nutrient field is considerably different at latitudes between 32-44 °N (Figure 4-5). Therefore the same MLD cannot supply the same amount of nutrients to the surface. This is particular true for latitudes to the south of 40 °N where MLD is progressively inefficient in supplying nutrients to the surface. The latitudinal changes in subsurface nutrient field provide an explanation for the different latitudinal biological responses. These results indicate that the MLD is not the main factor controlling SCHL latitudinal changes as discussed by Levy et al (2005) in a nearby region and that the nutrient subsurface field should also be taken in account. Extrapolating these results to a broader region, it is shown that the climatological SCHL field does not matches the climatological MLD maximum field, with the first one having a zonal distribution, while the second having a southwest-northeast orientation (Figure 4-4). Interestingly, the orientation of the nutrient subsurface field is nearly perpendicular to the orientation of the MLD maximum field (Figure 4-8 left and Figure 4-9 left). The combination of both fields, results in a nutrient pattern similar to the SCHL field (Figure 4-9, right). The nearly match of both SCHL and

nutrient (as a function of subsurface nutrient field and MLD), supports the hypothesis that these two factors are equally important in regulating the spatial patterns of biological production in the midlatitude region of the North Atlantic. It provides an explanation for why in the southwest part of the region despite deep MLD, SCHL is lower (Figure 4-6, see 1998). That is, in the southwest region, although MLD is deeper, there are less nutrients at depth.

Regarding the seasonal dynamics of SCHL in the Azores Archipelago, all groups are characterized by low SCHL during summer and an increase in autumn. The timing of the autumn increase is shown to be related to periods of rapid heat loss from the ocean (Figure 4-14). This can be associated to the passage of storms and associated convective mixing which erodes the seasonal thermocline. This first increase in SCHL after summer, has been described as the “fall”, or “entrainment” bloom, and is typically related to the input of nutrients from bellow the seasonal thermocline (Levy et al., 2005). One other reason, rarely mentioned, is the upward transport of phytoplankton cells from the deep chlorophyll maximum (DCM), and therefore not necessarily related to an increase in primary production. Regarding winter-spring SCHL dynamics it is shown that there are significant differences between each group of the islands (Figure 4-11, 4-12, 4-13, 4-15, 4-16 and 4-18). If the winter mixed layer depth is shallow (< 200 m), SCHL continues to increase through winter to spring. This is typically the case for the Central and Eastern Groups. If the mixed layer depth is deep (> 200 m) SCHL decreases or maintains. This is typically the case for the Western Group. This is shown from modeled and in-situ MLD (Figure 4-11, 4-12, 4-15, 4-16 and 4-18). The winter decrease in SCHL is typically observed in the Western group, but it should be noted that other groups also can have MLD higher than 200m.

The timing of the increases in SCHL in winter and spring were found to be related to periods of ocean heat gain (Qnet>0) (Figure 4-15, 4-16 and 4-17). Accordingly to Sverdrup (1953), to occur a bloom in regions with deep MLD, it requires that MLD gets shallower than a critical depth, which in the Azores latitudes is between 30 and 50 m (Follows and Dutkiewicz, 2001; Townsend et al., 1994). Other hypotheses for the initiation of spring blooms do not require a mixed layer shoaling, such has when the mixed layer turbulence decreases, allowing phytoplankton to grow within a deep, but weakly mixed layer (Townsend et al., 1992; Taylor and Ferrari, 2011). This mechanism occurs in the absence of convective mixing, such as in end of winter, when the daily average heat flux across the air-sea interface tends to zero (Qnet=0). In this work, it is found a match between periods of no convection (Qnet=0) and spring SCHL increases. In the southeast region, the MLD is shallower (~100m) and SCHL increases gradually, with the winter-spring episodic increases of

SCHL matching the periods of zero Qnet. In contrast, the northwest region decreases its SCHL during a deeper MLD (>200 m) and the spring increase occurs when Qnet is largely positive. The response of SCHL to Qnet appears to be not so fast as in the southeast, possibly because of the deeper MLD and dilution of phytoplankton in the water column. The spring bloom in these regions is stronger. These results are in agreement with the turbulence hypothesis (e.g. Taylor and Ferrari, 2011) since the MLD appears to be around 100 m during the episodic SCHL increases. As stated by LEV05, the euphotic depth of around 100 m in this region, allows phytoplankton populations to stay near the euphotic depth. Although several years show identical patterns, it is not possible to discard the Sverdrup hypothesis, which would require that the observed increases in SCHL are a result of short periods with shallower MLD not captured by the model and in-situ data used in this work. Finally, in terms of annual SCHL, it is suggested that the southern part of the Archipelago as lower annual SCHL due to weaker mixing and lower subsurface nutrient content. The northern part, at the same latitude, has similar annual SCHL possibly due to the combination of deeper/shallower mixing with lower/higher subsurface nutrient content.

Regarding interannual variability it is shown a decreasing trend in SCHL from 1998-2009 in the northern waters (Figure 4-22, 4-23 and 4-24). This trend has been identified by many authors (e.g. Vantrepotte and Melin, 2009). However until now, no study has been able to explain the responsible mechanisms. This trend can be found until latitudes of 50 °N (Figure 4-23 and 4-24). It was found an overall lack of relation between modelled MLD and SCHL at 40-45 °N and 20-30 °W (Figure 4-22). Similarly, the response of SCHL to winter wind speed fails to explain the interannual variability in the eastern basin, in contrary to the southwestern area (Figure 4-25). Despite all the myriad factors that might have led to the decreasing trend in 1997-2007 in the eastern basin, the idea of nutrient limitation is further explored. In concrete, it was explored the hypothesis that interannual changes in the subsurface nutrient field, as a result of different ambient water masses, might have resulted in lower biological production. Since in-situ nutrient data is scarce, interannual variability in the subsurface nutrient field was analyzed through changes in temperature and salinity. This is based on the fact that warm and saline subtropical waters have lower nutrient concentrations at 200-300 m than colder fresh subpolar waters (Figure 3-8 left). It was found, that the early years (1998-2000) of the SCHL time series coincide with colder and fresher water masses (Figure 4-26). After 2001 the waters in the region were consistent warmer and saline. It is speculated, that before 2000, the water masses in the region were from subpolar origin (as discussed in Chapter 3) and with a higher nutrient concentration. From 2001-2006, pulses of saline and warm waters, possibly changed the subsurface nutrient field which would supply less nutrients independent of MLD.

Changes in plankton communities are not excluded., but the decrease in nutrients has been showed to occur between 2003-2005 at 50 °N, 20 °W, and lateral advection of subtropical waters was suggest to be the responsible mechanisms (Hartman et al., 2010). It is suggested that after 2006, consecutive winters of deep mixing and typical southward flows (such has 2006-2007, see Figure 3-10) started to change the water masses. Finally, the 2009/2010 winter rapidly decreased temperatures and SCHL values returned to values of 1998-2000 (Figure 4-22). These mechanisms are speculative and should be addressed in a future work.

Finally it is shown from satellite images of SCHL, that during summer almost all islands produce an island-mass effect (Figure 4-28), although Terceira and S. Miguel show particular higher values. A more detailed analysis shows that the higher values are found at the east-west flanks of the islands and coincide with patches of colder waters (Silva *et al.*, 2013). Therefore the higher SCHL found during summer is either a result of: increase biological production, different phytoplankton communities (Silva *et al.*, 2013) or mixing of the deep chlorophyll maximum (DCM) found typically during summer at depths 50-100 m. Between November and February the island-mass effect appears to be weaker. In March-April there is an increase in SCHL around the islands and it can be observed a plume of higher values originating from Terceira island. Nevertheless it is suggested that the primary mechanisms for the spring increase in SCHL is the deepening of the MLD. Without a sufficient winter mixing, the spring bloom will be weak and also will be the island-mass effect. However the combined effect of island-mass effect and MLD could increase SCHL. It is plausible to think that a deep MLD would mix more nutrients from the rocky bottom of the islands coasts and together with an incident flow would be more effectively in irrigating waters downstream of the islands with nutrients.

Around February and March, there is typically a patch of high SCHL around the Central Group (Figure 4-29). In a first instance the pattern resembles an island-mass effect, but in the following month (April), the regions immediate to the northwest of the patch have a stronger bloom. The circulation patterns clearly show a southeastward current toward the islands. From the several years analysed, the presence of a current interacting with the islands does not appear sufficient to cause a bloom. The major factor controlling the SCHL signal appears again to be the mixed layer depth. Nevertheless in some years the maximum of SCHL in the entire midlatitude intergyre region was near the islands (see 2005 and 2010, Figure 4-20) which clearly indicates the presence of island-mass effect. However, as indicated by Figure 4-28, the dimensions of the island mass effect are apparently smaller than the patch observed in Figure 4-29. From the analyses performed in this

work it is not possible to give a clear answer on the mechanism responsible for the occurrence and non-occurrence of the large-scale patch around the Azores in different years, but the following hypothesis are suggested and can be investigated in future work: 1) southeastward advection of surface waters that have gained a higher nutrient content from deeper MLD to the northwest and find in the Azores favourable conditions for production (shallower mixed layer depths); 2) shallow (or weakly mixed) MLD in the region (due to milder atmospheric conditions) while the surrounding waters have deeper MLDs; 3) regional enrichment of nutrients as a result of mixing different water masses; 4) regional enrichment of nutrients derived by topographic disturbances; 5) a nutrient pool around the Archipelago derived from the continuously action of the previous two mechanisms.

REFERENCES

Alves, M., F. Gaillard, M. Sparrow, M. Knoll, and S.Giraud (2002). Circulation patterns and transport of the Azores Front-Current system. Deep-Sea Research II, 49, (19), 3983-4002.

Amante, C. and B. W. Eakins (2009). ETOPO1 1 Arc-Minute Global Relief Model: Procedures, Data Sources and Analysis. NOAA Technical Memorandum NESDIS NGDC-24, 19 pp, March 2009.

Antonov, J. I., R. A. Locarnini, T. P. Boyer, A. V. Mishonov, and H. E. Garcia (2006). World Ocean Atlas 2005, Volume 2: Salinity. S. Levitus, Ed. NOAA Atlas NESDIS 62, U.S. Government Printing Office, Washington, D.C., 182 pp.

Backhaus, J. O., E. Hegseth, H. Wehde, X. Irigoien, K. Hatten, and K. Logemann (2003). Convection and primary production in winter. Marine Ecology Progress Series 215:1–14.

Behrenfeld, M. J., R. T. O'Malley, D. A. Siegel, C. R. McClain, J. L. Sarmiento, G. C. Feldman, A. J. Milligan, P. G. Falkowski, R. M. Letelier, and E. S. Boss (2006). Climate-driven trends in contemporary ocean productivity, Nature, 444, 752– 755, doi: 10.1038/nature05317.

Behrenfeld, M. (2010). Abandoning Sverdrup's Critical Depth Hypothesis on phytoplankton blooms. Ecology 91:977–989. http://dx.doi.org/10.1890/09-1207.1

Bower, A. S., and W. J. Von Appen (2008). Interannual variability in the pathways of the North Atlantic current over the Mid-Atlantic Ridge and the impact of topography. Journal of Physical Oceanography, 38(1), 104-120, doi:10.1175/2007JPO3686.1.

Carton, J. A., G. A. Chepurin, X. Cao, and B. Giese (2000). A Simple Ocean Data Assimilation retrospective analysis of the global ocean 1950-1995. Part I: Methodology. J.Phys. Oceanogr., v.30, n. 2, pp. 294-309.

Cermeño P, S. Dutkiewicz, R. P. Harris, M. Follows, O. Schofield, and P. G. Falkowski (2008). The role of nutricline depth in regulating the ocean carbon cycle. Proceedings of the National Academy of Sciences of USA 105, (51) 20344-20349. Highlighted Faculty 1000.

CLS (Collecte Localisation Satellites) (2009). SSALTO/DUACS User Handbook : (M)SLA and (M)ADT Near-Real Time and Delayed Time Products. Ref. CLS-DOS-NT-06.034. Available from: http://www.aviso.oceanobs.com/fileadmin/documents/data/tools/hdbk_duacs.pdf.

Cummings, J. A. (2005). Operational multivariate ocean data assimilation. Quart. J. Roy. Meteor. Soc., 131, 3583–3604

de Boyer Montégut, C., G. Madec, A. S. Fischer, A. Lazar, and D. Iudicone (2004). Mixed layer depth over the global ocean: an examination of profile data and a profile-based climatology, J. Geophys. Res., 109, C12003

Doney, S. C. (2006). Plankton in a warmer world. Nature 444: z–696, doi: 10.1038/444695a.

Dutkiewicz, S., M. Follows, J. Marshall, and W.W. Gregg (2001). Interannual variability of phytoplankton abundances in the North Atlantic. Deep Sea Res. II 48, 2323–2344. doi:10.1016/S0967-0645(00)00178-8.

Ferry N., L. Parent, G. Garric, M. Drevillon, C. Desportes, C. Bricaud, and F. Hernandez (2012). Scientific Validation Report (ScVR) for Reprocessed Analysis and Reanalysis. MyOcean project report, MYO-WP04-ScCV-rea-MERCATOR-V1.0, 66pp. (available at http://www.mercator-ocean.fr/content/download/1624/12967/version/1/file/MYO-WP4-ScVR-rea-MERCATOR-V1.0.pdf)

Falkowski, P.G., Greene, R.M. and R.J. Geider (1992). Physiological limitations on phytoplankton productivity in the ocean, Oceanography 5, 84-91.

Follows, M., and S. Dutkiewicz (2001). Meteorological modulation of the North Atlantic spring bloom, Deep Sea Res., Part II, 49, 321 – 344, doi:10.1016/S0967-0645(01)00105-9.

Foltz, G. R., S. A. Grodsky, J. A. Carton, and M. J. McPhaden (2003). Seasonal mixed layer heat budget of the tropical Atlantic Ocean, J. Geophys. Res., 108(C5), 3146, doi: 10.1029/2002JC001584.

Garcia, H. E., R. A. Locarnini, T. P. Boyer, and J. I. Antonov (2006). World Ocean Atlas 2005, Volume 4: Nutrients (phosphate, nitrate, silicate). S. Levitus, Ed. NOAA Atlas NESDIS 64, U.S. Government Printing Office, Washington, D.C., 396 pp.

Gordon, H. R., and M. Wang (1994). Retrieval of water-leaving radiance and aerosol optical thickness over the oceans with SeaWiFS: A preliminary algorithm, Applied Optics 33, 443–452.

Gould, W. J. (1985). Physical oceanography of the Azores Front. Prog. Oceanogr., 14, 167–190.

Häkkinen, S., and P. B. Rhines (2009). Shifting surface currents in the northern North Atlantic Ocean, J. Geophys. Res., 114, C04005, doi: 10.1029/2008JC004883.

Häkkinen, S., P. B. Rhines, and D. L. Worthen (2011a). Warm and saline events embedded in the meridional circulation of the northern North Atlantic, J. Geophys. Res., 116, C03006, doi: 10.1029/2010JC006275

Häkkinen, S., P. B. Rhines, and D.L. Worthen (2011b). Atmospheric blocking and Atlantic Multidecadal Variability, Science 2011.

Hansen, J., Mki. Sato, R. Ruedy, K. Lo, D.W. Lea, and M. Medina-Elizade (2006). Global temperature change. *Proc. Natl. Acad. Sci.*,**103**, 14288-14293, doi:10.1073/pnas.0606291103

Hartman, S. E., K. E. Larkin, R. S. Lampitt, M. Lankhorst, and D. J. Hydes (2010) .Seasonal and inter-annual biogeochemical variations in the Porcupine Abyssal Plain 2003-2005 associated with winter mixing and surface circulation. Deep Sea Research Part II: Topical Studies in Oceanography, 57, 1303-1312.

Hasegawa, D., H. Yamazaki, T. Ishimaru, H. Nagashima, and Y. Koike (2008). Apparent phytoplankton bloom due to island mass effect. J. Mar. Syst., 69, 238– 246.

Hátún, H., B. Hansen, A. B. Sandø, H. Drange, and H. Valdimarsson (2005). Destabilization of the North Atlantic thermohaline circulation by a gyre mode, Science, 309, 1841–1844, doi:10.1126/science.1114777.

Henson, S. A., I. Robinson, J. T. Allen, and J. J. Waniek (2006). Effect of meteorological conditions on interannual variability in timing and magnitude of the spring bloom in the Irminger Basin, North Atlantic, Deep Sea Res., Part I, 53, 1601– 1615, doi:10.1016/j.dsr.2006.07.009.

Henson, S. A., J. P. Dunne, and J. L. Sarmiento (2009). Decadal variability in North Atlantic phytoplankton blooms, J. Geophys. Res., 114, C04013, doi: 10.1029/2008JC005139.

Holliday, N. P. (2003). Air-sea interaction and circulation changes in the northeast Atlantic, J. Geophys. Res., 108(C8), 3259, doi: 10.1029/2002JC001344

Holliday, N. P., S. L. Hughes, S. Bacon, A. Beszczynska-Möller, B. Hansen, A. Lavín, H. Loeng, K. A. Mork, S. Østerhus, T. Sherwin, and W. Walczowski (2008). Reversal of the 1960s to 1990s freshening trend in the northeast North Atlantic and Nordic Seas, Geophys. Res. Lett., 35, L03614, doi: 10.1029/2007GL032675.

Johnson, G. C., and N. Gruber (2007). Decadal water mass variations along 20 W in the northeastern Atlantic Ocean, Prog. Oceanogr., 73, 277–295, doi:10.1016/j.pocean.2006.03.022.

Kalnay, E., M. Kanamitsu, R. Kistler, W. Collins, D. Deaven, L. Gandin, M. Iredell, S. Saha, G. White, J. Woollen, Y. Zhu, A. Leetmaa, R. Reynolds, M. Chelliah, W. Ebisuzaki,W. Higgins, J. Janowiak, K. C. Mo, C. Ropelewski, J. Wang, R. Jenne, and D. Joseph (1996). The NCEP/NCAR 40-year reanalysis project, Bull. Amer. Meteor. Soc., 77, 437-470, doi: 10.1175/1520-0477(1996)077<0437:TNYRP>2.0.CO;2.

Lafon, V., Martins, A., Bashmachnikov, I., Jose, F., Melo-Rodriguez, M., Figueiredo, M., Mendonça, A., and Macedo, L. (2004). SST variability in the Azores region using AVHRR imagery: regional to local scale study. In: "Remote Sensing of Ocean and Sea Ice", Vol. 5569: 130-139. Proceedings of SPIE Vol. 5569, 130-139. Maspalomas, Gran Canaria, Espanha, 13 a 17 de Setembro.

Lagerloef,G. S. E., G. Mitchum, R. Lukas, and P. Niiler (1999). Tropical Pacific near-surface currents estimated from altimeter, wind and drifter data, J. Geophys. Res., 104, 23,313-23,326.

Le Cann, B., M. Assenbaum, J.C. Gascard, and G. Reverdin (2005). Observed mean and mesoscale upper ocean circulation in the midlatitude northeast Atlantic, J. Geophys. Res., 110, C07S05, doi: 10.1029/2004JC002768.

Levy, M., Y. Lehahn, J.M. Andre´, L. Me´mery, H. Loisel, and E. Heifetz (2005). Production regimes in the northeast Atlantic: A study based on Sea-viewing Wide Field-of-view Sensor (SeaWiFS) chlorophyll and ocean general circulation model mixed layer depth, J. Geophys. Res., 110, C07S10, doi: 10.1029/2004JC002771.

Locarnini, R. A., A. V. Mishonov, J. I. Antonov, T. P. Boyer, and H. E. Garcia (2006). World Ocean Atlas 2005, Volume 1: Temperature. S. Levitus, Ed. NOAA Atlas NESDIS 61, U.S. Government Printing Office, Washington, D.C., 182 pp.

Longhurst, A. (2006). The Atlantic Ocean. In: Longhurst A (ed) Ecological geography of the sea, 2nd edn. Elsevier Science Publishers, New York, p 131–268

Lozier, M. S., and N. M. Stewart (2008). On the temporally varying northward penetration of Mediterranean Overflow Water and eastward penetration of Labrador Sea Water, J. Phys. Oceanogr., 38, 2097–2103, doi:10.1175/2008JPO3908.1.

Marañon, E., Holligan, P. M., Varela, M., Mouriño, B. and A. J. Bale (2000). Basin-scale variability of phytoplankton biomass, production and growth in the Atlantic Ocean, Deep-Sea. Res. Pt I., 47, 825–857.

Mahadevan, A., E. D'Asaro, M. J. Perry, and C. Lee (2012). Eddy-driven stratification initiates North Atlantic Spring phytoplankton blooms Science, 337 (6090), 54-58, doi:10.1126/science.1218740.

Monterey, G., and S. Levitus (1997). Seasonal Variability of Mixed Layer Depth for the World Ocean, NOAA Atlas NESDIS 14, 100 pp., Natl. Oceanic and Atmos. Admin., Silver Spring, Md.

MWF, MeanWind Fields (MWF product) (2002).User Manual, Volume 2 : QuikSCAT, C2-MUT-W-04-IF, CERSAT – IFREMER, available at http://projets.ifremer.fr/cersat/content/download/2427/16800/file/mutwqscat.pdf

O’Reilly, J., S. Maritorena, B. G. Mitchell, D. A. Siegel, K. L. Carder, M. Kahru, S. A. Garver, and C. R. McClain (1998). Ocean color algorithms for SeaWiFS, J. Geophys. Res., 103, 24,937 – 24,953.

Palacios, D.M. (2002). Factors influencing the island-mass effect of the Galápagos Islands. Geophys. Res. Lett. 29 (23), 2134.

Palter, J. B., M. S. Lozier, and R. T. Barber (2005). The impact of advection on the nutrient reservoir in the North Atlantic subtropical gyre. Nature, 437, 687–692, doi: 10.1038/nature03969

Pelegri, J. L., A. Marrero Diaz, and A. W. Ratsimandresy (2006). Nutrient irrigation in the North Atlantic, Prog. Oceanogr., 70, 366–406.

Polovina, J. J., E. A. Howell, and M. Abecassis (2008). Ocean’s least productive waters are expanding, Geophys. Res. Lett., 35, L03618, doi:10.1029/2007GL031745

Raitsos, D., P.C. Reid, S. J. Lavender, M. Edwards, and A. J. Richardson (2005). Extending the SeaWiFS chlorophyll data set back 50 years in the northeast Atlantic. Geophysical Research Letters 32.

Reid, P. C., M. Edwards, H. G. Hunt, and A. J. Warner (1998). Phytoplankton change in the North Atlantic, Nature, 391, 546, doi: 10.1038/35290.

Reverdin, G., P. P. Niiler, and H. Valdimarsson (2003). North Atlantic Ocean surface currents, J. Geophys. Res., 108(C1), 3002, doi:10.1029/2001JC001020.

Reverdin, G. (2010). North Atlantic subpolar gyre surface variability (1895–2009), J. Clim., 23, 4571–4584, doi:10.1175/2010JCLI3493.1.

Reynolds, R. W., N. A. Rayner, T. M. Smith, D. C. Stokes, and W. Wang (2002). An improved in situ and satellite SST analysis for climate. J. Climate, 15, 1609-1625.

Sangrà, P., G. Baterretxea, J. L. Pelegrí, and J. Arístegui (2001). Chlorophyll Increase by Internal

Waves In The Shelf-Break Of Gran Canaria Island (CANARY Islands). Scientia Marina, 65, 89-97.

Seki, M. P., D. G. Foley, R. R. Bidigare, J. J. Polovina, C. L. Leonard, and R. E. Brainard (2001). Observations of biological enhancement at cyclonic eddies tracked with GOES thermal imagery in Hawaiian waters. Geophys. Res. Lett., 28, 1583–1586.

Siegel, D. A., S. C. Doney, and J. A. Yoder (2002). The North Atlantic spring phytoplankton bloom and Sverdrup's critical depth hypothesis, Science, 296, 730– 733, doi:10.1126/science.1069174.

Silva A, V. Brotas, A. Valente, T. Diniz, C. Sá, R. F. Patarra, N. V. Álvaro, and A. I. Neto (2013). Coccolithophore species as indicators of surface oceanographic conditions in the vicinity of Azores islands. Estuarine Costal and Shelf Science. 118: 50-59.

Simpson, J. H., P. B. Tett, M. L. Argote-Espinoza, A. Edwards, K.J. Jones, G. Savidge (1982). Mixing and phytoplankton growth around an island in a stratified sea. Cont. Shelf Res. 1, 15– 31

Smith, S. D. (1988). Coefficients for sea surface wind stress, heat flux, and wind profiles as a function of wind speed and temperature, Journal of Geophysical Research, Vol. 93, No. C12, P15, 467, doi: 10.1029/JC093iC12p15467

Spall, M. A., R. A. Weller, and P. W. Furey (2000). Modeling the threedimensional upper ocean heat budget and subduction rate during the Subduction Experiment, J. Geophys. Res., 105, 26,151–26,166.

Storto, A., I. Russo, S. Masina, S. Dobricic, and P. Di Pietro (2012). Scientific Validation Report (ScVR) for Reprocessed Analysis and Reanalysis. MyOcean project report, MYO-WP04-ScCV-rea-CMCC, 66pp.

Sun, C., A. Thresher, R. Keeley, N. Hall, M. Hamilton, P. Chinn, A. Tran, G. Goni, L. Petit de la Villeon T. Carval, L. Cowen, G. Manzella, V. Gopalakrishna, R. Guerrero, F. Reseghetti, Y. Kanno, B. Klein, L. Rickards, A. Baldoni, S. Lin, F. Ji, and Y. Nagaya (2010). The Data Management System for the Global Temperature and Salinity Profile Programme, in Proceedings of OceanObs.09: Sustained Ocean Observations and Information for Society, Vol. 2, Venice, Italy, 21-25 September 2009, Hall, J., Harrison, D.E. & Stammer, D., Eds., ESA Publication WPP-306,

doi:10.5270/OceanObs09.cwp.86

Sverdrup, H. U. (1953). On conditions for the vernal blooming of phytoplankton, J. Cons. Cons. Int. Explor. Mer, 18, 287– 295.

Taylor, J.R., and R. Ferrari (2011). Shutdown of turbulent convection as a new criterion for the onset of spring phytoplankton blooms. Limnology and Oceanography, 56(6) 2293-2307.

Teira, E., B. Mouriño, E. Marañón, V. Pérez, M. J. Pazó, P. Serret, E. Fernández (2005). Variability of chlorophyll and primary production in the Eastern North Atlantic subtropical gyre: potential factors affecting phytoplankton activity. Deep-Sea Research I, 52, 569-588.

Townsend D. W., L.M. Cammen, P. M. Holligan, D. E. Campbell, and N. R. Pettigrew (1994). Causes and concsequences of variability in the timing of spring phytoplankton blooms. Deep-Sea Res 41:747–765.

Vantrepotte, V., and Melin, F. (2009). Temporal variability of 10-year global SeaWiFS time-series of phytoplankton chlorophyll a concentration. –ICES Journal of Marine Science, 66: 1547–1556.

Williams, R. G., A. J. McLaren, and M. J. Follows (2000). Estimating the convective supply of nitrate and implied variability in export production over the North Atlantic, Global Biogeochem. Cycles, 14(4), 1299–1313, doi:10.1029/2000GB001260.

Williams, R. G., E. McDonagh, V. M. Roussenov, S. TorresValdes, B. King, R. Sanders, and D. A. Hansell (2011). Nutrient streams in the North Atlantic: Advective pathways of inorganic and dissolved organic nutrients, Global Biogeochem. Cycles, 25, GB4008, doi: 10.1029/2010GB003853.

Yentsch, C. S. (1989). An overview of mesoscales distribution of ocean color in the North Atlantic, Advances in Space Research (ISSN 0273-1177); 9; 7, 19; 435-442, doi:10.1016/0273-1177(89)90196-8